A lateralized pathway for associating nutrients with flavors

James C. R. Grove[1,2,3], Queenie Li[4], Heiko Backes[5], Bojana Kuzmanovic[5], Jaewon Choi[4], Violeta Ubadiah[4], Longhui Qiu[6], Jingkun Zhang[4], Zhengya Liu[1,2,3], Dana M. Small[7,8], Marc Tittgemeyer[5], Zachary A. Knight[1,2,3,4,9*].

[1]Department of Physiology, University of California, San Francisco
[2]Kavli Institute for Fundamental Neuroscience, University of California, San Francisco
[3]Neuroscience Graduate Program, University of California, San Francisco
[4]Howard Hughes Medical Institute
[5]Max Planck Institute for Metabolism Research, Cologne, Germany
[6]Department of Medicine, University of California, San Francisco
[7]Department of Psychiatry, Yale University School of Medicine
[8]Department of Psychology, Yale University School of Medicine
[9]Weill Institute for Neurosciences, University of California, San Francisco

[*]zachary.knight@ucsf.edu

Abstract

Animals learn about the external world, in part, via interoceptive signals[1,2]. For example, the nutrient content of food is first estimated in the mouth, in the form of flavor, and then measured again via slower signals from the gut. How these signals from the mouth and gut are integrated to drive learning is unknown. Here we identify a lateralized dopamine pathway that is specialized for learning about the nutrient content of food. We show that dopamine neurons in the ventral tegmental area (VTA_{DA}) are necessary for associating nutrients with flavors, but that this does not involve canonical dopamine targets in the striatum. Instead, post-ingestive nutrients trigger DA release selectively in a small region of the anterior basolateral amygdala (BLA). Remarkably, this hotspot for nutrient-triggered DA release is localized to the left side of the brain in both mice and humans, revealing that the DA system is lateralized. We identify the gut sensors that are responsible for nutrient-triggered DA release; show that they selectively activate BLA-projecting DA neurons defined by expression of cholecystokinin (CCK); and demonstrate that stimulation of DA axon terminals in the anterior BLA drives flavor-nutrient learning but not other aspects of behavior. Two-photon imaging of neurons in the left anterior BLA reveals that they encode food flavors, and these representations are strengthened by post-ingestive nutrients, whereas silencing of these neurons prevents flavor-nutrient learning. These

findings establish a neural basis for how animals learn about the nutrient content of their food. They also reveal unexpectedly that post-ingestive nutrients are differentially represented on the right and left sides of the brain.

Introduction

We learn about food during the process of eating[1–4]. For example, animals come to prefer calorie-rich foods after experiencing their post-ingestive effects[1,2]. This learning process is enabled by sensation along the alimentary canal that begins at the tip of the tongue and extends into the intestine. A fundamental challenge is to explain how these diverse interoceptive signals are integrated in the brain to create a coherent picture of what has been consumed.

Prior work has shown that there is a privileged connection between sensory signals that arise from the mouth and gut. For example, animals can learn to lick a flavored solution, but not press a lever, in order to receive an infusion of nutrients into the stomach[5,6]. This suggests that there may be hardwired pathways in the brain for linking orosensory and gut signals, but the identity and nature of these circuits is unknown.

DA neurons are required for learning about nutrients but not toxins

Pharmacological studies have suggested a role for DA in learning associations between nutrients and flavors[7–9]. We therefore first tested whether VTA_{DA} neurons are required for this process. We targeted the inhibitory opsin stGtACR to these cells for neural silencing, and, in a separate surgery, equipped mice with intragastric (IG) catheters for nutrient infusion. We then used a closed-loop paradigm for post-ingestive learning[5,10] in which mice are given access to two differentially flavored solutions, one of which is paired with lick-triggered IG glucose infusion and the other of which is paired with isovolumic infusions of water (see Methods, Fig. 1a). After six days of training, the preference of mice for these two flavors is measured ~~in a two-bottle test~~. Consistent with previous findings[10], we found that control mice developed a robust preference for the solution paired with sugar infusion (35±5% before vs. 81±7% after training, p=7.8e-5). In contrast, optogenetic silencing of VTA_{DA} neurons throughout training completely blocked the acquisition of a flavor preference (48±7% before vs. 53±7% after training, Fig. 1b). Importantly, silencing VTA_{DA} neurons did not reduce consumption of foods with known caloric value in hungry mice (Fig. 1d). However, it did reduce the consumption of food with a larger than expected caloric content (i.e. on the first day that a flavor was paired with closed-loop nutrient infusion; Fig. 1c). This indicates that VTADA neurons are necessary for updating food preferences and consumption in response to new information about a food's caloric content.

In addition to learning to prefer foods that have calories, animals also learn to avoid foods that are toxic, which occurs through an analogous post-ingestive learning process known as conditioned taste avoidance (CTA). To test whether VTA_{DA} neurons are involved in learning about toxins, we asked whether silencing these cells could block the CTA that results from pairing a novel flavor with LiCl injection, which causes visceral malaise (Fig. 1e). In contrast to flavor-nutrient learning (Fig. 1b), we found that silencing VTA neurons had no effect on flavor-toxin learning (Fig. 1e). This indicates that VTA_{DA} neurons are specifically required for learning about nutrients but are not necessary for all forms of post-ingestive learning.

Nutrients selectively trigger DA release in the BLA

We hypothesized that DA neurons contribute to flavor nutrient conditioning by supplying a signal of nutrient detection from the gut. Of note, previous studies have reported post-ingestive DA release in multiple brain regions[11–13], but the significance of these pathways for post-ingestive learning has not been tested.

We first directly compared nutrient-triggered DA release in three principal targets of VTA-DA neurons: the nucleus accumbens core (NAc), dorsolateral striatum (DLS), and basolateral amygdala (BLA). To do this, we targeted GRAB-DA3m[14] to these structures for fiber photometry recordings of extracellular DA in mice with IG catheters (Fig. 2a–b; Extended Fig. 1). Infusion of the complete diet Ensure caused dramatic DA release in BLA (18.2±3.5%, p=1e-5) which began 48±11 seconds after nutrients entered the stomach, and remained elevated for 9±1 minutes after the infusion ended (Extended Fig. 1e–i). This response was specific to nutrients, as it was also observed for infusion of glucose but not water (13.5±4.0% vs. -0.1±0.3% p=1e-4; Extended Fig. 1d), and it was independent of sex, as it was observed in both male and female mice (Extended Fig. 1c). In contrast, we observed no DA release in either dorsal or ventral striatum in response to IG nutrients (Fig. 2b). Of note, this is consistent with our previous finding that nutrient detection in the gut does not trigger DA release in the other major targets of the mesolimbic DA pathway[11].

To confirm that these DA dynamics in BLA also occur during natural ingestion, we next recorded DA release during self-paced consumption of Ensure (Fig. 2c; Extended Fig. 2). In BLA, we observed a dramatic increase in DA release that ramped over the first minute of ingestion and was sustained for the entire trial (Extended Fig. 2a–d). In contrast, DA release in NAc peaked almost immediately after ingestion and then rapidly declined, consistent with known responses

in NAc to appetitive tastes (Extended Fig. 2i–l). Interestingly, we observed a small but statistically significant (1.0±0.3%, p=1e-4; Extended Fig. 2p) increase in DA release in DLS after ingestion that may correspond to previous observations using microdialysis[12]. Together, this indicates that the BLA is the major site of DA release in response to nutrient detection in the gut.

DA release in response to nutrients is restricted to the anterior BLA

The BLA is an extended structure that spans 2.5 mm in the rostro-caudal axis in the mouse, and its anterior and posterior subdivisions have differences in cytoarchitecture and connectivity[15–17]. We therefore set out to systematically localize the site of nutrient-triggered DA release in the BLA. We first noted that we observed larger and more specific responses to nutrients in recordings from magnocellular cells, which extend from the central-medial to anterior BLA (Extended Fig. 1n). Therefore, we prepared mice for DA recordings in anterior vs. posterior BLA to test directly whether there is differential DA release across the rostro-caudal axis. This revealed that nutrient infusion caused much larger DA release in the anterior versus posterior BLA (e.g. Ensure: 10.0±2.3% vs. 3.1±0.4%, p=0.0085; Fig. 2d). Importantly, we found that the DA release in response to licking – which is immediate and does not involve GI signals – was the same in the anterior and posterior BLA, indicating that the difference in GI responses was not due to a technical defect in our posterior BLA recordings (Fig. 2e, Extended Fig. 3). Indeed, we found that DA release in posterior BLA was preferentially triggered by aversive GI stimuli, such as injection of LiCl (Extended Fig. 3g) and LPS (Extended Fig. 3h), which did not cause DA release in anterior BLA. This shows that the anterior and posterior BLA respond to fundamentally different visceral signals.

Prior work has identified specific gut sensors that are required for flavor-nutrient learning. We therefore reasoned that, if DA release in the anterior BLA is involved in this learning process, it should depend on these same gut receptors. For sugar, it has been shown that the key sensor is the intestinal sodium glucose transporter SGLT1[18,19]. Consistently, we found that IG infusion of a variety of SGLT1 agonists (glucose, galactose, and MDG) induced strong DA release in anterior BLA, whereas sugars that do not activate SGLT1 (mannitol and fructose) did not stimulate DA release (Extended Fig. 4d). Conversely, blocking intestinal SGLT1 with a specific antagonist was sufficient to prevent anterior BLA DA release in response IG glucose infusion (Extended Fig. 4e), indicating that this transporter is necessary. For fat, the key sensors that drive flavor-nutrient learning are GPR40/120 and CD36[20–22]. Accordingly, we found that blocking all three of these intestinal receptors abolished DA release in the anterior BLA during fat

infusion (Extended Fig. 4i). Thus, DA release in the anterior BLA depends on the same gut sensors that are known to drive flavor-nutrient conditioning.

The left side of the brain preferentially responds to nutrients in mice and humans

There have been reports that stimuli that induce fear[23,24] and pain[25] preferentially engage the right amygdala, whereas all the recordings we have described thus far were performed in the left amygdala. We therefore wondered whether internal nutrient signals might be differentially represented on the right and left hemispheres of the brain. To test this, we prepared mice for matched recordings in the right and left BLA during nutrient infusions. Remarkably, we found that IG Ensure triggered much greater DA release in left BLA compared to right (18.2±3.5% vs 5.3±1.0%, p=5.3e-4; Fig. 2f). We also observed a greater response in left BLA to IG infusion of glucose (Extended Fig. 5a–c). Of note, the short-timescale DA release in response to licking was actually greater on the right compared to the left BLA, confirming that the lateralized responses to prolonged GI signals were not due to a technical defect in our right hemisphere recordings (Fig. 2g; Extended Fig. 5d–f). This demonstrates that interoceptive cues such ingested nutrients can be specifically represented in one hemisphere of the mouse brain.

We wondered whether humans show similar lateralized responses to post-ingestive nutrients. While dopamine responses to IG nutrient infusion have not been measured in humans, one study[26] reported dopamine release (measured by 11C-raclopride PET) at fixed intervals during and after ingestion of a milkshake, enabling isolation of putative internal nutrient driven signals. Reanalysis of this data showed that, as in the mouse, the BLA is a major site of post-ingestive DA release in humans (Fig. 2h). Remarkably, this post-ingestive DA release was localized to the left BLA, specifically in the anterior portion, revealing that this small region is a hotspot for nutrient-triggered DA in both mice and humans. In a separate experiment utilizing fMRI in humans, we found that there was increased activity in BLA following consumption of glucose compared to water, and this was again localized to the anterior BLA in the left hemisphere (Fig. 2i). Thus, these data reveal that there is an evolutionarily conserved, dopaminergic pathway conveying nutrient signals to the left anterior BLA.

CCK+ DA neurons that project to BLA preferentially respond to nutrients

Our finding that nutrients trigger DA release only in the anterior BLA suggests that these responses are driven by only a small percentage of all VTA-DA neurons. Indeed, when we performed single-cell calcium imaging of VTA-neurons, we observed that only 11% of cells were

activated during IG nutrient infusion[11,27] (Fig. 3a; Extended Fig. 6a–b). We therefore set out to identify these nutrient-responsive DA neurons.

We used a combination of intersectional genetics and single-cell imaging to test candidate molecular markers, which revealed that VTA-DA neurons expressing CCK were highly enriched for nutrient responsive cells (Fig. 3b–d). A majority of these VTA-DA-CCK cells (61%) were activated during nutrient infusion and their dynamics during IG infusion mirrored the dynamics of downstream DA release in the BLA. For example, somatic calcium ramped in the first minute after the onset of infusion (rise time: 35±7s for calcium vs. 41±12s for DA in BLA; see Methods; Extended Fig. 1f–g, 6g) and then remained elevated for many minutes after nutrient infusion ended (Extended Fig. 6i). Importantly, VTA-DA neurons expressing CCK are known to project to BLA[28], which we confirmed (Fig. 3b), indicating that this subtype is very likely the source of the nutrient-triggered DA release in anterior BLA.

We noticed that, while most VTA-DA-CCK neurons responded to IG nutrients, these responses were not homogeneous. Indeed, k-means clustering revealed two populations of VTA-DA-CCK cells, one that was activated primarily during IG infusion and a second population of cells that showed more sustained responses (Fig. 3e). Consistently, principle component analysis (PCA) revealed two distinct phases of activity - one during nutrient infusion (PC2) and one after (PC1) (Fig. 3f) – and this first principle component was sufficient to segregate the two clusters of cells identified by k-means (Extended Fig. 6h). This reveals that internal signals of nutrient ingestion – which persist for tens for minutes – are encoded in two parts by two discrete populations of CCK+ cells at the level of the VTA.

The VTA→aBLA pathway is specialized for post-ingestive learning

The fact that the VTA→aBLA pathway responds to internal nutrients (Fig. 2) via the same gut sensors that drive flavor learning (Extended Fig. 4) suggests that this pathway is involved in this process. To test this possibility, we prepared mice for optogenetic stimulation of VTA_{DA} terminals in the anterior BLA and, as a control, two other sites: the NAc, which is important for many other forms of DA-mediated learning[29–31], and the posterior BLA, which responded to aversive visceral signals (Fig. 2, Extended Fig. 3).

We first tested whether optogenetic activation of these pathways could substitute for nutrient signals in driving flavor learning. Mice were given access to two differently flavored, non-caloric solutions, one of which was paired with delayed, tonic stimulation (to mimic post-ingestive DA

release; see Methods and Extended Data Fig. 2e), while the other solution did not trigger
195 stimulation. Strikingly, this delayed stimulation of DA release in anterior BLA conditioned a robust flavor preference (Fig. 4b). In contrast, no change in preference was observed after stimulation of axon terminals in the posterior BLA or NAc (Fig. 4c–d) or for mCherry controls (Extended Data Fig. 7a–d). This indicates that only the anterior BLA projection is sufficient to drive flavor learning.

200 To evaluate the specificity of these results, we tested these mice in a battery of assays measuring different aspects of feeding behavior or reinforcement. In contrast to the effects on flavor learning, stimulation of axon terminals in the anterior BLA had no effect on total food intake, regardless of the timing of optogenetic stimulation (either continuous or closed-loop to lick onset or offset; see Methods and Fig. 4f and Extended Figs. 8b,f) and also failed to
205 condition avoidance of a paired flavor (Fig. 4j and Extended Fig. 8j). Moreover, this pathway did not support self-stimulation, indicating it is not reinforcing in the absence of a flavor cue. As a control, we tested stimulation of the VTA→NAc pathway in the same assays, which confirmed that DA release in NAc modulated food intake[32] (Fig. 4h and Extended Fig. 8d) and supported vigorous lever pressing, as previously reported[31] (Fig. 4l). Taken together, these results reveal a
210 double dissociation in which the aBLA pathway specifically drives flavor learning but not other aspects of motivated behavior or reinforcement, which are instead mediated by canonical DA pathways.

aBLA neurons integrate nutrient and flavor signals to drive learning

The fact that nutrients trigger DA release selectively in anterior BLA raises the question of how
215 flavors and post-ingestive signals are integrated in this structure. In pilot studies, we found that IG nutrient infusion was unable to condition a preference when it was separated in time from the paired flavor (Extended Fig. 9a), implying that these signals must overlap for learning to occur (which is in contrast to CTA, which permits long delays between flavor and toxin). We therefore prepared mice for two-photon imaging of left anterior BLA neurons expressing dopamine
220 receptor 1 (D1R), which labels most DA-responsive BLA cells[33] (Fig. 5a), and examined how these cells integrate ongoing nutrient and flavor signals.

We first sought to isolate BLA responses to flavor cues by recording activity during brief-access taste tests (5 seconds, each trial initiated by an auditory cue) for sucrose, sucralose (a non-caloric sweetener), or water. To distinguish taste-driven activity from other cue responses[34] or
225 licking itself, in 10% of trials (mock trials) the cue was played but liquid access was withheld (Fig. 5b).

We found that 58% of anterior BLA_{D1R} neurons were activated by sucrose ingestion with dynamics that were time-locked to the start of licking (Fig. 5c; peak time: 3.4±0.3s from the first lick in each bout; Extended Data Fig. 9e). In contrast, we observed only weak activation of these cells during mock trials (1.0±0.2z vs. 0.08±0.09z, sucrose vs. mock, p=1e-5; Extended Data Fig. 9h), and these differences persisted when we controlled for the number of licks (Extended Data Fig. 9i–k), indicating these responses depend on ingestion. In addition, the responses to sucrose and sucralose were highly correlated, both at the level of individual neurons (p=7.7e-8; Fig. 5d–e; Extended Data Fig. 9m–o) and population dynamics (Fig. 5f; Extended Data Fig. 9r). In contrast, ingestion of water produced less activation (Extended Data Fig. 9o–p) and a distinct population trajectory (Fig. 5f; Extended Data Fig. 9r). Together, this demonstrates that many anterior BLA neurons specifically represent sweet tastes.

We next investigated how anterior BLA_{D1R} neurons respond to purely post-ingestive signals by recording their activity during and after IG infusion of sucrose. This revealed a slow ramping activation that began during sucrose infusion and remained elevated for many minutes after the infusion ended (Fig. 5g; Extended Data Fig. 9s–v). We observed a similar ramping activity following infusion of Intralipid or Ensure (Fig. 5h; Extended Data Fig. 9u–v) but not following sham infusion, confirming that these are bona fide nutrient responses.

We wondered how the phasic signal representing sweet taste and the tonic signal represent GI feedback are integrated in individual neurons. Of note, if learning happens in the anterior BLA, then we might expect that these flavor and post-ingestive signals to converge on the same anterior BLA neurons (Fig. 5i). Alternatively, these two signals could be represented in separate cells, which would suggest that learning happens in a downstream structure. To test this, we examined the activity in-between trials of brief-access to sucrose, which would potentially include GI but not oral signals. We found that this inter-trial activity increased in the second half of the session in cells that were activated by taste cues, and did so only in cells that were also phasically activated by sweet tastes (Fig. 5j–k; Extended Data Fig. 9w). In contrast, there was no similar increase in inter-trial activity following consumption of sucralose or water, indicating this depends on caloric content. We also found that the phasic taste responses changed over the course of the trial in a nutrient-dependent way: lick responses to sucralose and water diminished over time, whereas lick responses to sucrose were stable at the single-cell (Fig. 9y–z) and population level (Fig. 5l). Together, these two observations indicate that nutrient and gustatory responses converge on the same cells in anterior BLA, and that this integration strengthens responses to tastes associated with calories.

260 The integration of taste and post-ingestive signals in anterior BLA_{D1R} neurons suggests that these cells could be critical for learning about the nutrient content of food. To test their necessity, we optogenetically silenced anterior BLA_{D1R} neurons during flavor-nutrient conditioning, which completely prevented mice from learning which flavor was associated with calories (Fig. 6a–b). Importantly, silencing these neurons did not result in a decrease in food
265 intake when hungry animals were given Ensure (Fig. 6d), indicating that anterior BLA_{D1R} neurons are not required for ingestion per se. However, silencing these neurons did decrease consumption of a non-caloric solution newly paired with IG glucose infusion (Fig. 6c), indicating that they are important for updating the value of flavors when the nutrient content of food is uncertain. This effect was specific to flavor-nutrient learning, as inhibition of these neurons did
270 not block a different form of post-ingestive learning, CTA (Fig. 6e). Thus anterior BLA_{D1R} neurons integrate flavor cues with nutrient signals to assign value to calorie-rich foods.

Summary

Animals must learn which foods are nutritious based on their post-ingestive effects[1–4]. While
275 these post-ingestive effects could in principle be associated with any sensory cue, there is much evidence that there is a privileged pathway connecting the flavor of food, sensed in the mouth, with its nutrient content sensed in the gut. For example, animals can readily learn to lick a flavored solution, but not press a lever, in order to receive an IG infusion of nutrients[5,6]. Similarly, animals will learn to prefer a place associated with IG nutrient infusion only if it is
280 coupled with an orosensory cue[35]. This suggests that there is a hardwired pathway in the brain that connects flavors and nutrients in order to drive learning about food, but the underlying circuits have been unknown.

Here, we have shown that there is a genetically and anatomically-distinct pathway within the midbrain dopamine system that is specialized for associating nutrients and flavors. This
285 pathway is defined by CCK-expressing VTA_{DA} neurons that relay internal nutrient signals to a remarkably specific subregion of the amygdala, namely the anterior portion of the BLA on the left side of the brain. A variety of functional tests show that this pathway receives the specific GI signals known to drive flavor preference, and that the underlying neurons are necessary and sufficient for flavor learning. This establishes a neural basis for how animals learn which foods
290 are nutritious.

Learning about food involves making associations with both its nutrient content and its environmental context. The latter is known to be mediated by phasic DA release in NAc in response to reward-predicting exterosensory cues. A salient feature of this form of learning is that it is temporally precise, meaning that DA must be released within (at most) a few seconds of the cue[36,37]. In contrast, nutrient detection in the gut is inherently slow and, as we show, involves DA signals that ramp over tens of minutes in the BLA. Consistent with the distinct properties of these two pathways, we found that acute stimulation of NAc DA projections invigorated ongoing behavior, but delayed and prolonged stimulation did not drive flavor learning. Conversely, acute stimulation of BLA projections did not alter behavior, but delayed stimulation drove robust flavor learning. This reveals a hierarchy in which learning about food involves first associating flavors with nutrients via the VTA-BLA pathway and then associating those flavors with exterosensory cues via the VTA–NAc pathway (Fig. 6f).

A surprising feature of this BLA pathway is that it is lateralized to the left hemisphere in both mice and humans. This could account for the unexplained alterations in ingestive behavior observed in individuals with lesions to the left BLA[38–40]. While a few functions, such as speech processing in humans, are known to be localized to one side of the brain, the neural circuits that govern core survival behaviors such as feeding are generally thought to be symmetric. We do not know the origin of the asymmetry in BLA nutrient responses, but it could originate from asymmetry in the vagus nerve[12,41] that relays signals from gut to brain, or, alternatively, from lateralized responses to visceral stimuli in insular cortex[42,43]. As almost no studies of feeding behavior in rodents have examined the possibility that the underlying circuits are lateralized, it will be important in future studies to determine the anatomic origin of this functional asymmetry in the BLA. More broadly, these findings raise the possibility that there is a general role for hemispheric specialization in the control of feeding behavior.

Bibliography

1. Sclafani, A. Learned controls of ingestive behaviour. *Appetite* **29**, 153–158 (1997).
2. Capaldi, E. D. Conditioned Food Preferences. in *Psychology of Learning and Motivation* (ed. Medin, D. L.) vol. 28 1–33 (Academic Press, 1992).
3. Havermans, R. C. & van den Heuvel, E. 10 - Acquired tastes: on the learning of human food preferences. in *Flavor (Second Edition)* (eds. Guichard, E. & Salles, C.) 283–299 (Woodhead Publishing, 2023). doi:10.1016/B978-0-323-89903-1.00005-0.
4. Rozin, P. & Zellner, D. The role of Pavlovian conditioning in the acquisition of food likes and dislikes. *Ann. N. Y. Acad. Sci.* **443**, 189–202 (1985).
5. Sclafani, A. Conditioned food preferences. *Bull. Psychon. Soc.* **29**, 256–260 (1991).
6. Holman, G. L. Intragastric reinforcement effect. *J. Comp. Physiol. Psychol.* **69**, 432–441 (1969).
7. Azzara, A. V., Bodnar, R. J., Delamater, A. R. & Sclafani, A. D1 but not D2 dopamine receptor antagonism blocks the acquisition of a flavor preference conditioned by intragastric carbohydrate infusions. *Pharmacol. Biochem. Behav.* **68**, 709–720 (2001).
8. Touzani, K., Bodnar, R. J. & Sclafani, A. Dopamine D1-like receptor antagonism in amygdala impairs the acquisition of glucose-conditioned flavor preference in rats. *Eur. J. Neurosci.* **30**, 289–298 (2009).
9. Touzani, K., Bodnar, R. & Sclafani, A. Activation of dopamine D1-like receptors in nucleus accumbens is critical for the acquisition, but not the expression, of nutrient-conditioned flavor preferences in rats. *Eur. J. Neurosci.* **27**, 1525–1533 (2008).
10. Zukerman, S., Ackroff, K. & Sclafani, A. Post-oral glucose stimulation of intake and conditioned flavor preference in C57BL/6J mice: A concentration–response study. *Physiol. Behav.* **109**, 33–41 (2013).

11. Grove, J. C. R. *et al.* Dopamine subsystems that track internal states. *Nature* **608**, 374–380 (2022).

12. Han, W. *et al.* A Neural Circuit for Gut-Induced Reward. *Cell* **175**, 665-678.e23 (2018).

13. Alhadeff, A. L. *et al.* Natural and Drug Rewards Engage Distinct Pathways that Converge on Coordinated Hypothalamic and Reward Circuits. *Neuron* **103**, 891-908.e6 (2019).

14. Zhuo, Y. *et al.* Improved green and red GRAB sensors for monitoring dopaminergic activity in vivo. *Nat. Methods* **21**, 680–691 (2024).

15. Krettek, J. E. & Price, J. L. A description of the amygdaloid complex in the rat and cat with observations on intra-amygdaloid axonal connections. *J. Comp. Neurol.* **178**, 255–279 (1978).

16. Wang, L. *et al.* The coding of valence and identity in the mammalian taste system. *Nature* **558**, 127–131 (2018).

17. Hintiryan, H. *et al.* Connectivity characterization of the mouse basolateral amygdalar complex. *Nat. Commun.* **12**, 2859 (2021).

18. Sclafani, A., Koepsell, H. & Ackroff, K. SGLT1 sugar transporter/sensor is required for post-oral glucose appetition. *Am. J. Physiol.-Regul. Integr. Comp. Physiol.* **310**, R631–R639 (2016).

19. Zukerman, S., Ackroff, K. & Sclafani, A. Post-oral appetite stimulation by sugars and nonmetabolizable sugar analogs. *Am. J. Physiol.-Regul. Integr. Comp. Physiol.* **305**, R840–R853 (2013).

20. Ackroff, K. & Sclafani, A. Post-oral fat stimulation of intake and conditioned flavor preference in C57BL/6J mice: A concentration-response study. *Physiol. Behav.* **129**, 64–72 (2014).

21. Sclafani, A., Zukerman, S. & Ackroff, K. GPR40 and GPR120 fatty acid sensors are critical for postoral but not oral mediation of fat preferences in the mouse. *Am. J. Physiol.-Regul. Integr. Comp. Physiol.* **305**, R1490–R1497 (2013).

22. Sclafani, A., Ackroff, K. & Abumrad, N. A. CD36 gene deletion reduces fat preference and intake but not post-oral fat conditioning in mice. *Am. J. Physiol.-Regul. Integr. Comp. Physiol.* **293**, R1823–R1832 (2007).

23. Baas, D., Aleman, A. & Kahn, R. S. Lateralization of amygdala activation: a systematic review of functional neuroimaging studies. *Brain Res. Rev.* **45**, 96–103 (2004).

24. Baker, K. B. & Kim, J. J. Amygdalar Lateralization in Fear Conditioning: Evidence for Greater Involvement of the Right Amygdala. *Behav. Neurosci.* **118**, 15–23 (2004).

25. Allen, H. N., Bobnar, H. J. & Kolber, B. J. Left and right hemispheric lateralization of the amygdala in pain. *Prog. Neurobiol.* **196**, 101891 (2021).

26. Thanarajah, S. E. *et al.* Food Intake Recruits Orosensory and Post-ingestive Dopaminergic Circuits to Affect Eating Desire in Humans. *Cell Metab.* **29**, 695-706.e4 (2019).

27. Fernandes, A. B. *et al.* Postingestive Modulation of Food Seeking Depends on Vagus-Mediated Dopamine Neuron Activity. *Neuron* **106**, 778-788.e6 (2020).

28. Poulin, J.-F. *et al.* Mapping projections of molecularly defined dopamine neuron subtypes using intersectional genetic approaches. *Nat. Neurosci.* **21**, 1260–1271 (2018).

29. Flagel, S. B. *et al.* A selective role for dopamine in stimulus–reward learning. *Nature* **469**, 53–57 (2011).

30. Saddoris, M. P., Cacciapaglia, F., Wightman, R. M. & Carelli, R. M. Differential Dopamine Release Dynamics in the Nucleus Accumbens Core and Shell Reveal Complementary Signals for Error Prediction and Incentive Motivation. *J. Neurosci.* **35**, 11572–11582 (2015).

31. Han, X. *et al.* Role of dopamine projections from ventral tegmental area to nucleus accumbens and medial prefrontal cortex in reinforcement behaviors assessed using optogenetic manipulation. *Metab. Brain Dis.* **32**, 1491–1502 (2017).

32. Boekhoudt, L. *et al.* Does activation of midbrain dopamine neurons promote or reduce feeding? | International Journal of Obesity. *Int. J. Obes.* **41**, 1131–1140 (2017).

33. Wei, X. *et al.* Dopamine D1 or D2 receptor-expressing neurons in the central nervous system. *Addict. Biol.* **23**, 569–584 (2018).

34. Lutas, A. *et al.* State-specific gating of salient cues by midbrain dopaminergic input to basal amygdala. *Nat. Neurosci.* **22**, 1820–1833 (2019).

35. Matsumura, S. *et al.* Intragastric infusion of glucose enhances the rewarding effect of sorbitol fatty acid ester ingestion as measured by conditioned place preference in mice. *Physiol. Behav.* **99**, 509–514 (2010).

36. Izhikevich, E. M. Solving the Distal Reward Problem through Linkage of STDP and Dopamine Signaling. *Cereb. Cortex* **17**, 2443–2452 (2007).

37. Yagishita, S. *et al.* A critical time window for dopamine actions on the structural plasticity of dendritic spines. *Science* **345**, 1616–1620 (2014).

38. Ghika-Schmid, F., Assal, G., De Tribolet, N. & Regli, F. Klüver-Bucy syndrome after left anterior temporal resection. *Neuropsychologia* **33**, 101–113 (1995).

39. Anson, J. A. & Kuhlman, D. T. Post-ictal Kluver-Bucy syndrome after temporal lobectomy. *J. Neurol. Neurosurg. Psychiatry* **56**, 311–313 (1993).

40. Boronat, S., Newberry, P., Mehan, W., Thiele, E. A. & Duhaime, A.-C. Klüver–Bucy syndrome after unilateral frontotemporal resection in a child with tuberous sclerosis. *Childs Nerv. Syst.* **29**, 1391–1394 (2013).

41. de Araujo, A. M. *et al.* Asymmetric control of food intake by left and right vagal sensory neurons. *bioRxiv* 2023.05.08.539627 (2023) doi:10.1101/2023.05.08.539627.

42. Qian, K., Liu, J., Cao, Y., Yang, J. & Qiu, S. Intraperitoneal injection of lithium chloride induces lateralized activation of the insular cortex in adult mice. *Mol. Brain* **14**, 71 (2021).

43. Wu, Y. *et al.* The anterior insular cortex unilaterally controls feeding in response to aversive visceral stimuli in mice. *Nat. Commun.* **11**, 640 (2020).

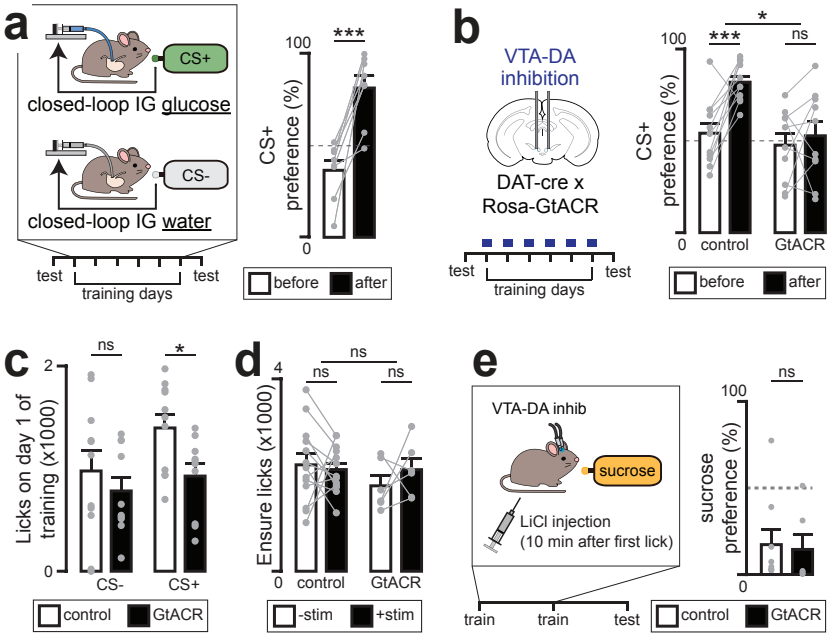

Figure 1. Dopamine neurons are necessary for nutrient learning. a. (Left) Flavor-nutrient conditioning protocol. (Right) Mice learn to prefer flavored solution paired with glucose infusion (CS+). **b.** (Left) Method for inhibition of VTA-DA neurons during flavor-nutrient conditioning. (Right) Inhibiting VTA-DA neurons prevents flavor-nutrient conditioning. **c.** VTA-DA inhibition decreases CS+ solution intake on the first day of training. **d.** VTA-DA inhibition does not decrease intake of familiar nutritive solution Ensure. **e.** (Left) Method for taste aversion conditioning. (Right) VTA-DA inhibition does not prevent aquisition of a conditioned taste aversion (CTA). ns.P>0.05, *P<0.05, **P<0.01, ***P<0.001. See Extended Data Table 1.

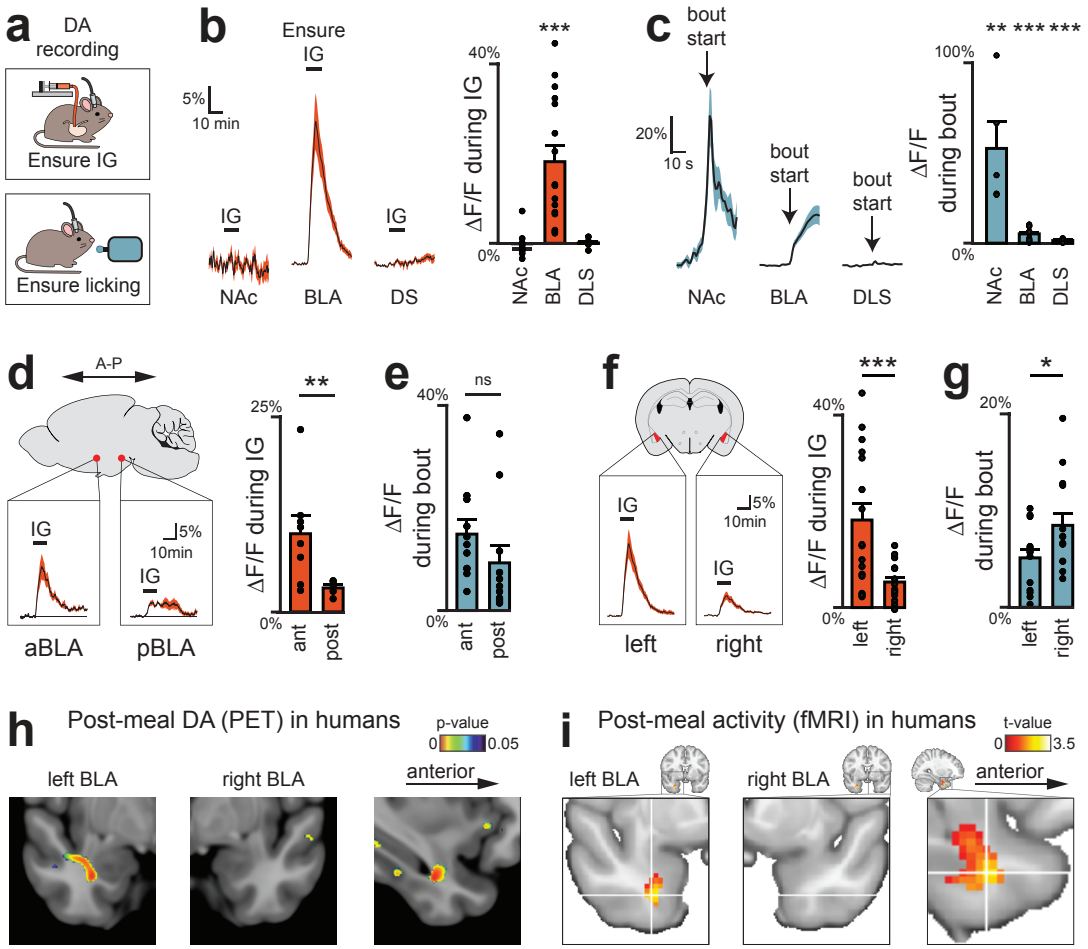

Figure 2. Lateralized DA pathway tracks internal nutrients. **a.** Recording DA release in mice (with GRAB-DA) during IG infusion or consumption of liquid diet Ensure. **b.** Mean traces (left) and summary plot (right) showing DA release during IG is localized to the BLA. **c.** Mean traces (left) and summary plot (right) showing DA release during the first lick bout is largest in NAc. **d.** Mean traces (left) and summary plot (right) showing DA release during IG is largest in anterior BLA (aBLA). **e.** Summary plot showing equal DA release in across BLA during the first lick bout. **f.** Mean traces (left) and summary plot (right) showing DA release during IG is largest in the left hemisphere. **g.** Summary plot showing DA release during the first lick bout is not also larger in the left hemisphere. **h.** DA release after milkshake consumption (recorded in humans using 11C-raclopride) is increased in left but not right BLA, and is greatest in the anterior pole. **i.** Increased activity after glucose consumption compared to water control (recorded in humans using fMRI) in left but not right aBLA. Brains are shown in neurological orientation with the subject's left on the left side of the image. ns.P>0.05, *P<0.05, **P<0.01, ***P<0.001. See Extended Data Table 2.

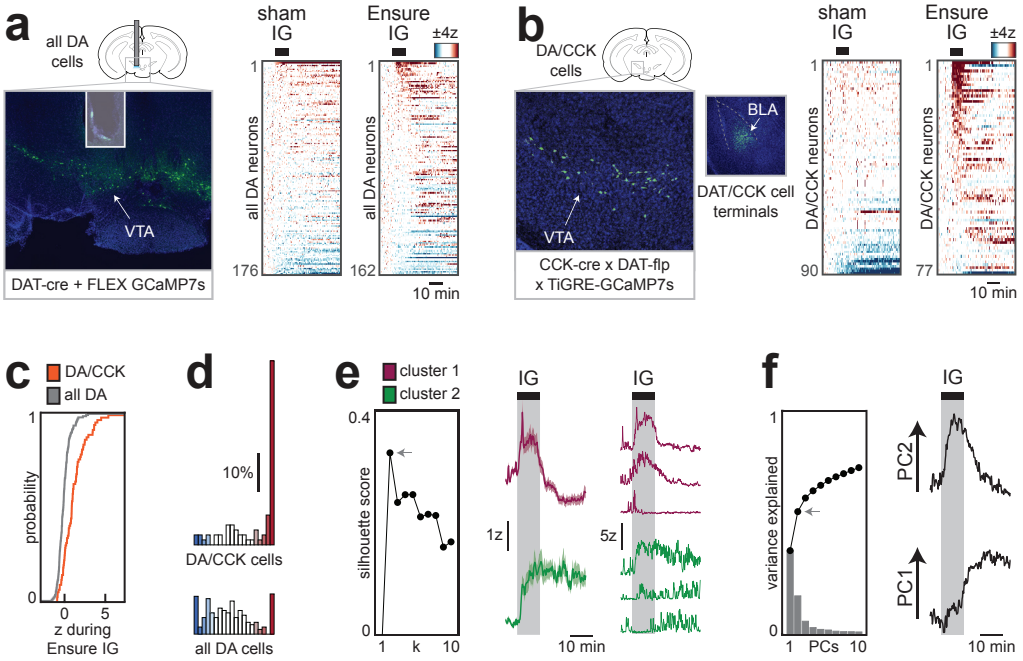

Figure 3. Genetically-defined VTA DA projection tracking nutrient ingestion. a. Single cell imaging of VTA-DA neurons. (Left) Histology showing fiber placement. (Right) Individual DA neuron dynamics during infusion of Ensure or sham. **b.** Single cell imaging of VTA-DA/CCK neurons. (Left) Histology showing location of DA/CCK cell bodies in VTA and location of terminals in BLA. (Right) Individual DA/CCK neuron dynamics during infusion of Ensure or sham. **c–d.** Cumulative distribution plot (c) and binned activity plot (d) show greater activation during Ensure infusion in VTA-DA/CCK subpopulation (p=4.2e-11, KS test). **e.** K-means clustering of VTA-DA/CCK activity during Ensure infusion reveals two clusters (left). These two clusters correspond to neurons exhibiting transient activation (purple) or prolonged activation (green) in response to infusion, shown with mean activity (middle) and representative single neuron activity (right). **f.** Principal component (PC) analysis of VTA-DA/CCK activity during Ensure infusion reveals two PCs explain 55% of total variance (left). These two PCs correspond to activity changes during and after infusion (right). *P < 0.05, **P < 0.01, ***P < 0.001. See Extended Data Table 3.

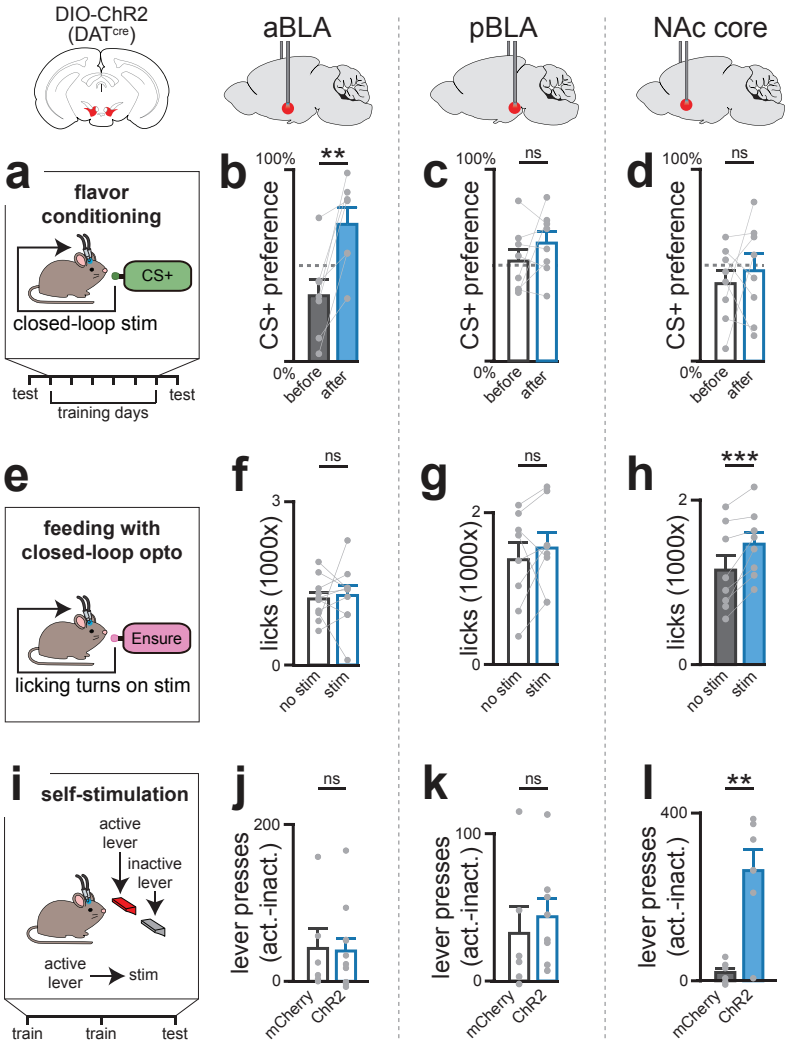

Figure 4. Specific role of BLA dopamine projection in flavor conditioning. (Top) Schematic for activation of VTA-DA terminals in aBLA, pBLA, or NAc, using the excitatory opsin ChR2 (with mCherry controls). **a.** Schematic for flavor-stimulation conditioning assay, where each lick of a flavored solution triggers terminal stimulation with a delay of 20s (to simulate IG transit delay; Extended Fig. 3h). Conditioning of flavor preference is tested using a two-bottle test before and after training. **b–d.** Mice learn to prefer flavor associated with stimulation of terminals in aBLA, but not for stimulation of NAc or pBLA. **e.** Schematic for feeding assay, where each lick triggers terminal stimulation. **f–h.** Mice consume more Ensure when paired with stimulation of of terminals in NAc, but not in aBLA or pBLA. **i.** Schematic for self-stimulation assay, where mice can lever press for terminal stimulation. **j–k.** Mice lever press for stimulation of terminals in NAc, but not in aBLA or pBLA. For visual presentation, bars are filled only in tests with significant effects. ns.P>0.05, *P < 0.05, **P < 0.01, ***P < 0.001, after Benjamini-Hochberg correction for multiple comparisons. See Extended Data Table 1.

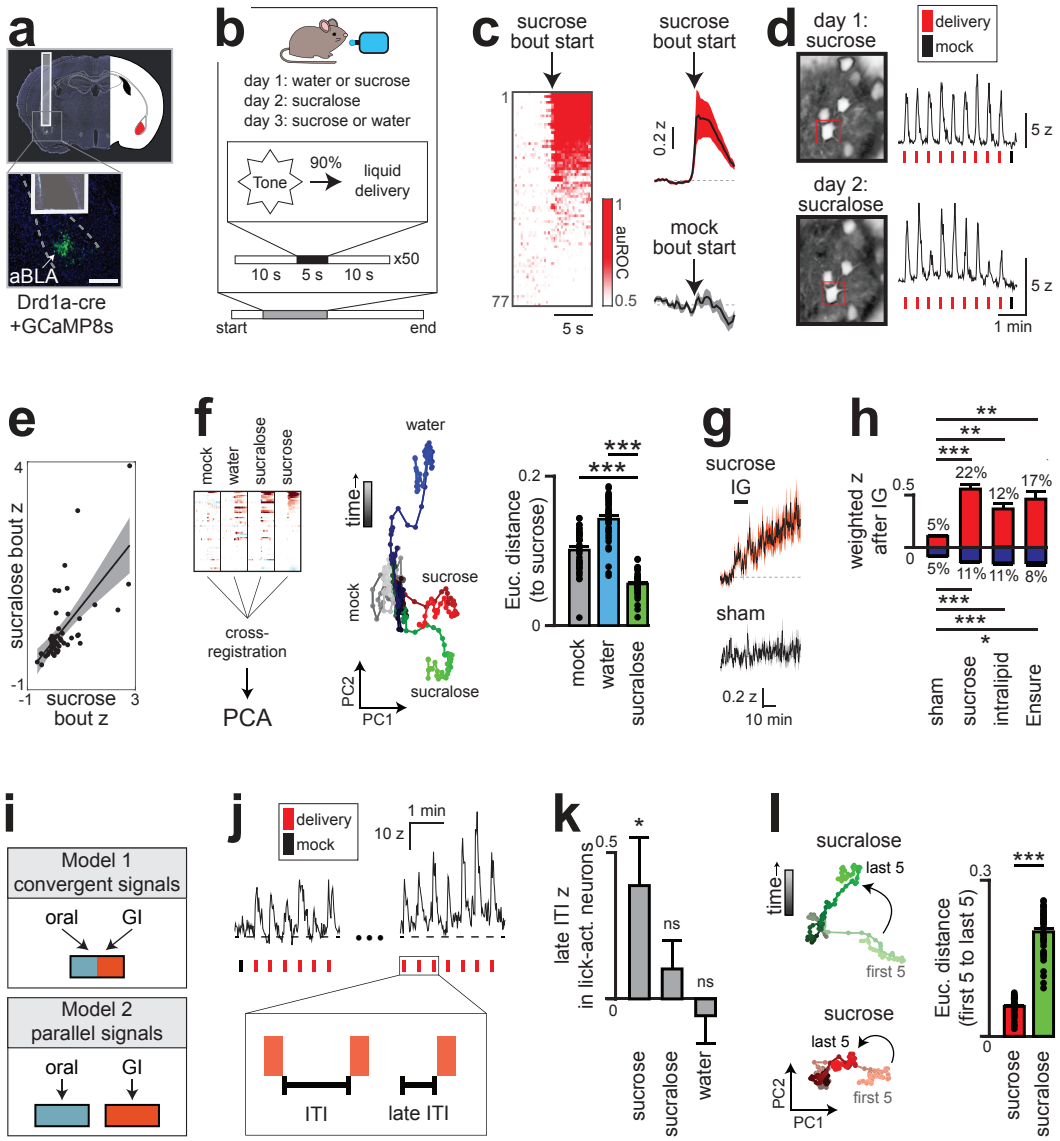

Figure 5. aBLA neurons integrate oral and post-ingestive nutrient signals. a. Imaging aBLA neurons expressing D1R (scale bar, 0.5 mm). **b.** Protocol for recording responses to tastants. **c.** (Left) Single cell dynamics averaged across all trials with sucrose delivery quantified using auROC, or area under the receiver operator curve. (Right) Mean activity across lick bouts during trials with sucrose delivery (red) or no delivery (grey) quantified using z-score. **d.** (Left) Example FOVs from two separate experimental days. (Right) Activity traces from an example cross-registered neuron (in red box) during sucrose delivery (top, day 1) and during sucralose delivery (bottom, day 2). Lines below traces indicate when tone was played (red lines are trials with liquid delivery). **e.** Correlation plot of activity during sucrose and sucralose bouts (R^2=0.45, p=7.7e-8). **f.** Principal component analysis (PCA) of neuron activity cross-registered across all three days (left) reveals similar activity trajectories during sucrose and sucralose bouts, as shown in PC space (middle) and euclidian (euc.) distance across PC1,2 for each timepoint (right). **g.** Mean activity during sucrose infusion showing prolonged activation compared to sham. **h.** Population-weighted z-score of activity of activated (red) and inhibited (blue) neurons during IG infusions. **i.** Competing models where gustatory and internal signals either converge on the same cells (model 1) or are represented in separate cells (model 2). **j.** (Top) Example neuron activity during sucrose bouts separated by ten minutes, showing increased activity over the trial. (Bottom) The second half of the intertrial interval (ITI) can be used to separately analyze post-ingestive signals. **k.** Summary plots of late ITI activity of lick-activated neurons in between trials 25–50. **l.** Lick-triggered activity diverges across early and late bouts of sucralose (but not sucrose), as shown in PC space (left) and euclidian distance across PC1,2 for each timepoint (right). ns.P>0.05, *P<0.05, **P<0.01, ***P<0.001. See Extended Data Table 3.

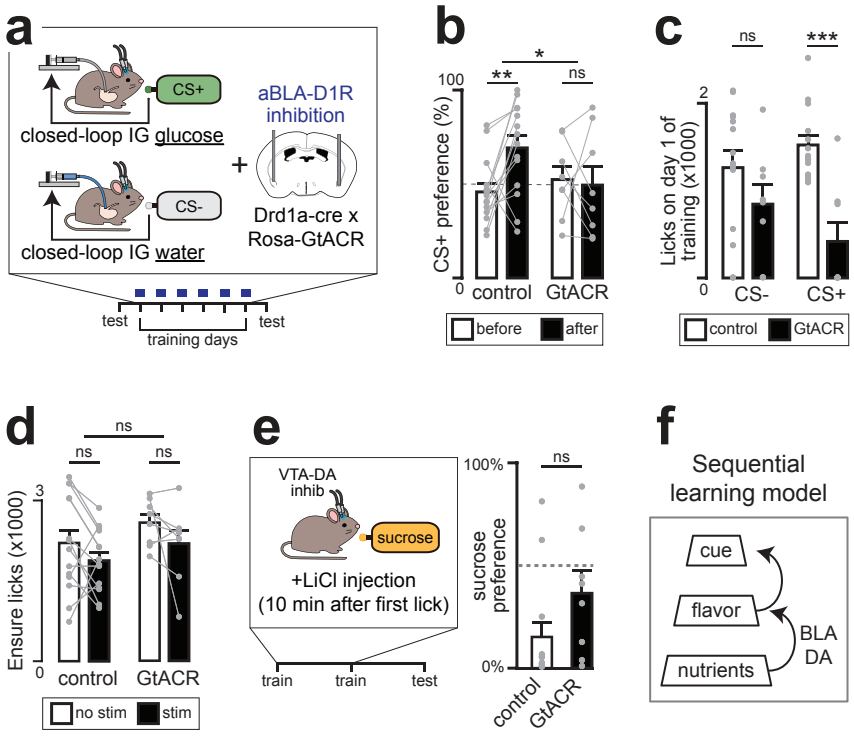

Figure 6. aBLA neurons are necessary for flavor-nutrient learning. a. Method for inhibition of aBLA-D1R neurons during flavor-nutrient conditioning. **b.** Silencing aBLA neurons prevents flavor-nutrient conditioning. **c.** aBLA-D1R inhibition decreases CS+ solution intake on the first day of training. **d.** Continuous inhibition of aBLA-D1R neurons does not effect consumption of familiar caloric solution Ensure. **e.** (Left) Schematic for conditioned taste aversion assay, where mice are given 1-hour access to a novel sucrose solution and injected with LiCl 10 minutes after their first lick. Conditioning of taste avoidance is tested using a two-bottle test against water after training. (Right) Continuous inhibition during training does not prevent taste aversion conditioning. **f.** Sequential model for learning about foods, where a primary association is made between the flavor of a food and its nutrient content (mediated by aBLA dopamine) and a secondary association is made between the flavor of a food and environmental cues (mediated in part by NAc dopamine). ns.P>0.05, *P<0.05, **P<0.01, ***P<0.001. See Extended Data Table 1.

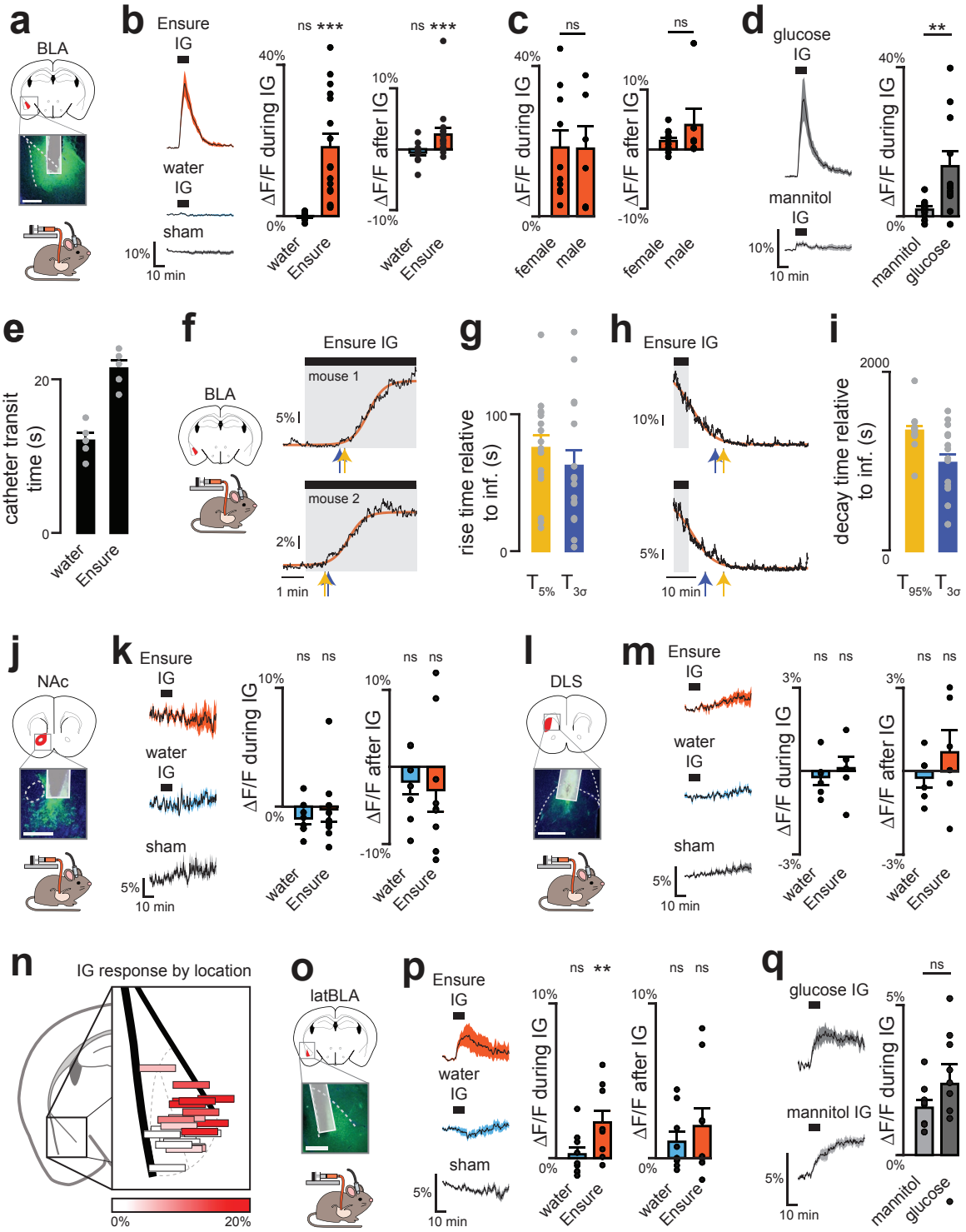

Extended Data Figure 1. Dopamine dynamics across brain regions during IG infusions. a. Recording DA release (using GRAB-DA) in BLA. Dotted lines show external capsule. Scale bar, 0.5 mm. **b.** Mean traces (left) and summary plots during (middle) and after (right) infusion showing increased DA release in BLA during and after infusion of Ensure compared to water. **c.** Summary plots showing no difference between male and female mice in BLA DA release during (left) and after (right) Ensure infusion. **d.** Mean traces (left) and summary plot (right) showing increased DA release in BLA during infusion of glucose compared to non-caloric mannitol. **e.** Transit time for water and Ensure through internal catheters, showing a delay of 12±1 seconds for water to reach the stomach, and 21±1 seconds for Ensure. **f.** Example recordings with fitted sigmoid curves to estimate 5% rise time ($T_{5\%}$), shown by yellow arrow. The blue arrow indicates the timepoint that the signal rises 3σ above baseline ($T_{3\sigma}$, blue arrow). **g.** Summary plots showing dopamine rise times relative to onset of infusion. Subtracting Ensure transit time (in e), we can calculate rise times relative to stomach entry for $T_{5\%}$ and $T_{3\sigma}$ as 54±9 seconds and 41±12 seconds respectively (averaging these values gives a rise time of 48±11 seconds, as reported in the results). **h.** Example recordings with fitted sigmoid curves to estimate 95% decay time ($T_{95\%}$), shown by yellow arrow. The blue arrow indicates the timepoint that the signal falls below 3σ above final value ($T_{3\sigma}$, blue arrow). **i.** Summary plots showing dopamine decay times relative to onset of infusion. Subtracting the time of infusion end, we calculate $T_{95\%}$ and $T_{3\sigma}$ as 749±51 seconds and 388±100 seconds respectively (averaging these values gives a decay time of 569±79 seconds, reported in the results as minutes). **j.** Recording DA release in NAc core. Dotted lines show anterior commissure. Scale bar, 0.5 mm. **k.** Mean traces (left) and summary plots during (middle) and after (right) infusion of Ensure or water show no change in DA release in NAc. **l.** Recording DA release in DLS. Dotted lines show corpus callosum. Scale bar, 0.5 mm. **m.** Mean traces (left) and summary plots during (middle) and after (right) infusion of Ensure or water show no significant change in DA release in DLS. **n.** Reconstructed placements of fibers used for imaging BLA and lateral BLA, with color scale indicating ΔF/F during Ensure IG. Mean coronal slice shown, with dotted lines around parvocellular (lateral) and magnocellular (medial) subregions, showing greater DA release in magnocellular BLA. **o.** Recording DA release in lateral BLA. Dotted lines show external capsule. Scale bar, 0.5 mm. **p.** Mean traces (left) and summary plots during (middle) and after (right) infusion show increased DA release in lateral BLA during but not after infusion of Ensure compared to water. **q.** Mean traces (left) and summary plot showing no difference in DA release in lateral BLA during infusion of glucose compared to non-caloric mannitol. ns.P>0.05, *P<0.05, **P<0.01, ***P<0.001. See Extended Data Table 2.

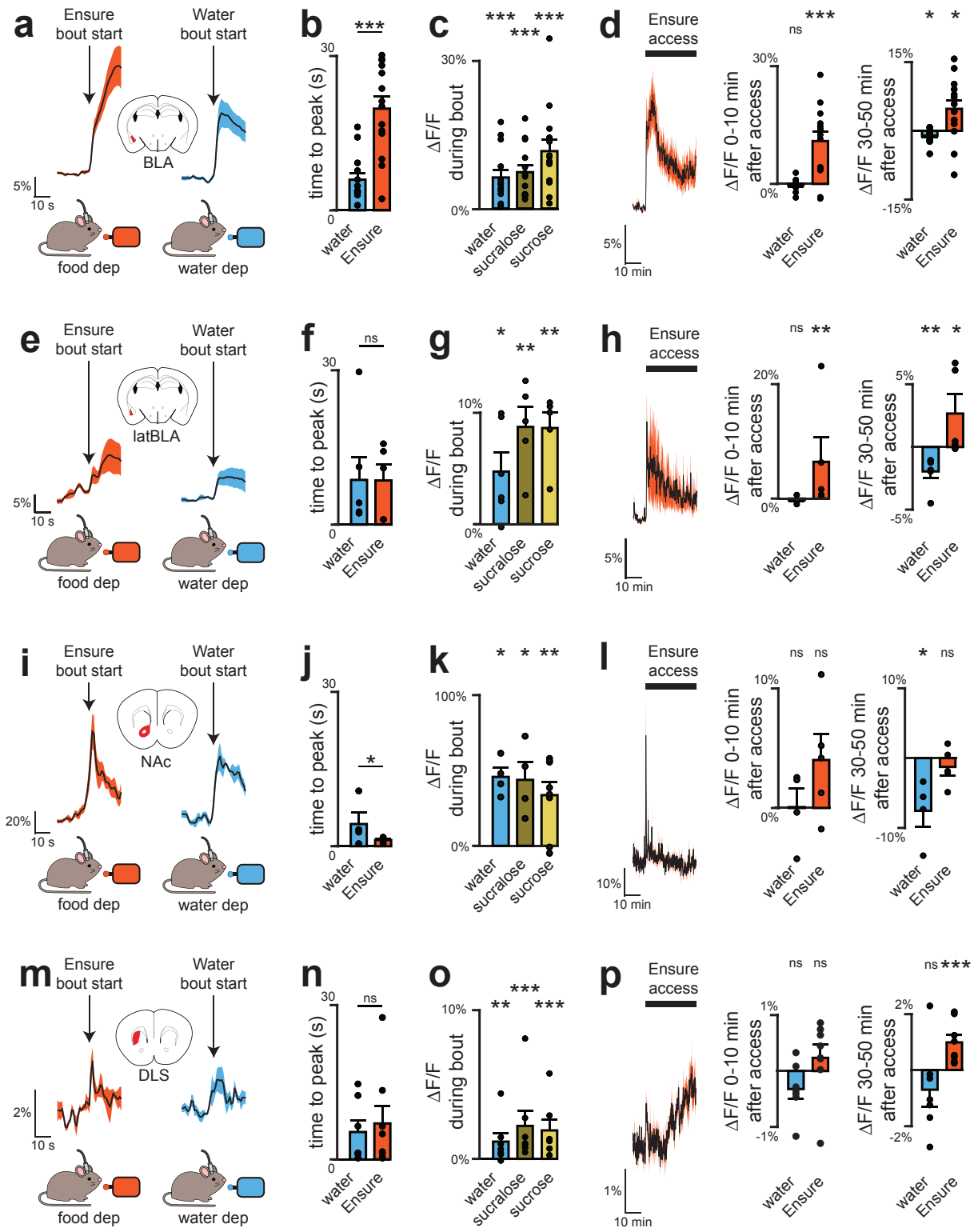

Extended Data Figure 2. Dopamine dynamics across brain regions during natural consumption. a. Recording DA release (using GRAB-DA) in BLA during the first lick bout of Ensure (left) and water (right). **b.** Summary plot showing BLA dopamine peak time is later following the first lick bout of Ensure compared to water. **c.** Summary plots of DA release during first lick bouts. **d.** Mean trace of DA release during Ensure access (left) and summary plots (middle, right) showing DA increases in BLA at various time points during consumption of Ensure. **e.** Recording DA release in lateral BLA during the first lick bout of Ensure (left) and water (right). **f.** Summary plot showing lateral BLA dopamine peak time. **g.** Summary plots of DA release during first lick bouts. **h.** Mean trace of DA release during Ensure access (left) and summary plots (middle, right) showing DA increases in lateral BLA at various time points during consumption of Ensure. **i.** Recording DA release in NAc during the first lick bout of Ensure (left) and water (right). **j.** Summary plot showing NAc dopamine peak time. **k.** Summary plots of DA release during first lick bouts. **l.** Mean trace of DA release during Ensure access (left) and summary plots (middle, right) showing DA increases in NAc at various time points during consumption of Ensure. **m.** Recording DA release in DS during the first lick bout of Ensure (left) and water (right). **n.** Summary plot showing DS dopamine peak time. **o.** Summary plots of DA release during first lick bouts. **p.** Mean trace of DA release during Ensure access (left) and summary plots (middle, right) showing DA increases in DS at various time points during consumption of Ensure. ns.P>0.05, *P<0.05, **P<0.01, ***P<0.001. See Extended Data Table 2.

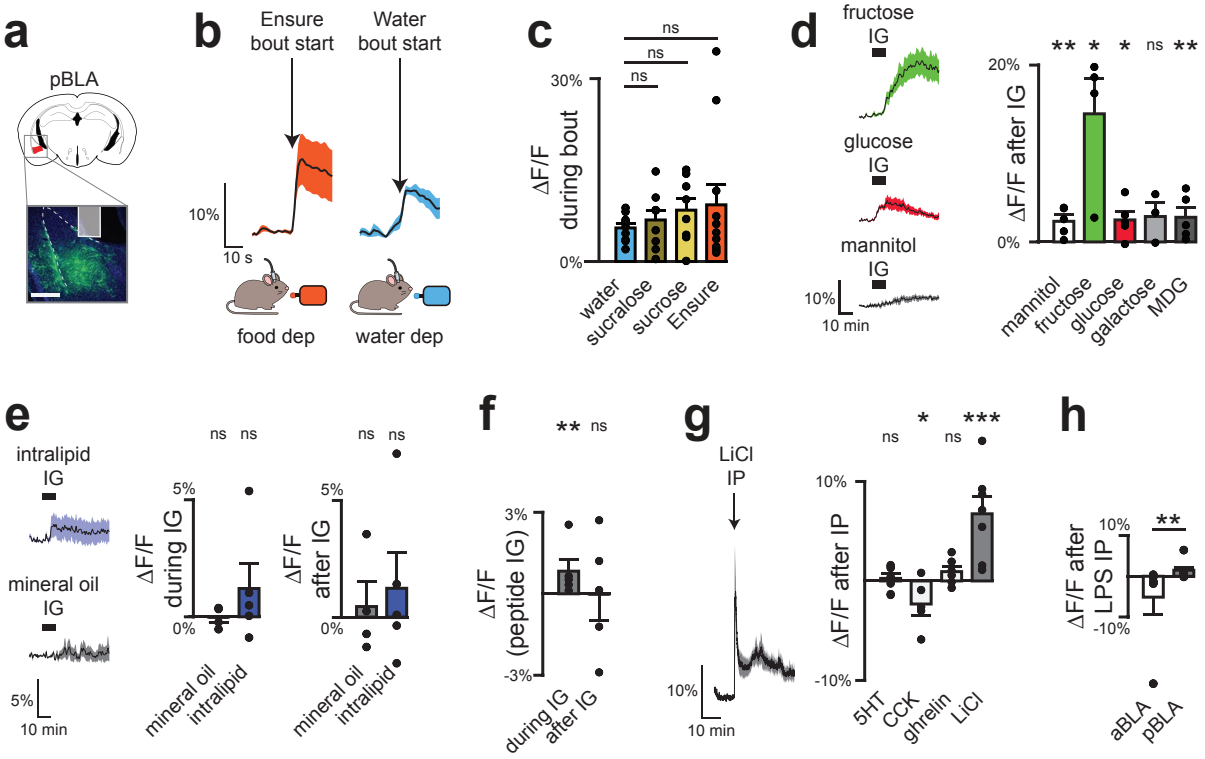

Extended Data Figure 3. Dopamine release in pBLA does not depend on nutrients. a. Recording DA release (using GRAB-DA) in posterior BLA. Dotted lines show external capsule. Scale bar, 0.5 mm. **b.** DA dynamics during first lick bout of water and Ensure. **c.** Summary plot showing no difference in DA release during bouts of water compared to nutrients. **d.** (Left) Mean traces during IG infusion of sugars, (right) alongside summary plot showing increased DA release after sugar infusion independent of SGLT1 activity. **e.** (Left) Mean traces during IG infusion of fats, (right) alongside summary plots showing no increased DA release after nutritive or non-nutritive fats. **f.** Summary plot showing small but significant DA release during peptide infusion. **g.** (Left) Mean trace during IP infusion of LiCl, (right) alongside summary plots showing no DA release in response to feeding hormones, but significant release following aversive LiCl. **h.** Summary plot showing increased pBLA DA and decreased aBLA DA following aversive LPS injection. ns.P>0.05, *P<0.05, **P<0.01, ***P<0.001. See Extended Data Table 2.

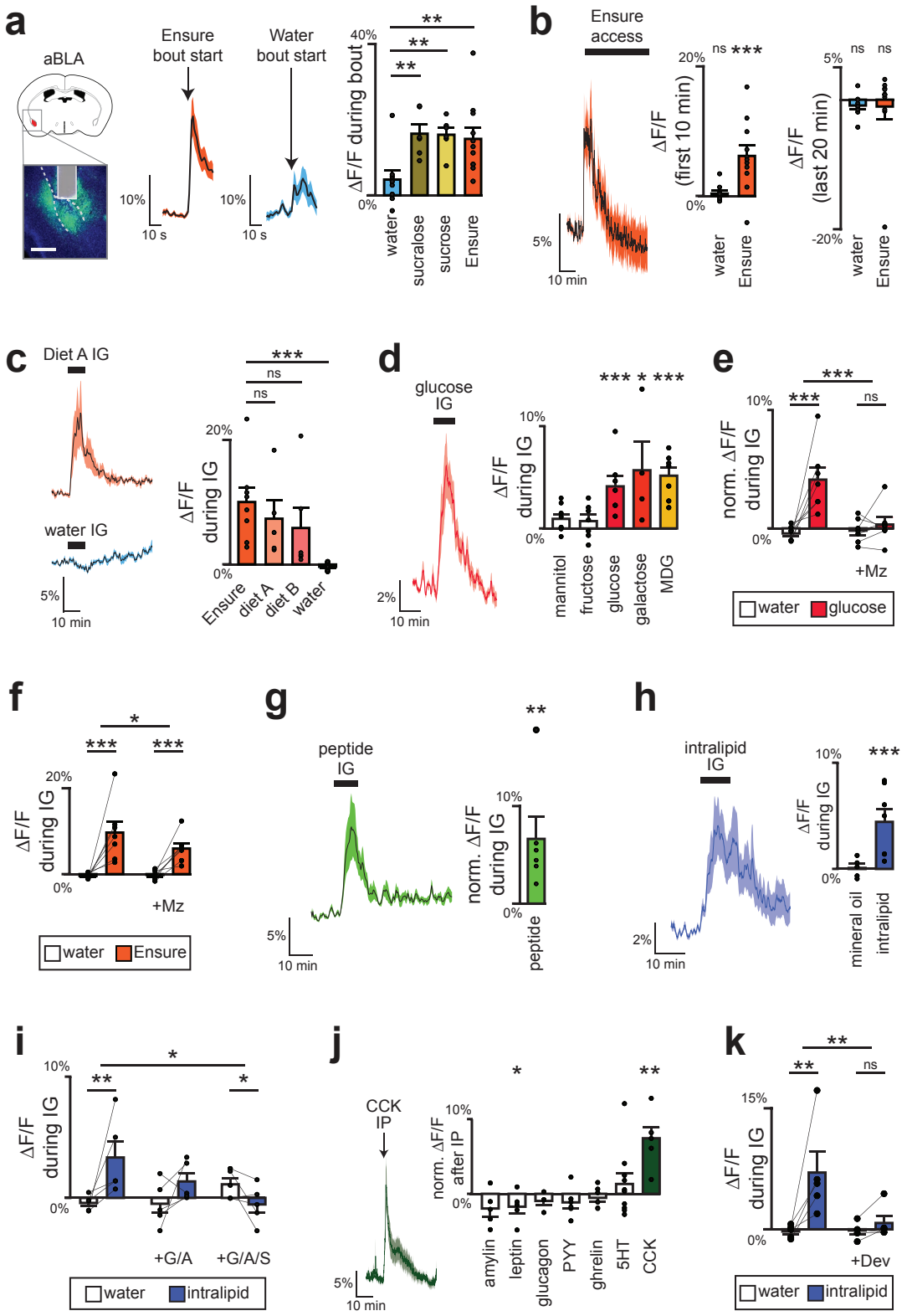

Extended Data Figure 4. Specific nutrients drive aBLA dopamine release. **a.** (Left) Recording DA release (using GRAB-DA) in anterior BLA. Dotted lines show external capsule. Scale bar, 0.5 mm. (Middle) Dopamine dynamics during first lick bout of water and Ensure. (Right) Summary plot showing increased DA release during bouts of sweet solutions compared to water. **b.** (Left) Dopamine dynamics throughout Ensure access, (right) alongside summary plots of release at different timepoints after access was given. **c.** (Left) Dopamine dynamics in response to different calorie-matched liquid diets, (right) alongside summary plots. The sugar/fat/protein composition of diet A is matched to Ensure (55%/14%/31% by calories); whereas the composition of diet B is matched to the preferred diet of mice (20%/20%/60% by calories). **d.** (Left) Dopamine dynamics during glucose IG, (right) alongside summary plot of responses to different sugars and analogs. **e.** Summary plot of dopamine response during water or glucose IG, with and without co-infused SGLT1 antagonist mizaglifozin (Mz). **f.** Summary plot of dopamine response during water or Ensure IG, with and without co-infused SGLT1 antagonist mizaglifozin (Mz). **g.** (Left) Dopamine dynamics during peptide IG, (right) alongside summary plot of dopamine response. **h.** (Left) Dopamine dynamics during intralipid IG, (right) alongsdie summary plot of responses during infusion of intralipid or non-nutritive mineral oil. **i.** Summary plot of dopamine response during water or intralipid IG, with and without co-infused GPR40 antagonist GW1100 (G), GPR120 antagonist AH7614 (A), and CD36 antagonist sulfosuccinimidyl oleate (S). **j.** (Left) Dopamine dynamics during intraperitoneal (IP) injection of CCK, (right) alongside summary plots of release during various injections. **k.** Summary plot of release during water or intralipid IG, with and without prior injection of CCK antagonist devazepide (Dev). ns.P>0.05, *P<0.05, **P<0.01, ***P<0.001. See Extended Data Table 2.

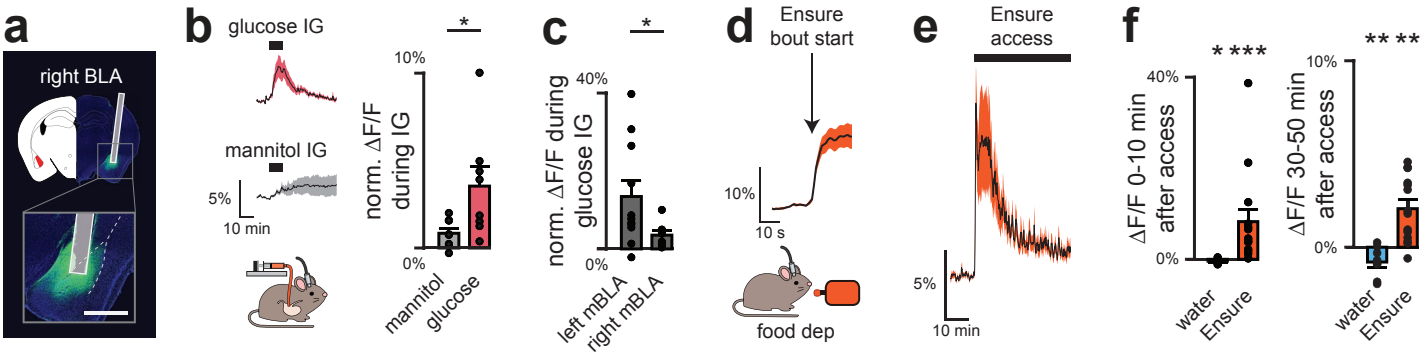

Extended Data Figure 5. Lateralization of BLA dopamine release. a. Recording DA release in right BLA (with GRAB-DA). Dotted line shows external capsule. Scale bar, 1 mm. **b.** Mean traces (left) and summary plots (right) showing increased DA release in right BLA during infusion of glucose compared to non-caloric mannitol. **c.** Summary plot showing increased DA release during glucose infusion in left BLA compared to right BLA. **d.** Mean trace showing DA release in right BLA during the first bout of Ensure consumption. **e.** Mean trace of DA release in right BLA throughout Ensure consumption. **f.** Summary plots showing increased DA release in rightBLA at various time points during consumption of Ensure compared to water consumption. ns.P>0.05, *P<0.05, **P<0.01, ***P<0.001. See Extended Data Table 2.

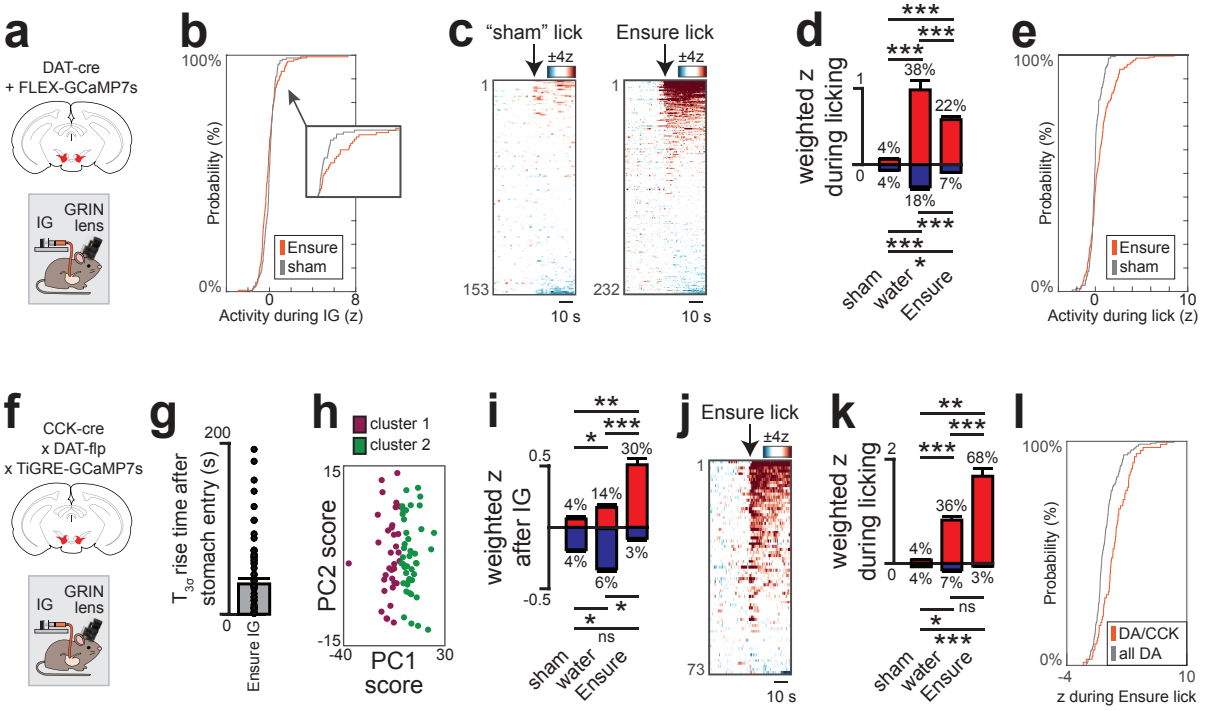

Extended Figure 6. Subpopulation responses across different stages of ingestion. a. Single-cell imaging of all VTA-DA neurons during Ensure IG. **b.** Cumulative distribution plot showing greater activation during infusion of Ensure compared to sham in a small VTA-DA subpopulation (p=0.018, KS test). **c.** Individual VTA-DA neuron dynamics during sham (left) and Ensure consumption (right). **d.** Population-weighted VTA-DA neuron activity (see Methods) during the first bout of consumption. **e.** Cumulative distribution plot showing greater activation during the first bout of Ensure consumption comapred to sham in VTA-DA neurons (p=2.6e-6, KS test). **f.** Single-cell imaging of the VTA-DA/CCK subpopulation during Ensure IG. **g.** VTA-DA/CCK neuron activity rise time relative to adjusted onset of infusion, using $T_{3\sigma}$ method (activity rises 35.5±6.9 seconds after Ensure reaches the stomach, compare to DA rise time calculated using the same method to be 41±12 seconds; see Methods). **h.** PC scores for each neuron, showing k-means separated clusters along PC1.**i.** Population-weighted VTA-DA/CCK neuron activity showing increased activation after infusion of Ensure compared to water or sham. **j.** Individual VTA-DA/CCK neuron dynamics during Ensure consumption. **k.** Population-weighted VTA-DA/CCK neuron activity, showing increased activation during the first bout of consumption of Ensure compared to water or sham. **l.** Cumulative distribution plot showing greater activation during the first bout of Ensure consumption in VTA-DA/CCK neurons, compared to all VTA-DA neurons (p=0.0005, KS test). ns>0.05, *P < 0.05, **P < 0.01, ***P < 0.001, ****P < 0.0001. See Extended Data Table 3.

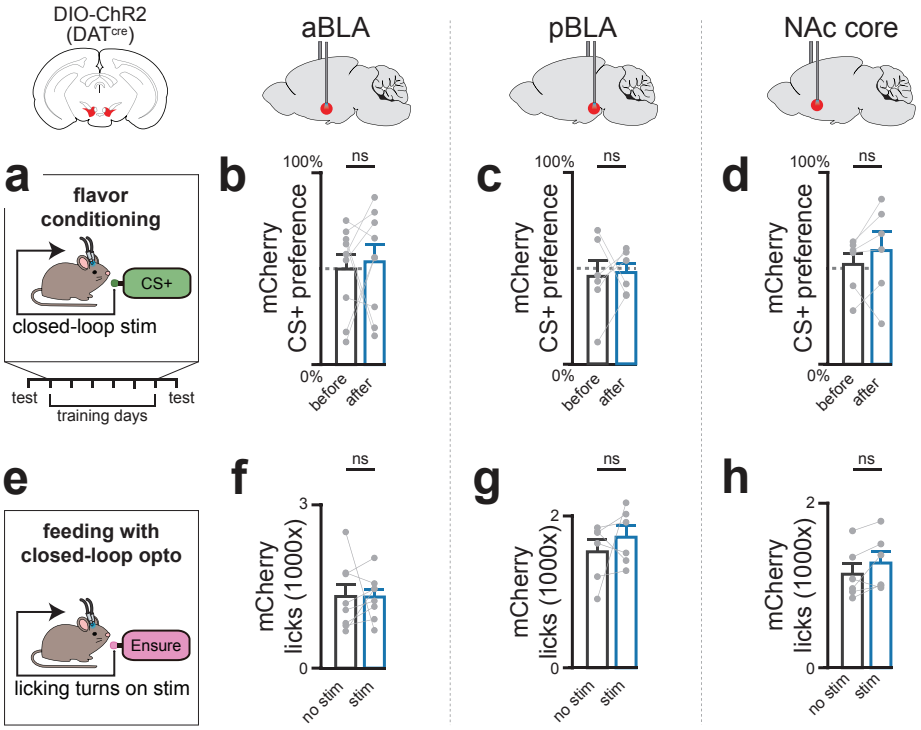

Extended Data Figure 7. Controls for dopamine projection experiments. (Top) Schematic for activation of VTA-DA terminals in aBLA, pBLA, or NAc, using the excitatory opsin ChR2 (with mCherry controls). **a–d.** Flavor-stimulation assay (Fig. 3a–d) with mCherry controls. For visual presentation, bars are filled only in tests with significant effects. **e–h.** Feeding assay, where each lick triggers terminal stimulation (Fig. 3e–h) with mCherry controls. *P < 0.05, **P < 0.01, ***P < 0.001, after Benjamini-Hochberg correction for multiple comparisons (see Extended Data Table 1).

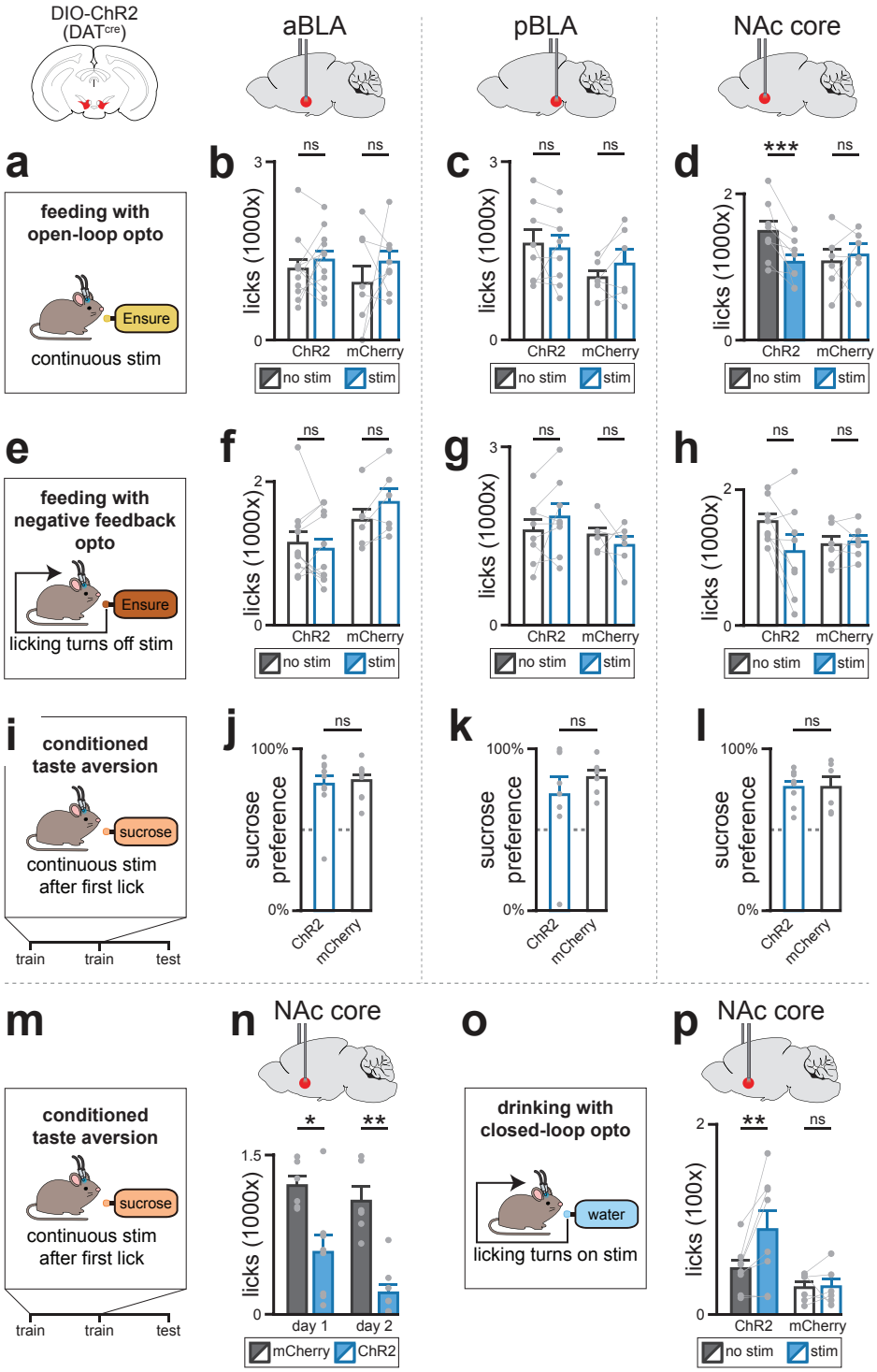

Extended Data Figure 8. Temporally-precise effects of NAc projection on feeding. (Top) Schematic for activation of VTA-DA terminals in aBLA, pBLA, or NAc, using the excitatory opsin ChR2 (with mCherry controls). **a.** Schematic for feeding assay, with continuous terminal stimulation. Different flavors of Ensure (vanilla, chocolate, and strawberry) were used in the feeding assays here (i–l), in m–p, and in Fig. 3e–h, as shown by the different solution colors. **b–d.** Mice consume less Ensure with continuous stimulation of terminals in NAc, but not in either BLA subregion. **e.** Schematic for feeding assay, where each lick turns off otherwise continuous terminal stimulation. **f–h.** No significant effect of this stimulation protocol on consumption. **i.** Schematic for conditioned taste aversion assay, where consumption of a novel sucrose solution triggers terminal stimulation with a delay of 20s until the end of the training session. Conditioning of taste avoidance is tested using a two-bottle test against water after training. **j–l.** Stimulation of these terminals does not condition taste aversion. **m–n.** Stimulation of terminals in NAc decreased sucrose intake during conditioned taste aversion training. **o.** Schematic for drinking assay, where each lick triggers terminal stimulation. **p.** Mice consume more water when paired with stimulation of of terminals NAc. *P < 0.05, **P < 0.01, ***P < 0.001, after Benjamini-Hochberg correction for multiple comparisons (see Extended Data Table 1).

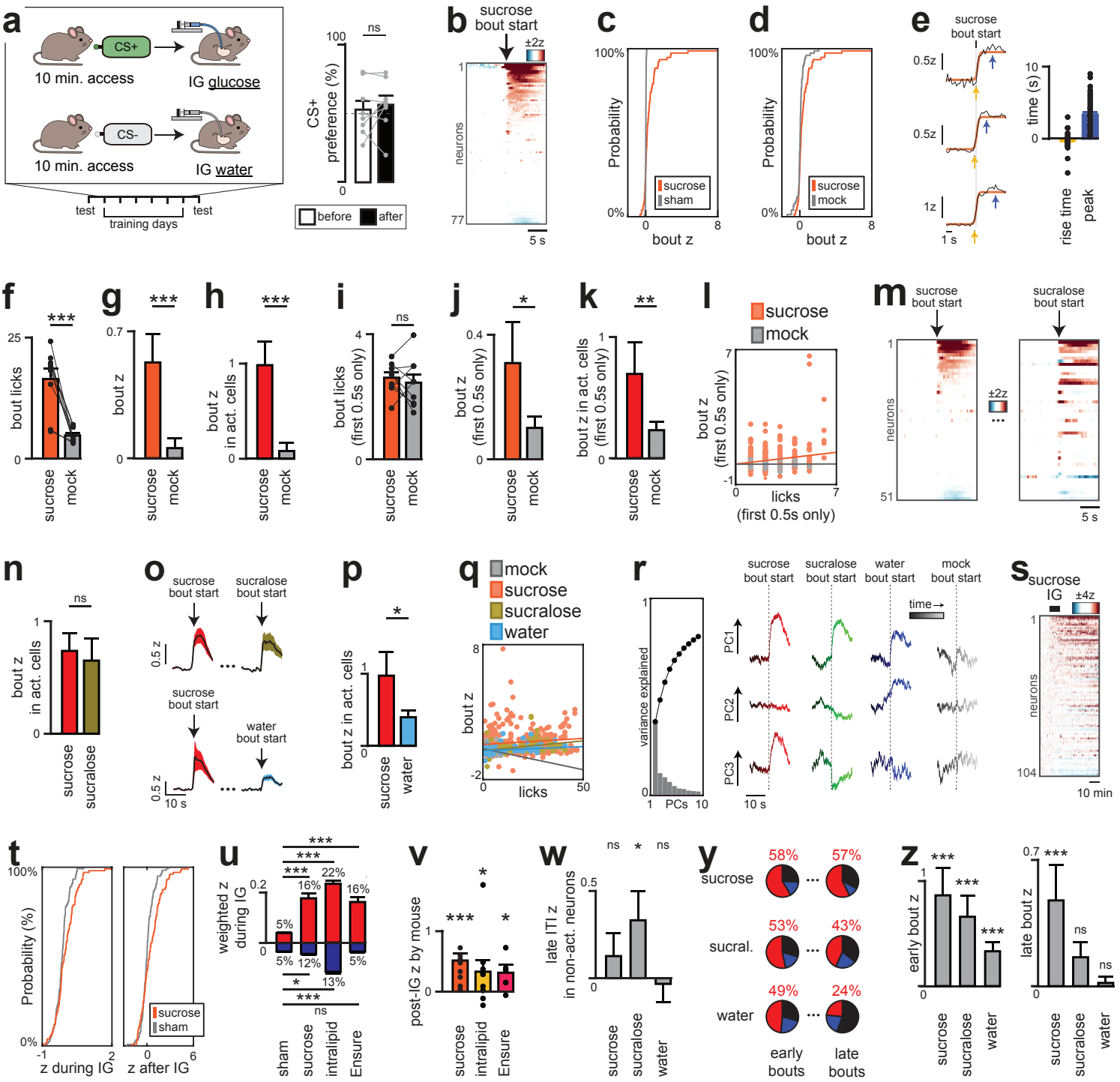

Extended Figure 9. aBLA neurons track nutrient ingestion. a. (Left) Protocol for delayed flavor-nutrient conditioning. Mice are given 10 minute access to a flavored saccharin solution, after which water or glucose is infused intragastrically. (Right) Mice do not learn to prefer glucose-paired flavor if IG is exclusively given after ingestion ceases **b.** aBLA neuron dynamics averaged across sucrose bouts, shown using z-score. **c.** Distribution of aBLA neuron activity during bouts with sucrose delivery compared to "sham" bouts (p=6.7e-15, KS test). See Methods for creation of "sham" dataset. **d.** Distribution of aBLA neuron activity during sucrose and mock lick bouts (p=0.005, KS test). **e.** Time of peak response (blue) and 5% rise time (yellow), shown with example cells (left) and summary plots (right). **f.** Lick count averaged across mice. **g.** Activity averaged across trials. **h.** Activity of sucrose-activated cells averaged across trials. **i.** Lick count during the first 0.5 seconds of lick bouts averaged across mice. **j.** Activity during the first 0.5 seconds of lick bouts averaged across trials. **k.** Activity of sucrose-activated cells during the first 0.5 seconds oflick bouts averaged across trials. **l.** Correlation plot of activity and lick count during the first 0.5 seconds of sucrose and mock lick bouts (sucrose: R^2=0.030, p=0.0017; mock: R^2=0.00014, p=0.95). **m.** Cross-registered neuron dynamics during sucrose trials (left) and sucralose trials (right). **n.** Activity of sucrose-activated cells during sucrose and sucralose trials. **o.** Mean dynamics of cross-registered sucrose-activated neurons during sucrose vs. sucralose bouts (top) or during sucrose vs. water bouts (bottom). **p.** Activity of sucrose-activated cells during sucrose and water trials. **q.** Correlation plot of activity and lick count during mock, sucrose, sucralose, and water lick bouts (mock: R^2=0.062, p=0.21; sucrose: R^2=0.018, p=0.016; sucralose: R^2=0.17, p=1e-7; water: R^2=0.076, p=0.0089). **r.** (Left) Scree plot for principal component analysis (PCA) of bout activity of neurons cross-registered across sucrose, sucralose, and water sessions. (Right) First three PCs during each bout. **s.** Single-neuron dynamics during sucrose IG infusion. **t.** (Left) Distribution of aBLA neuron activity during sucrose IG infusion compared to sham infusion (p=0.002, KS test). (Right) Distribution of aBLA neuron activity after sucrose IG infusion compared to sham infusion (p=0.002, KS test). **u.** Population-weighted z-score of activity during IG infusions. **v.** Summary plot of aBLA activity after IG infusions averaged by mouse. **w.** Summary plots of trial 25–50 ITI activity of neurons not activated during licking. **y.** Pie charts showing distribution of aBLA neurons activated (in red), inhibited (in blue), and unchanged (in black) during early vs late bouts. Percent neurons activated is given in red above each pie chart. **z.** (Left) Activity traces from example neurons during early (2–6) and late bouts (last 5) of sucrose consumption. (Right) Summary plots of activity from all neurons during early and late bouts. ns.P>0.05, *P<0.05, **P<0.01, ***P<0.001. See Extended Data Table 3.

Manipulation	Experiment	Cohort	Test	Comparison	Statistics	n	i	m	p	p'
n/a	Flavor conditioning, 2 bottle test	WT	perm. (1-sided, paired)	pre vs. post	35.2±5.3 vs. 81.3±6.7%	8			7.77E-05	
VTA-DA inhibition	Flavor conditioning, 2 bottle test	control	perm. (1-sided, paired)	pre vs. post	53.7±4.8 vs. 81.1±3.0%	11			**1.00E-05**	
VTA-DA inhibition	Flavor conditioning, 2 bottle test	GtACR	perm. (1-sided, paired)	pre vs. post	48.5±6.9 vs. 53.4±7.4%	10			3.14E-01	
VTA-DA inhibition	Flavor conditioning, 2 bottle test		perm. (2-sided)	control vs. GtACR	27.3±5.3 vs. 5.0±9.0 Δ%	11, 10			**1.97E-02**	
VTA-DA inhibition	Flavor conditioning, CS- day 1		perm. (2-sided)	control vs. GtACR	977.1±200.7 vs. 782.4±135.7 licks	11, 10			4.34E-01	
VTA-DA inhibition	Flavor conditioning, CS+ day 1		perm. (2-sided)	control vs. GtACR	1396.4±131.3 vs. 927.4±122.7 licks	11, 10			**1.90E-02**	
VTA-DA inhibition	Ensure licks, continuous laser	control	perm. (2-sided, paired)	control vs. stim	484.2±51.5 vs. 458±37.3 licks	13			6.66E-01	
VTA-DA inhibition	Ensure licks, continuous laser	GtACR	perm. (2-sided, paired)	control vs. stim	322.9±47.2 vs. 422.3±84.6 licks	6			4.08E-01	
VTA-DA inhibition	Ensure licks, continuous laser	GtACR	perm. (2-sided)	control vs. GtACR	-26.2±58.9 vs. 99.4±113 Δlicks	6, 13			3.69E-01	
VTA-DA inhibition	CTA, 2-bottle test	GtACR	perm. (2-sided)	control vs. GtACR	17.3±8.5 vs 14.4±8.9%	9, 6			5.86E-01	
VTA-DA→aBLA excitation	Flavor conditioning, 2 bottle test	mCherry	perm. (1-sided, paired)	pre vs. post	49.8±7.7 vs 53.6±8.8%	9	5	6	3.74E-01	4.48E-01
VTA-DA→aBLA excitation	Flavor conditioning, 2 bottle test	ChR2	perm. (1-sided, paired)	pre vs. post	34.3±8.7 vs 71.5±8.8%	7	1	6	**2.91E-04**	**1.75E-03**
VTA-DA→pBLA excitation	Flavor conditioning, 2 bottle test	mCherry	perm. (1-sided, paired)	pre vs. post	45.6±8.5 vs. 47.6±4.6%	6	6	6	4.06E-01	4.06E-01
VTA-DA→pBLA excitation	Flavor conditioning, 2 bottle test	ChR2	perm. (1-sided, paired)	pre vs. post	52.1±6 vs. 61.4±5.8%	8	2	6	1.40E-01	4.19E-01
VTA-DA→NAc excitation	Flavor conditioning, 2 bottle test	mCherry	perm. (1-sided, paired)	pre vs. post	52±5.9 vs. 59.3±9.8%	6	3	6	1.37E-01	2.75E-01
VTA-DA→NAc excitation	Flavor conditioning, 2 bottle test	ChR2	perm. (1-sided, paired)	pre vs. post	40.4±6.8 vs. 47.1±8.7%	8	4	6	2.55E-01	3.82E-01
VTA-DA→aBLA excitation	Ensure licks, continuous laser	mCherry	perm. (2-sided, paired)	control vs. stim	955.7±289.2 vs 1313±186.3 licks	8	3	6	3.97E-01	7.93E-01
VTA-DA→aBLA excitation	Ensure licks, continuous laser	ChR2	perm. (2-sided, paired)	control vs. stim	1194.5±163.8 vs 1346.3±155.8 licks	11	4	6	3.95E-01	5.93E-01
VTA-DA→pBLA excitation	Ensure licks, continuous laser	mCherry	perm. (2-sided, paired)	control vs. stim	1046.8±120.5 vs. 1276.4±248.8 licks	6	2	6	1.78E-01	5.35E-01
VTA-DA→pBLA excitation	Ensure licks, continuous laser	ChR2	perm. (2-sided, paired)	control vs. stim	1612.1±237.1 vs. 1533.1±222 licks	8	5	6	5.52E-01	6.62E-01
VTA-DA→NAc excitation	Ensure licks, continuous laser	mCherry	perm. (2-sided, paired)	control vs. stim	1071.2±165.9 vs. 1164.3±154 licks	6	6	6	5.72E-01	5.72E-01
VTA-DA→NAc excitation	Ensure licks, continuous laser	ChR2	perm. (2-sided, paired)	control vs. stim	1487.2±142.3 vs. 1065.4±106.1 licks	8	1	6	7.77E-05	**4.66E-04**
VTA-DA→aBLA excitation	Ensure licks, closed loop laser	mCherry	perm. (2-sided, paired)	control vs. stim	1316.3±222.4 vs. 1306.6±146.2 licks	8	6	6	9.95E-01	9.95E-01
VTA-DA→aBLA excitation	Ensure licks, closed loop laser	ChR2	perm. (2-sided, paired)	control vs. stim	1213.7±123.3 vs. 1277.3±179.5 licks	10	5	6	7.84E-01	9.41E-01
VTA-DA→pBLA excitation	Ensure licks, closed loop laser	mCherry	perm. (2-sided, paired)	control vs. stim	1528.1±157.2 vs. 1720.2±149.4 licks	6	4	6	5.91E-01	8.87E-01
VTA-DA→pBLA excitation	Ensure licks, closed loop laser	ChR2	perm. (2-sided, paired)	control vs. stim	1380.1±221.3 vs. 1533.7±200.8 licks	8	3	6	4.31E-01	8.62E-01
VTA-DA→NAc excitation	Ensure licks, closed loop laser	mCherry	perm. (2-sided, paired)	control vs. stim	1136.9±127.1 vs. 1272.9±136.3 licks	6	2	6	4.65E-02	1.39E-01
VTA-DA→NAc excitation	Ensure licks, closed loop laser	ChR2	perm. (2-sided, paired)	control vs. stim	1148.9±181.4 vs. 1464.5±144 licks	8	1	6	7.77E-05	**4.66E-04**
VTA-DA→aBLA excitation	Ensure licks, neg. feedback laser	mCherry	perm. (2-sided, paired)	control vs. stim	1461.5±159.6 vs. 1710.9±188.7 licks	6	2	6	4.65E-02	1.39E-01
VTA-DA→aBLA excitation	Ensure licks, neg. feedback laser	ChR2	perm. (2-sided, paired)	control vs. stim	1142.5±155.9 vs. 1058.4±146.1 licks	11	5	6	5.23E-01	6.27E-01
VTA-DA→pBLA excitation	Ensure licks, neg. feedback laser	mCherry	perm. (2-sided, paired)	control vs. stim	1516±116.5 vs. 1341.6±146.7 licks	6	4	6	3.19E-01	4.78E-01
VTA-DA→pBLA excitation	Ensure licks, neg. feedback laser	ChR2	perm. (2-sided, paired)	control vs. stim	1586±193.1 vs. 1819.2±227.7 licks	8	3	6	1.81E-01	3.62E-01
VTA-DA→NAc excitation	Ensure licks, neg. feedback laser	mCherry	perm. (2-sided, paired)	control vs. stim	1190±127.8 vs. 1230.6±101.8 licks	6	6	6	6.48E-01	6.48E-01
VTA-DA→NAc excitation	Ensure licks, neg. feedback laser	ChR2	perm. (2-sided, paired)	control vs. stim	1529.9±113.8 vs. 1088.4±244.9 licks	8	1	6	2.43E-02	1.46E-01
VTA-DA→aBLA excitation	CTA, 2-bottle test		perm. (1-sided)	mCherry vs. ChR2	80.4±3.8 vs. 78.2±5.1%	9, 11	2	3	4.01E-01	6.01E-01
VTA-DA→pBLA excitation	CTA, 2-bottle test		perm. (1-sided)	mCherry vs. ChR2	82.2±4.6 vs. 71.7±11.2%	6, 8	1	3	2.64E-01	7.91E-01
VTA-DA→NAc excitation	CTA, 2-bottle test		perm. (1-sided)	mCherry vs. ChR2	76.2±6.3 vs. 76.2±3.9%	6, 8	3	3	5.01E-01	5.01E-01
VTA-DA→aBLA excitation	CTA, day 1		perm. (2-sided)	mCherry vs. ChR2	337.1±145 vs. 416.5±109.5 licks	9, 11	3	3	6.54E-01	6.54E-01
VTA-DA→pBLA excitation	CTA, day 1		perm. (2-sided)	mCherry vs. ChR2	349.2±66.5 vs. 187.4±45 licks	6, 8	2	3	5.86E-02	8.79E-02
VTA-DA→NAc excitation	CTA, day 1		perm. (2-sided)	mCherry vs. ChR2	1212.2±89.3 vs. 584±165.5 licks	6, 8	1	3	1.53E-02	**4.59E-02**
VTA-DA→aBLA excitation	CTA, day 2		perm. (2-sided)	mCherry vs. ChR2	793.9±186.6 vs. 521.3±212.3	9, 11	2	3	3.84E-01	5.76E-01
VTA-DA→pBLA excitation	CTA, day 2		perm. (2-sided)	mCherry vs. ChR2	455.8±140.1 vs. 286.3±138.5 licks	6, 8	3	3	4.19E-01	4.19E-01
VTA-DA→NAc excitation	CTA, day 2		perm. (2-sided)	mCherry vs. ChR2	1065.8±135.2 vs. 202±81.8 licks	6, 8	1	3	6.66E-04	**2.00E-03**
VTA-DA→aBLA excitation	self-stimulation, test		perm. (1-sided)	mCherry vs. ChR2	42±25 vs. 38.7±15.9 'presses	6, 11	2	3	5.50E-01	8.25E-01
VTA-DA→pBLA excitation	self-stimulation, test		perm. (1-sided)	mCherry vs. ChR2	43.6±12.2 vs. 32.3±18 'presses	6, 8	3	3	7.00E-01	7.00E-01
VTA-DA→NAc excitation	self-stimulation, test		perm. (1-sided)	mCherry vs. ChR2	262.9±49.2 vs. 19.8±10.6 'presses	6, 7	1	3	2.33E-03	**6.99E-03**
VTA-DA→NAc excitation	water licks, closed loop laser	mCherry	perm. (2-sided, paired)	control vs. stim	48.3±8.6 vs. 89.4±20.1 licks	8			**1.32E-03**	
VTA-DA→NAc excitation	water licks, closed loop laser	ChR2	perm. (2-sided, paired)	control vs. stim	28.3±6.1 vs. 29.3±8.3 licks	6			8.77E-01	
n/a	bout licks within 5 seconds	aBLA	perm. (2-sided, paired)	mock vs. sucrose	4.8±0.5 vs. 16.5±2.2 licks	9			**2.06E-05**	
n/a	bout licks within 0.5 seconds	aBLA	perm. (2-sided, paired)	mock vs. sucrose	2.5±0.3 vs. 2.6±0.2 licks	9			5.55E-01	
aBLA-D1R inhibition	Flavor conditioning, 2 bottle test	control	perm. (1-sided, paired)	pre vs. post	45.8±4.7 vs. 69.2±6.5%	14			**2.46E-03**	
aBLA-D1R inhibition	Flavor conditioning, 2 bottle test	GtACR	perm. (1-sided, paired)	pre vs. post	52.4±7.2 vs. 49.4±9.9%	8			6.02E-01	
aBLA-D1R inhibition	Flavor conditioning, 2 bottle test		perm. (2-sided)	control vs. GtACR	23.4±7.6 vs. -3±10.9 Δ%	14, 8			**2.90E-02**	
aBLA-D1R inhibition	Flavor conditioning, CS- day 1		perm. (2-sided)	control vs. GtACR	1263.5±198.6 vs. 845±226.6 licks	14, 8			1.97E-01	
aBLA-D1R inhibition	Flavor conditioning, CS+ day 1		perm. (2-sided)	control vs. GtACR	1522.6±110.3 vs. 418.1±216.8 licks	14, 8			**1.50E-04**	
aBLA-D1R inhibition	Ensure licks, continuous laser	control	perm. (2-sided, paired)	control vs. stim	2207.2±241.4 vs. 1876.1±155.6 licks	14			1.07E-01	
aBLA-D1R inhibition	Ensure licks, continuous laser	GtACR	perm. (2-sided, paired)	control vs. stim	2577.9±154 vs. 2186.1±251 licks	8			1.37E-01	
aBLA-D1R inhibition	Ensure licks, continuous laser	GtACR	perm. (2-sided)	control vs. GtACR	-331.1±197.5 vs. -391.8±279.3 Δlicks	14, 8			2.12E-01	
aBLA-D1R inhibition	CTA, 2-bottle test	GtACR	perm. (2-sided)	control vs. GtACR	15.2±7.3 vs. 36.4±10.9%	13, 8			5.82E-02	

Extended Data Table 1. Behavior statistics. Summary information for all behavioral tests for each manipulation. Values are reported to 1 decimal place. P-values are reported for all statistical tests, and are shown in bold if below standard significance level (α=0.05). In cases where a Benjamini-Hochberg correction was made for multiple comparisons, an adjusted p-value (p') is shown (where p'=p*m/i, where i is rank and m is number of cohorts tested; see Methods). X' corresponds to the normalized value of X. For self-stimulation, 'presses means the number of inactive lever presses have been subtracted from the number of active lever presses. Permutation (perm.) tests use an exact test (or 100,000 iterations if n>9) and are unpaired, unless otherwise mentioned (note: this means the lowest calculable p is 1E-5).

Area	Experiment	Phase	Test	Comparison	Statistics	n	p
BLA	water drinking	oral	perm. (2-sided, paired)	vs. baseline	6.269±1.466 vs. 0±0 dF'/F'	14	**1.00E-05**
BLA	water drinking	GI	perm. (2-sided, paired)	vs. baseline	-0.287±0.385 vs. 0±0 dF'/F'	14	4.78E-01
BLA	water drinking	post-GI	perm. (2-sided, paired)	vs. baseline	-1.05±0.415 vs. 0±0 dF'/F'	14	**9.58E-03**
BLA	Ensure drinking	oral	perm. (2-sided, paired)	vs. baseline	5.11±0.871 vs. 0±0 dF'/F'	14	**1.00E-05**
BLA	Ensure drinking	oral	perm. (2-sided)	vs. water	5.11±0.871 vs 6.269±1.466 dF'/F'	14, 14	5.06E-01
BLA	Ensure drinking	oral	peak time, perm. (2-sided)	vs. water	19.821±2.352 vs 5.982±1.19 s'	14, 14	**4.00E-05**
BLA	Ensure drinking	GI	perm. (2-sided, paired)	vs. baseline	10.914±2.405 vs. 0±0 dF'/F'	14	**7.00E-05**
BLA	Ensure drinking	GI	perm. (2-sided)	vs. water	10.914±2.405 vs -0.287±0.385 dF'/F'	14,14	**1.40E-04**
BLA	Ensure drinking	post-GI	perm. (2-sided, paired)	vs. baseline	4.804±1.828 vs. 0±0 dF'/F'	14	**1.29E-02**
BLA	Ensure drinking	post-GI	perm. (2-sided)	vs. water	4.804±1.828 vs -1.05±0.415 dF'/F'	14, 14	**3.88E-03**
BLA	sucralose drinking	oral	perm. (2-sided, paired)	vs. baseline	7.345±1.375 vs. 0±0 dF'/F'	14	**1.00E-05**
BLA	sucralose drinking	oral	perm. (2-sided)	vs. water	7.345±1.375 vs 6.269±1.466 dF'/F'	14, 14	5.96E-01
BLA	sucrose drinking	oral	perm. (2-sided, paired)	vs. baseline	11.597±2.259 vs. 0±0 dF'/F'	14	**1.00E-05**
BLA	sucrose drinking	oral	perm. (2-sided)	vs. water	11.597±2.259 vs 6.269±1.46 dF'/F'	14, 14	5.26E-02
BLA	water IG	GI	perm. (2-sided, paired)	vs. sham	-0.010±0.280 vs. 0±0 dF'/F'	12	7.34E-01
BLA	water IG	post-GI	perm. (2-sided, paired)	vs. sham	-0.563±0.484 vs. 0±0 dF'/F'	12	2.88E-01
BLA	Ensure IG	GI	perm. (2-sided, paired)	vs. sham	18.20±3.517 vs. 0±0 dF'/F'	16	**1.00E-05**
BLA	Ensure IG	GI	perm. (2-sided)	vs. water	18.20±3.517 vs. -0.010±0.280 dF'/F'	16, 12	**1.50E-04**
BLA	Ensure IG	GI	rise time (3 sd)	N/A	62.25±11.652 s	16	N/A
BLA	Ensure IG	GI	rise time (sigmoid fit)	N/A	75.25±9.206 s	16	N/A
BLA	Ensure IG	post-GI	perm. (2-sided, paired)	vs. sham	2.397±1.102 vs. 0±0 dF'/F'	16	**7.70E-04**
BLA	Ensure IG	post-GI	perm. (2-sided)	vs. water	2.397±1.102 vs. -0.563±0.484 dF'/F'	16, 12	**7.86E-03**
BLA	Ensure IG	post-GI	fall time (3 sd)	N/A	387.8±99.862 s'	16	N/A
BLA	Ensure IG	post-GI	fall time (sigmoid fit)	N/A	748.2±51.241 s'	16	N/A
BLA	glucose IG	GI	perm. (2-sided, paired)	vs. sham	13.449±4.018 vs. 0±0 dF'/F'	11	**2.30E-04**
BLA	glucose IG	GI	perm. (2-sided)	vs. mannitol	13.449±4.018 vs. 1.811±0.836 dF'/F'	11, 10	**6.81E-03**
BLA	glucose IG	GI	perm. (2-sided)	vs. water	13.449±4.018 vs. -0.010±0.280 dF'/F'	16, 12	**5.00E-05**
BLA	glucose IG	post-GI	perm. (2-sided, paired)	vs. sham	1.609±1.045 vs. 0±0 dF'/F'	11	1.43E-01
BLA	glucose IG	post-GI	perm. (2-sided)	vs. mannitol	1.609±1.045 vs. 1.261±1.565 dF'/F'	11, 10	8.60E-01
BLA	glucose IG	post-GI	perm. (2-sided)	vs. water	1.609±1.045 vs. -0.563±0.486 dF'/F'	16, 12	6.55E-02
BLA	intralipid IG	GI	perm. (2-sided, paired)	vs. sham	6.094±1.704 vs. 0±0 dF'/F'	11	**1.00E-05**
BLA	intralipid IG	GI	perm. (2-sided)	vs. water	6.094±1.704 vs. -0.010±0.280 dF'/F'	11, 12	**1.00E-05**
BLA	intralipid IG	post-GI	perm. (2-sided, paired)	vs. sham	2.323±0.952 vs. 0±0 dF'/F'	11	**1.79E-02**
BLA	intralipid IG	post-GI	perm. (2-sided)	vs. water	2.323±0.952 vs. -0.563±0.484 dF'/F'	11, 12	**8.72E-03**
BLA	mannitol IG	GI	perm. (2-sided, paired)	vs. sham	1.811±0.836 vs. 0±0 dF'/F'	10	**2.80E-02**
BLA	mannitol IG	post-GI	perm. (2-sided, paired)	vs. sham	1.261±1.565 vs. 0±0 dF'/F'	10	5.40E-01
BLA	MDG IG	GI	perm. (2-sided, paired)	vs. sham	17.803±10.452 vs. 0±0 dF'/F'	3	**4.76E-02**
BLA	MDG IG	post-GI	perm. (2-sided, paired)	vs. sham	5.023±0.875 vs. 0±0 dF'/F'	3	**4.76E-02**
BLA	peptide IG	GI	perm. (2-sided, paired)	vs. sham	5.223±2.185 vs. 0±0 dF'/F'	3	**4.76E-02**
BLA	peptide IG	post-GI	perm. (2-sided, paired)	vs. sham	1.767±0.885 vs. 0±0 dF'/F'	3	**4.76E-02**
latBLA	water drinking	oral	perm. (2-sided, paired)	vs. baseline	4.719±1.723 vs. 0±0 dF'/F'	6	**1.41E-02**
latBLA	water drinking	GI	perm. (2-sided, paired)	vs. baseline	-0.276±0.21 vs. 0±0 dF'/F'	6	2.74E-01
latBLA	water drinking	post-GI	perm. (2-sided, paired)	vs. baseline	-1.942±0.529 vs. 0±0 dF'/F'	6	**1.08E-03**
latBLA	Ensure drinking	oral	perm. (2-sided, paired)	vs. baseline	4.432±2.172 vs. 0±0 dF'/F'	5	1.23E-01
latBLA	Ensure drinking	oral	perm. (2-sided)	vs. water	4.432±2.172 vs 4.719±1.723 dF'/F'	5, 6	9.24E-01
latBLA	Ensure drinking	oral	peak time, perm. (2-sided)	vs. water	8.6±3.196 vs 8.708±4.439 s'	5, 6	9.85E-01
latBLA	Ensure drinking	GI	perm. (2-sided, paired)	vs. baseline	6.422±4.318 vs. 0±0 dF'/F'	5	**3.95E-03**
latBLA	Ensure drinking	GI	perm. (2-sided)	vs. water	6.422±4.318 vs -0.276±0.21 dF'/F'	5, 6	**4.32E-03**
latBLA	Ensure drinking	post-GI	perm. (2-sided, paired)	vs. baseline	2.667±1.53 vs. 0±0 dF'/F'	5	**4.35E-02**
latBLA	Ensure drinking	post-GI	perm. (2-sided)	vs. water	2.667±1.53 vs -1.942±0.529 dF'/F'	5, 6	**2.16E-03**
latBLA	sucralose drinking	oral	perm. (2-sided, paired)	vs. baseline	8.732±1.789 vs. 0±0 dF'/F'	5	**3.95E-03**
latBLA	sucralose drinking	oral	perm. (2-sided)	vs. water	8.732±1.789 vs 4.719±1.723 dF'/F'	5, 6	1.47E-01
latBLA	sucrose drinking	oral	perm. (2-sided, paired)	vs. baseline	8.632±1.435 vs. 0±0 dF'/F'	5	**3.95E-03**
latBLA	sucrose drinking	oral	perm. (2-sided)	vs. water	8.632±1.435 vs 4.719±1.723 dF'/F'	5, 6	1.27E-01
latBLA	water IG	GI	perm. (2-sided, paired)	vs. sham	0.247±0.467 vs. 0±0 dF'/F'	9	6.60E-01
latBLA	water IG	post-GI	perm. (2-sided, paired)	vs. sham	1.051±0.644 vs. 0±0 dF'/F'	9	1.63E-01
latBLA	Ensure IG	GI	perm. (2-sided, paired)	vs. sham	2.309±0.750 vs 0±0 dF'/F'	9	**1.87E-03**
latBLA	Ensure IG	GI	perm. (2-sided)	vs. water	2.309±0.750 vs 0.247±0.467 dF'/F'	9, 9	**3.40E-02**
latBLA	Ensure IG	post-GI	perm. (2-sided, paired)	vs. sham	2.070±1.174 vs 0±0 dF'/F'	9	8.05E-02
latBLA	Ensure IG	post-GI	perm. (2-sided)	vs. water	2.070±1.174 vs 1.051±0.644 dF'/F'	9, 9	4.61E-01
latBLA	glucose IG	GI	perm. (2-sided, paired)	vs. sham	2.372±0.648 vs. 0±0 dF'/F'	9	**3.35E-03**
latBLA	glucose IG	GI	perm. (2-sided)	vs. mannitol	2.372±0.648 vs 1.579±0.256 dF'/F'	9, 9	2.78E-01
latBLA	glucose IG	GI	perm. (2-sided)	vs. water	2.372±0.648 vs 0.247±0.467 dF'/F'	9, 9	**1.88E-02**
latBLA	glucose IG	post-GI	perm. (2-sided, paired)	vs. sham	3.438±0.543 vs. 0±0 dF'/F'	9	**2.06E-05**
latBLA	glucose IG	post-GI	perm. (2-sided)	vs. mannitol	3.438±0.543 vs 4.163±0.511 dF'/F'	9, 9	3.47E-01
latBLA	glucose IG	post-GI	perm. (2-sided)	vs. water	3.438±0.543 vs 1.051±0.644 dF'/F'	9, 9	**1.45E-02**
latBLA	intralipid IG	GI	perm. (2-sided, paired)	vs. sham	1.470±0.320 vs. 0±0 dF'/F'	9	**3.91E-04**
latBLA	intralipid IG	GI	perm. (2-sided)	vs. water	1.470±0.320 vs 0.247±0.467 dF'/F'	9, 9	**4.78E-02**
latBLA	intralipid IG	post-GI	perm. (2-sided, paired)	vs. sham	0.963±0.202 vs. 0±0 dF'/F'	9	**3.91E-04**
latBLA	intralipid IG	post-GI	perm. (2-sided)	vs. water	0.963±0.202 vs 1.051±0.644 dF'/F'	9, 9	8.95E-01
latBLA	mannitol IG	GI	perm. (2-sided, paired)	vs. sham	1.579±0.256 vs. 0±0 dF'/F'	9	**2.06E-05**
latBLA	mannitol IG	post-GI	perm. (2-sided, paired)	vs. sham	4.163±0.511 vs. 0±0 dF'/F'	9	**2.06E-05**
latBLA	MDG IG	GI	perm. (2-sided, paired)	vs. sham	1.760±0.832 vs. 0±0 dF'/F'	8	**3.18E-02**
latBLA	MDG IG	post-GI	perm. (2-sided, paired)	vs. sham	1.966±0.774 vs. 0±0 dF'/F'	8	**7.77E-05**
latBLA	peptide IG	GI	perm. (2-sided, paired)	vs. sham	1.366±0.276 vs. 0±0 dF'/F'	8	**7.77E-05**
latBLA	peptide IG	post-GI	perm. (2-sided, paired)	vs. sham	3.126±0.338 vs. 0±0 dF'/F'	8	**7.77E-05**
NAc	water drinking	oral	perm. (2-sided, paired)	vs. baseline	45.709±6.122 vs. 0±0 dF'/F'	4	**1.41E-02**
NAc	water drinking	GI	perm. (2-sided, paired)	vs. baseline	0.073±1.588 vs. 0±0 dF'/F'	4	9.72E-01

Area	Experiment	Phase	Test	Comparison	Statistics	n	p
NAc	water drinking	post-GI	perm. (2-sided, paired)	vs. baseline	-7.554±2.288 vs. 0±0 dF'/F'	4	**1.41E-02**
NAc	Ensure drinking	oral	perm. (2-sided, paired)	vs. baseline	52.516±14.77 vs. 0±0 dF'/F'	5	**3.95E-03**
NAc	Ensure drinking	oral	perm. (2-sided)	vs. water	52.516±14.77 vs 45.709±6.122 dF'/F'	5, 4	7.64E-01
NAc	Ensure drinking	oral	peak time, perm. (2-sided)	vs. water	1.2±0.215 vs 4.313±2.228 s'	5, 4	**4.72E-02**
NAc	Ensure drinking	GI	perm. (2-sided, paired)	vs. baseline	4.013±2.162 vs. 0±0 dF'/F'	5	1.23E-01
NAc	Ensure drinking	GI	perm. (2-sided)	vs. water	4.013±2.162 vs 0.073±1.588 dF'/F'	5, 4	1.97E-01
NAc	Ensure drinking	post-GI	perm. (2-sided, paired)	vs. baseline	-1.262±1.189 vs. 0±0 dF'/F'	5	3.99E-01
NAc	Ensure drinking	post-GI	perm. (2-sided)	vs. water	-1.262±1.189 vs -7.554±2.288 dF'/F'	5, 4	**2.36E-02**
NAc	sucralose drinking	oral	perm. (2-sided, paired)	vs. baseline	43.748±12.002 vs. 0±0 dF'/F'	4	**1.41E-02**
NAc	sucralose drinking	oral	perm. (2-sided)	vs. water	43.748±12.002 vs 45.709±6.122 dF'/F'	4, 4	8.87E-01
NAc	sucrose drinking	oral	perm. (2-sided, paired)	vs. baseline	33.617±8.766 vs. 0±0 dF'/F'	8	**6.91E-03**
NAc	sucrose drinking	oral	perm. (2-sided)	vs. water	33.617±8.766 vs 45.709±6.122 dF'/F'	8, 4	3.93E-01
NAc	water IG	GI	perm. (2-sided, paired)	vs. sham	-0.998±0.490 vs. 0±0 dF'/F'	8	6.13E-02
NAc	water IG	post-GI	perm. (2-sided, paired)	vs. sham	-1.896±1.672 vs. 0±0 dF'/F'	8	2.78E-01
NAc	Ensure IG	GI	perm. (2-sided, paired)	vs. sham	-0.233±1.0252 vs. 0±0 dF'/F'	9	8.96E-01
NAc	Ensure IG	GI	perm. (2-sided)	vs. water	-0.233±1.0252 vs -0.998±0.490 dF'/F'	9	6.25E-01
NAc	Ensure IG	post-GI	perm. (2-sided, paired)	vs. sham	-3.005±2.784 vs. 0±0 dF'/F'	9	2.95E-01
NAc	Ensure IG	post-GI	perm. (2-sided)	vs. water	-3.005±2.784 vs -1.896±1.672 dF'/F'	9, 8	7.44E-01
DLS	water drinking	oral	perm. (2-sided, paired)	vs. baseline	1.159±0.572 vs. 0±0 dF'/F'	7	**4.37E-03**
DLS	water drinking	GI	perm. (2-sided, paired)	vs. baseline	-0.315±0.174 vs. 0±0 dF'/F'	7	9.41E-02
DLS	water drinking	post-GI	perm. (2-sided, paired)	vs. baseline	-0.697±0.598 vs. 0±0 dF'/F'	7	2.69E-01
DLS	Ensure drinking	oral	perm. (2-sided, paired)	vs. baseline	1.404±0.337 vs. 0±0 dF'/F'	8	**7.77E-05**
DLS	Ensure drinking	oral	perm. (2-sided)	vs. water	1.404±0.337 vs 1.159±0.572 dF'/F'	8, 7	7.28E-01
DLS	Ensure drinking	oral	peak time, perm. (2-sided)	vs. water	7.031±3.349 vs 5.357±2.285 s'	8, 7	7.28E-01
DLS	Ensure drinking	GI	perm. (2-sided, paired)	vs. baseline	0.23±0.235 vs. 0±0 dF'/F'	8	3.58E-01
DLS	Ensure drinking	GI	perm. (2-sided)	vs. water	0.23±0.235 vs -0.315±0.174 dF'/F'	8, 7	9.51E-02
DLS	Ensure drinking	post-GI	perm. (2-sided, paired)	vs. baseline	0.984±0.26 vs. 0±0 dF'/F'	8	**7.77E-05**
DLS	Ensure drinking	post-GI	perm. (2-sided)	vs. water	0.984±0.26 vs -0.697±0.598 dF'/F'	8, 7	**1.88E-02**
DLS	sucralose drinking	oral	perm. (2-sided, paired)	vs. baseline	2.214±1.019 vs. 0±0 dF'/F'	7	**2.91E-04**
DLS	sucralose drinking	oral	perm. (2-sided)	vs. water	2.214±1.019 vs 1.159±0.572 dF'/F'	7, 7	4.56E-01
DLS	sucrose drinking	oral	perm. (2-sided, paired)	vs. baseline	1.914±0.711 vs. 0±0 dF'/F'	7	**2.91E-04**
DLS	sucrose drinking	oral	perm. (2-sided)	vs. water	1.914±0.711 vs 1.159±0.572 dF'/F'	7, 7	4.34E-01
DLS	water IG	GI	perm. (2-sided, paired)	vs. sham	-0.214±0.296 vs. 0±0 dF'/F'	6	4.57E-01
DLS	water IG	post-GI	perm. (2-sided, paired)	vs. sham	-0.225±0.354 vs. 0±0 dF'/F'	6	5.16E-01
DLS	Ensure IG	GI	perm. (2-sided, paired)	vs. sham	0.091±0.410 vs. 0±0 dF'/F'	6	7.43E-01
DLS	Ensure IG	GI	perm. (2-sided)	vs. water	0.091±0.410 vs -0.215±0.296 dF'/F'	6, 6	5.57E-01
DLS	Ensure IG	post-GI	perm. (2-sided, paired)	vs. sham	0.689±0.788 vs. 0±0 dF'/F'	6	3.19E-01
DLS	Ensure IG	post-GI	perm. (2-sided)	vs. water	0.689±0.788 vs -0.225±0.354 dF'/F'	6, 6	3.15E-01
aBLA	water drinking	oral	perm. (2-sided, paired)	vs. baseline	4.156±2.357 vs. 0±0 dF'/F'	9	**4.79E-02**
aBLA	water drinking	GI	perm. (2-sided, paired)	vs. baseline	0.355±0.442 vs. 0±0 dF'/F'	9	5.41E-01
aBLA	water drinking	post-GI	perm. (2-sided, paired)	vs. baseline	-0.9±0.574 vs. 0±0 dF'/F'	9	1.47E-01
aBLA	Ensure drinking	oral	perm. (2-sided, paired)	vs. baseline	14.907±2.88 vs. 0±0 dF'/F'	11	**1.00E-05**
aBLA	Ensure drinking	oral	perm. (2-sided)	vs. water	14.907±2.88 vs 4.156±2.357 dF'/F'	11, 9	**9.05E-03**
aBLA	Ensure drinking	oral	perm. (2-sided)	vs. pBLA	14.907±2.88 vs 9.299±3.324 dF'/F'	11, 11	2.20E-01
aBLA	Ensure drinking	GI	perm. (2-sided, paired)	vs. baseline	6.168±1.66 vs. 0±0 dF'/F'	11	**3.60E-04**
aBLA	Ensure drinking	GI	perm. (2-sided)	vs. water	6.168±1.66 vs 0.355±0.442 dF'/F'	11, 9	**4.79E-03**
aBLA	Ensure drinking	post-GI	perm. (2-sided, paired)	vs. baseline	-1.057±1.912 vs. 0±0 dF'/F'	11	9.51E-01
aBLA	Ensure drinking	post-GI	perm. (2-sided)	vs. water	-1.057±1.912 vs -0.9±0.574 dF'/F'	11, 9	9.92E-01
aBLA	sucralose drinking	oral	perm. (2-sided, paired)	vs. baseline	16.287±2.474 vs. 0±0 dF'/F'	6	**1.08E-03**
aBLA	sucralose drinking	oral	perm. (2-sided)	vs. water	16.287±2.474 vs 4.156±2.357 dF'/F'	6, 9	**6.19E-03**
aBLA	sucrose drinking	oral	perm. (2-sided, paired)	vs. baseline	16.007±1.901 vs. 0±0 dF'/F'	6	**1.08E-03**
aBLA	sucrose drinking	oral	perm. (2-sided)	vs. water	16.007±1.901 vs 4.156±2.357 dF'/F'	6, 9	**6.39E-03**
aBLA	water IG	GI	perm. (2-sided, paired)	vs. sham	-0.364±0.215 vs. 0±0 dF'/F'	8	1.23E-01
aBLA	water IG	post-GI	perm. (2-sided, paired)	vs. sham	0.472±0.296 vs. 0±0 dF'/F'	8	1.34E-01
aBLA	Ensure IG	GI	perm. (2-sided, paired)	vs. sham	10.013±2.285 vs. 0±0 dF'/F'	8	**7.77E-05**
aBLA	Ensure IG	GI	perm. (2-sided)	vs. water	10.013±2.285 vs -0.364±0.215 dF'/F'	8, 8	**7.77E-05**
aBLA	Ensure IG	GI	perm. (2-sided)	vs. pBLA	10.013±2.285 vs 3.069±0.427 dF'/F'	8, 5	**2.87E-02**
aBLA	Ensure IG	GI	perm. (2-sided, paired)	vs. Ensure IG	10.838±2.89 vs 6.367±2.745	6	3.17E-01
aBLA	Ensure IG	post-GI	perm. (2-sided, paired)	vs. sham	1.939±0.36 vs. 0±0 dF'/F'	8	**7.77E-05**
aBLA	Ensure IG	post-GI	perm. (2-sided)	vs. water	1.939±0.36 vs 0.472±0.296 dF'/F'	8, 8	**8.00E-03**
aBLA	Ensure IG	post-GI	perm. (2-sided)	vs. pBLA	1.939±0.36 vs 1.608±0.743 dF'/F'	8, 5	6.59E-01
aBLA	Ensure IG	post-GI	perm. (2-sided, paired)	vs. Ensure IG	2.275±0.442 vs 2.311±2.154	6	9.98E-01
aBLA	diet A IG	GI	perm. (2-sided, paired)	vs. sham	7.332±2.952 vs. 0±0 dF'/F'	5	**3.95E-03**
aBLA	diet A IG	GI	perm. (2-sided)	vs. Ensure	7.332±2.952 vs 10.013±2.285 dF'/F'	5, 8	4.88E-01
aBLA	diet A IG	post-GI	perm. (2-sided, paired)	vs. sham	1.292±0.234 vs. 0±0 dF'/F'	5	**3.95E-03**
aBLA	diet A IG	post-GI	perm. (2-sided)	vs. Ensure	1.292±0.234 vs 1.939±0.36 dF'/F'	5, 8	2.15E-01
aBLA	diet B IG	GI	perm. (2-sided, paired)	vs. sham	5.838±3.212 vs. 0±0 dF'/F'	6	**1.08E-03**
aBLA	diet B IG	GI	perm. (2-sided)	vs. Ensure	5.838±3.212 vs 10.013±2.285 dF'/F'	6, 8	3.01E-01
aBLA	diet B IG	post-GI	perm. (2-sided, paired)	vs. sham	0.643±0.675 vs. 0±0 dF'/F'	6	3.95E-01
aBLA	diet B IG	post-GI	perm. (2-sided)	vs. Ensure	0.643±0.675 vs 1.939±0.36 dF'/F'	6, 8	9.45E-02
aBLA	peptide IG	GI	perm. (2-sided, paired)	vs. sham	6.634±2.311 vs. 0±0 dF'/F'	6	**1.08E-03**
aBLA	peptide IG	post-GI	perm. (2-sided, paired)	vs. sham	1.889±0.509 vs. 0±0 dF'/F'	6	**1.08E-03**
aBLA	mineral oil IG	GI	perm. (2-sided, paired)	vs. sham	0.11±0.413 vs. 0±0 dF'/F'	5	8.34E-01
aBLA	mineral oil IG	post-GI	perm. (2-sided, paired)	vs. sham	0.829±0.591 vs. 0±0 dF'/F'	5	2.81E-01
aBLA	intralipid IG	GI	perm. (2-sided, paired)	vs. sham	4.547±1.271 vs. 0±0 dF'/F'	7	**2.91E-04**
aBLA	intralipid IG	GI	perm. (2-sided)	vs. mineral oil	4.547±1.271 vs 0.11±0.413 dF'/F'	7,5	**1.39E-02**
aBLA	intralipid IG	post-GI	perm. (2-sided, paired)	vs. sham	1.017±0.997 vs. 0±0 dF'/F'	7	3.47E-01
aBLA	intralipid IG	post-GI	perm. (2-sided)	vs. mineral oil	1.017±0.997 vs 0.829±0.591 dF'/F'	7, 5	8.90E-01

Area	Experiment	Phase	Test	Comparison	Statistics	n	p
aBLA	mannitol IG	GI	perm. (2-sided, paired)	vs. sham	0.986±0.48 vs. 0±0 dF'/F'	8	5.26E-02
aBLA	mannitol IG	post-GI	perm. (2-sided, paired)	vs. sham	0.416±0.866 vs. 0±0 dF'/F'	8	6.68E-01
aBLA	fructose IG	GI	perm. (2-sided, paired)	vs. sham	0.759±0.635 vs. 0±0 dF'/F'	7	2.65E-01
aBLA	fructose IG	post-GI	perm. (2-sided, paired)	vs. sham	3.026±2.211 vs. 0±0 dF'/F'	7	1.67E-01
aBLA	glucose IG	GI	perm. (2-sided, paired)	vs. sham	4.277±1.083 vs. 0±0 dF'/F'	7	**2.91E-04**
aBLA	glucose IG	post-GI	perm. (2-sided, paired)	vs. sham	-0.842±0.312 vs. 0±0 dF'/F'	7	**2.88E-02**
aBLA	galactose IG	GI	perm. (2-sided, paired)	vs. sham	5.933±2.90 vs. 0±0 dF'/F'	4	**1.41E-02**
aBLA	galactose IG	post-GI	perm. (2-sided, paired)	vs. sham	1.048±0.722 vs. 0±0 dF'/F'	4	2.96E-01
aBLA	MDG IG	GI	perm. (2-sided, paired)	vs. sham	5.337±0.878 vs. 0±0 dF'/F'	7	**2.91E-04**
aBLA	MDG IG	post-GI	perm. (2-sided, paired)	vs. sham	0.617±0.58 vs. 0±0 dF'/F'	7	3.10E-01
aBLA	glucose IG	GI	perm. (2-sided, paired)	vs. water	-0.447±0.228 vs 4.277±1.083 dF'/F'	7	**2.91E-04**
aBLA	glucose +Mz IG	GI	perm. (2-sided, paired)	vs. water + Mz	-0.187±0.382 vs 0.342±0.601 dF'/F'	7	4.49E-01
aBLA	glucose +Mz IG	GI	perm. (2-sided, paired)	glucose - water vs. (glucose+Mz) -(water+Mz)	-0.447±0.228 - 4.277±1.083 dF'/F' vs. -0.187±0.382 - 0.342±0.601 dF'/F'	7	**2.91E-04**
aBLA	glucose IG	post-GI	perm. (2-sided, paired)	vs. water	-0.842±0.312 vs 0.524±0.336 dF'/F'	7	**2.91E-04**
aBLA	glucose +Mz IG	post-GI	perm. (2-sided, paired)	vs. water + Mz	1.228±0.478 vs -0.641±0.297 dF'/F'	7	**4.37E-03**
aBLA	glucose +Mz IG	post-GI	perm. (2-sided, paired)	glucose - water vs. (glucose+Mz) -(water+Mz)	-0.842±0.312 - 0.524±0.336 dF'/F' vs. 1.228±0.478 - -0.641±0.297 dF'/F'	7	**4.40E-03**
aBLA	Ensure IG	GI	perm. (2-sided, paired)	vs. water	-0.447±0.228 vs 9.679±2.61 dF'/F'	7	**2.91E-04**
aBLA	Ensure +Mz IG	GI	perm. (2-sided, paired)	vs. water + Mz	-0.187±0.382 vs 5.957±1.254 dF'/F'	7	**2.91E-04**
aBLA	Ensure +Mz IG	GI	perm. (2-sided, paired)	Ensure - water vs. (Ensure+Mz) - (water+Mz)	-0.447±0.228 - 9.679±2.61 dF'/F' vs. -0.187±0.382 - 5.957±1.254 dF'/F'	7	**1.66E-02**
aBLA	Ensure IG	post-GI	perm. (2-sided, paired)	vs. water	0.524±0.336 vs 1.925±0.415 dF'/F'	7	**4.37E-03**
aBLA	Ensure +Mz IG	post-GI	perm. (2-sided, paired)	vs. water + Mz	-0.641±0.297 vs 1.619±0.496 dF'/F'	7	**2.91E-04**
aBLA	Ensure +Mz IG	post-GI	perm. (2-sided, paired)	Ensure - water vs. (Ensure+Mz) - (water+Mz)	0.524±0.336 - 1.925±0.415 dF'/F' vs. -0.641±0.297 - 1.619±0.496 dF'/F'	7	9.41E-02
aBLA	intralipid IG	GI	perm. (2-sided, paired)	vs. water	-0.429±0.288 vs 3.433±1.466 dF'/F'	5	**3.95E-03**
aBLA	intralipid +G/A IG	GI	perm. (2-sided, paired)	vs. water + G/A	-0.493±0.845 vs 1.411±0.756 dF'/F'	5	2.02E-01
aBLA	intralipid +G/A IG	GI	perm. (2-sided, paired)	intralipid - water vs. (intralipid+G/A) - (water+G/A)	-0.429±0.288 - 3.433±1.466 dF'/F' vs. -0.493±0.845 - 1.411±0.756 dF'/F'	5	4.39E-01
aBLA	intralipid +G/A/S IG	GI	perm. (2-sided, paired)	vs. water + G/A/S	1.171±0.555 vs -0.585±0.732 dF'/F'	5	**4.35E-02**
aBLA	intralipid +G/A/S IG	GI	perm. (2-sided, paired)	intralipid - water vs. (intralipid+G/A/S) -(water+G/A/S)	-0.429±0.288 - 3.433±1.466 dF'/F' vs. 1.171±0.555 vs -0.585±0.732 dF'/F'		**4.00E-03**
aBLA	intralipid IG	post-GI	perm. (2-sided, paired)	vs. water	0.392±0.311 vs 0.975±1.422 dF'/F'	5	5.57E-01
aBLA	intralipid +G/A IG	post-GI	perm. (2-sided, paired)	vs. water + G/A	0.138±0.41 vs 0.077±0.669 dF'/F'	5	9.13E-01
aBLA	intralipid +G/A IG	post-GI	perm. (2-sided, paired)	intralipid - water vs. (intralipid+G/A) - (water+G/A)	0.392±0.311 - 0.975±1.422 dF'/F' vs. 0.138±0.41 - 0.077±0.669 dF'/F'	5	7.55E-01
aBLA	intralipid +G/A/S IG	post-GI	perm. (2-sided, paired)	vs. water + G/A/S	0.351±0.992 vs -0.118±1.159 dF'/F'	5	6.36E-01
aBLA	intralipid +G/A/S IG	post-GI	perm. (2-sided, paired)	intralipid - water vs. (intralipid+G/A/S) -(water+G/A/S)	0.392±0.311 - 0.975±1.422 dF'/F' vs. 0.351±0.992 - -0.118±1.159 dF'/F'	5	7.55E-01
aBLA	intralipid +Dev IG	GI	perm. (2-sided, paired)	vs. water + Dev	-0.151±0.481 vs 0.818±0.947 dF'/F'	5	2.81E-01
aBLA	intralipid +Dev IG	GI	perm. (2-sided, paired)	intralipid - water vs. (intralipid+Dev) - (water+Dev)	-0.263±0.37 - 7.26±2.762 vs. -0.151±0.481 - 0.818±0.947 dF'/F'	5	**4.00E-03**
aBLA	intralipid +Dev IG	post-GI	perm. (2-sided, paired)	vs. water + Dev	-0.619±0.781 vs -2.161±0.933 dF'/F'	5	3.20E-01
aBLA	intralipid +Dev IG	post-GI	perm. (2-sided, paired)	intralipid - water vs. (intralipid+Dev) - (water+Dev)	-1.288±0.674 - -0.98±0.741 vs. -0.619±0.781 - -2.161±0.933 dF'/F'	5	7.55E-01
aBLA	amylin IP	hormone	perm. (2-sided, paired)	vs. saline IP	-1.964±1.061 vs. 0±0 dF'/F'	5	1.23E-01
aBLA	leptin IP	hormone	perm. (2-sided, paired)	vs. saline IP	-1.723±0.931 vs. 0±0 dF'/F'	5	**4.35E-02**
aBLA	glucagon IP	hormone	perm. (2-sided, paired)	vs. saline IP	-0.95±0.575 vs. 0±0 dF'/F'	4	1.27E-01
aBLA	PYY IP	hormone	perm. (2-sided, paired)	vs. saline IP	-1.146±0.793 vs. 0±0 dF'/F'	6	1.87E-01
aBLA	ghrelin IP	hormone	perm. (2-sided, paired)	vs. saline IP	-0.534±0.501 vs. 0±0 dF'/F'	7	3.10E-01
aBLA	5HT IP	hormone	perm. (2-sided, paired)	vs. saline IP	1.316±1.384 vs. 0±0 dF'/F'	10	4.33E-01
aBLA	CCK IP	hormone	perm. (2-sided, paired)	vs. saline IP	7.435±1.437 vs. 0±0 dF'/F'	6	**1.08E-03**
aBLA	CCK IP (10 ug/kg)	hormone	perm. (2-sided, paired)	vs. saline IP	3.77±1.011 vs. 0±0 dF'/F'	4	**1.41E-02**
aBLA	LPS IP	malaise	perm. (2-sided, paired)	vs. saline IP	-5.129±4.261 vs. 0±0 dF'/F'	6	**4.65E-02**
aBLA	LPS IP	malaise	perm. (2-sided)	vs. pBLA	-5.129±4.261 vs 1.474±0.731 dF'/F'	6, 8	**1.33E-03**
pBLA	water drinking	oral	perm. (2-sided, paired)	vs. baseline	5.506±0.764 vs. 0±0 dF'/F'	9	**2.06E-05**
pBLA	Ensure drinking	oral	perm. (2-sided, paired)	vs. baseline	9.299±3.324 vs. 0±0 dF'/F'	11	**1.00E-05**
pBLA	Ensure drinking	oral	perm. (2-sided)	vs. water	9.299±3.324 vs 5.506±0.764 dF'/F'	11, 9	3.98E-01
pBLA	sucralose drinking	oral	perm. (2-sided, paired)	vs. baseline	6.816±1.508 vs. 0±0 dF'/F'	9	**2.06E-05**
pBLA	sucralose drinking	oral	perm. (2-sided)	vs. water	6.816±1.508 vs 5.506±0.764 dF'/F'	9, 9	4.53E-01

Area	Experiment	Phase	Test	Comparison	Statistics	n	p
pBLA	sucrose drinking	oral	perm. (2-sided, paired)	vs. baseline	8.424±1.915 vs. 0±0 dF'/F'	8	**7.77E-05**
pBLA	sucrose drinking	oral	perm. (2-sided)	vs. water	8.424±1.915 vs 5.506±0.764 dF'/F'	8, 9	1.60E-01
pBLA	water drinking	GI	perm. (2-sided, paired)	vs. baseline	-0.156±0.879 vs. 0±0 dF'/F'	9	7.75E-01
pBLA	Ensure drinking	GI	perm. (2-sided, paired)	vs. baseline	4.859±1.645 vs. 0±0 dF'/F'	11	**6.00E-05**
pBLA	Ensure drinking	GI	perm. (2-sided)	vs. water	4.859±1.645 vs -0.156±0.879 dF'/F'	11, 9	**5.21E-03**
pBLA	water drinking	post-GI	perm. (2-sided, paired)	vs. baseline	-0.569±1.259 vs. 0±0 dF'/F'	9	7.61E-01
pBLA	Ensure drinking	post-GI	perm. (2-sided, paired)	vs. baseline	2.323±0.792 vs. 0±0 dF'/F'	11	**5.30E-04**
pBLA	Ensure drinking	post-GI	perm. (2-sided)	vs. water	2.323±0.792 vs -0.569±1.259 dF'/F'	11, 9	**4.31E-02**
pBLA	water IG	GI	perm. (2-sided, paired)	vs. sham	0.206±0.197 vs. 0±0 dF'/F'	5	3.99E-01
pBLA	water IG	post-GI	perm. (2-sided, paired)	vs. sham	-0.111±0.338 vs. 0±0 dF'/F'	5	7.94E-01
pBLA	Ensure IG	GI	perm. (2-sided, paired)	vs. sham	3.069±0.427 vs. 0±0 dF'/F'	5	**3.95E-03**
pBLA	Ensure IG	GI	perm. (2-sided)	vs. water	3.069±0.427 vs 0.206±0.197 dF'/F'	5, 5	**3.95E-03**
pBLA	Ensure IG	post-GI	perm. (2-sided, paired)	vs. sham	1.608±0.743 vs. 0±0 dF'/F'	5	**4.35E-02**
pBLA	Ensure IG	post-GI	perm. (2-sided)	vs. water	1.608±0.743 vs -0.111±0.338 dF'/F'	5, 5	5.14E-02
pBLA	diet A IG	GI	perm. (2-sided, paired)	vs. sham	1.638±0.33 vs. 0±0 dF'/F'	3	**4.76E-02**
pBLA	diet A IG	GI	perm. (2-sided)	vs. water	1.638±0.33 vs 0.206±0.197 dF'/F'	3, 5	**1.75E-02**
pBLA	diet A IG	post-GI	perm. (2-sided, paired)	vs. sham	0.676±0.303 vs. 0±0 dF'/F'	3	**4.76E-02**
pBLA	diet A IG	post-GI	perm. (2-sided)	vs. water	0.676±0.303 vs -0.111±0.338 dF'/F'	3, 5	1.58E-01
pBLA	mannitol IG	GI	perm. (2-sided, paired)	vs. sham	0.596±0.698 vs. 0±0 dF'/F'	5	4.39E-01
pBLA	mannitol IG	post-GI	perm. (2-sided, paired)	vs. sham	2.334±0.72 vs. 0±0 dF'/F'	5	**3.95E-03**
pBLA	fructose IG	GI	perm. (2-sided, paired)	vs. sham	1.236±0.603 vs. 0±0 dF'/F'	4	1.27E-01
pBLA	fructose IG	post-GI	perm. (2-sided, paired)	vs. sham	14.492±3.961 vs. 0±0 dF'/F'	4	**1.41E-02**
pBLA	glucose IG	GI	perm. (2-sided, paired)	vs. sham	3.199±0.561 vs. 0±0 dF'/F'	5	**3.95E-03**
pBLA	glucose IG	post-GI	perm. (2-sided, paired)	vs. sham	2.494±0.949 vs. 0±0 dF'/F'	5	**4.35E-02**
pBLA	galactose IG	GI	perm. (2-sided, paired)	vs. sham	3.074±1.646 vs. 0±0 dF'/F'	3	**4.76E-02**
pBLA	galactose IG	post-GI	perm. (2-sided, paired)	vs. sham	2.877±1.599 vs. 0±0 dF'/F'	3	3.33E-01
pBLA	MDG IG	GI	perm. (2-sided, paired)	vs. sham	2.755±0.77 vs. 0±0 dF'/F'	5	**3.95E-03**
pBLA	MDG IG	post-GI	perm. (2-sided, paired)	vs. sham	2.787±1.124 vs. 0±0 dF'/F'	5	**3.95E-03**
pBLA	mineral oil IG	GI	perm. (2-sided, paired)	vs. sham	-0.014±0.221 vs. 0±0 dF'/F'	4	9.72E-01
pBLA	mineral oil IG	post-GI	perm. (2-sided, paired)	vs. sham	0.448±1.078 vs. 0±0 dF'/F'	4	8.59E-01
pBLA	intralipid IG	GI	perm. (2-sided, paired)	vs. sham	1.209±1.087 vs. 0±0 dF'/F'	5	2.81E-01
pBLA	intralipid IG	post-GI	perm. (2-sided, paired)	vs. sham	1.228±1.536 vs. 0±0 dF'/F'	5	6.76E-01
pBLA	peptide IG	GI	perm. (2-sided, paired)	vs. sham	0.833±0.437 vs. 0±0 dF'/F'	5	**3.95E-03**
pBLA	peptide IG	post-GI	perm. (2-sided, paired)	vs. sham	-0.01±0.966 vs. 0±0 dF'/F'	5	9.13E-01
pBLA	5HT IP	hormone	perm. (2-sided, paired)	vs. saline IP	0.744±0.608 vs. 0±0 dF'/F'	7	2.33E-01
pBLA	CCK IP	hormone	perm. (2-sided, paired)	vs. saline IP	-2.143±0.964 vs. 0±0 dF'/F'	5	**4.35E-02**
pBLA	ghrelin IP	hormone	perm. (2-sided, paired)	vs. saline IP	0.996±0.571 vs. 0±0 dF'/F'	6	1.35E-01
pBLA	LiCl IP	hormone	perm. (2-sided, paired)	vs. saline IP	5.931±1.403 vs. 0±0 dF'/F'	7	**2.91E-04**
pBLA	LiCl IP	malaise	perm. (2-sided, paired)	vs. saline IP	5.537±1.705 vs. 0±0 dF'/F'	7	**4.37E-03**
pBLA	LPS IP	malaise	perm. (2-sided, paired)	vs. saline IP	1.474±0.731 vs. 0±0 dF'/F'	8	**1.32E-03**
right BLA	water drinking	oral	perm. (2-sided, paired)	vs. baseline	4.732±0.962 vs. 0±0 dF'/F'	8	**7.77E-05**
right BLA	Ensure drinking	oral	perm. (2-sided, paired)	vs. baseline	8.472±1.274 vs. 0±0 dF'/F'	14	**1.00E-05**
right BLA	Ensure drinking	oral	perm. (2-sided)	vs. water	8.472±1.274 vs 4.732±0.962 dF'/F'	14, 8	5.38E-02
right BLA	Ensure drinking	oral	perm. (2-sided)	vs. (left) BLA	8.472±1.274 vs. 5.110±0.871 dF'/F'		**3.57E-02**
right BLA	sucralose drinking	oral	perm. (2-sided, paired)	vs. baseline	5.422±1.168 vs. 0±0 dF'/F'	10	**7.00E-05**
right BLA	sucralose drinking	oral	perm. (2-sided)	vs. water	5.422±1.168 vs 4.732±0.962 dF'/F'	10, 8	6.66E-01
right BLA	sucrose drinking	oral	perm. (2-sided, paired)	vs. baseline	6.453±1.712 vs. 0±0 dF'/F'	8	**7.77E-05**
right BLA	sucrose drinking	oral	perm. (2-sided)	vs. water	6.453±1.712 vs 4.732±0.962 dF'/F'	8, 8	4.04E-01
right BLA	water drinking	GI	perm. (2-sided, paired)	vs. baseline	-0.435±0.168 vs. 0±0 dF'/F'	8	**2.31E-02**
right BLA	Ensure drinking	GI	perm. (2-sided, paired)	vs. baseline	8.275±2.753 vs. 0±0 dF'/F'	14	**1.00E-05**
right BLA	Ensure drinking	GI	perm. (2-sided)	vs. water	8.275±2.753 vs -0.435±0.168 dF'/F'	14, 8	**1.35E-02**
right BLA	water drinking	post-GI	perm. (2-sided, paired)	vs. baseline	-0.795±0.285 vs. 0±0 dF'/F'	8	**6.91E-03**
right BLA	Ensure drinking	post-GI	perm. (2-sided, paired)	vs. baseline	2.067±0.466 vs. 0±0 dF'/F'	14	**7.00E-05**
right BLA	Ensure drinking	post-GI	perm. (2-sided)	vs. water	2.067±0.466 vs -0.795±0.285 dF'/F'	14, 8	**3.40E-04**
right BLA	water IG	GI	perm. (2-sided, paired)	vs. baseline	-0.278±0.362 vs. 0±0 dF'/F'	8	7.07E-01
right BLA	water IG	post-GI	perm. (2-sided, paired)	vs. baseline	-1.173±0.597 vs. 0±0 dF'/F'	8	**4.05E-02**
right BLA	Ensure IG	GI	perm. (2-sided, paired)	vs. baseline	5.309±1.033 vs. 0±0 dF'/F'	15	**1.00E-05**
right BLA	Ensure IG	GI	perm. (2-sided)	vs. water	5.309±1.033 vs -0.278±0.362 dF'/F'	15, 8	**1.16E-03**
right BLA	Ensure IG	GI	perm. (2-sided)	vs. (left) BLA	5.309±1.033 vs 18.203±3.517 dF'/F'	15, 16	**1.54E-03**
right BLA	Ensure IG	post-GI	perm. (2-sided, paired)	vs. baseline	1.725±0.264 vs. 0±0 dF'/F'	15	**1.00E-05**
right BLA	Ensure IG	post-GI	perm. (2-sided)	vs. water	1.725±0.264 vs -1.173±0.597 dF'/F'	15, 8	**4.00E-05**
right BLA	Ensure IG	post-GI	perm. (2-sided)	vs. (left) BLA	1.725±0.264 vs 2.397±1.102 dF'/F'	15, 16	7.71E-01
right BLA	mannitol IG	GI	perm. (2-sided, paired)	vs. baseline	0.842±0.287 vs. 0±0 dF'/F'	8	**1.00E-02**
right BLA	mannitol IG	post-GI	perm. (2-sided, paired)	vs. baseline	1.95±1.475 vs. 0±0 dF'/F'	8	2.13E-01
right BLA	glucose IG	GI	perm. (2-sided, paired)	vs. baseline	3.539±1.094 vs. 0±0 dF'/F'	8	**7.77E-05**
right BLA	glucose IG	GI	perm. (2-sided)	vs. mannitol	3.539±1.094 vs 0.842±0.287 dF'/F'	8, 8	**1.58E-02**
right BLA	glucose IG	GI	perm. (2-sided)	vs. (left) BLA	3.539±1.094 vs 13.449±4.018 dF'/F'	8, 11	5.26E-02
right BLA	glucose IG	post-GI	perm. (2-sided, paired)	vs. baseline	1.077±0.387 vs. 0±0 dF'/F'	8	**1.56E-02**
right BLA	glucose IG	post-GI	perm. (2-sided)	vs. mannitol	1.077±0.387 vs 1.95±1.475 dF'/F'	8, 8	7.07E-01
right BLA	glucose IG	post-GI	perm. (2-sided)	vs. (left) BLA	1.077±0.387 vs 1.609±1.045 dF'/F'	8, 11	6.88E-01

Extended Data Table 2. Dopamine imaging statistics. Summary information for all recordings of dopamine release in each brain region. Values are reported to 2 decimal places. P-values are reported for all statistical tests, and are shown in bold if below standard significance level (α=0.05).
X' corresponds to the normalized value of X. For photometry traces, dF'/F' means the dF/F values seen during sham infusion have been subtracted. For rise times, s' means the time is relative to approximate entry of liquid into the stomach. For fall times, s' means the time is relative to the end of the infusion. For peak times during licking, s' means the time is relative to the start of the first licking bout. Baseline is defined as the first 10 minutes of the recording for GI and post-GI measurements, or 0–20 seconds before the start of the first licking bout for oral measurements. Permutation (perm.) tests use an exact test (or 100,000 iterations if n>9) and are unpaired, unless otherwise mentioned (note: this means the lowest calculable p is 1E-5).

Cells	Experiment	Phase	Test	Comparison	Statistics	n (mice)	n (cells)	p
VTA-DA	Ensure IG	GI	perm. (2-sided) of activated neurons	vs. sham IG	0.200±0.039 vs. 0.075±0.018 pop-z	8, 5	162, 176	3.01E-02
VTA-DA	Ensure IG	GI	perm. (2-sided) of inhibited neurons	vs. sham IG	–0.059±0.01 vs. –0.064±0.003 pop-z	8, 5	162, 176	6.45E-01
VTA-DA	Ensure IG	post–GI	perm. (2-sided) of activated neurons	vs. sham IG	0.131±0.013 vs. 0.283±0.095 pop-z	8, 5	162, 176	2.26E-01
VTA-DA	Ensure IG	post–GI	perm. (2-sided) of inhibited neurons	vs. sham IG	–0.230±0.043 vs. –0.115±0.012 pop-z	8, 5	162, 176	**9.10E-03**
VTA-DA	Ensure IG	GI	KS test	vs. sham IG		8, 5	162, 176	**1.80E-02**
VTA-DA	Ensure IG	post–GI	KS test	vs. sham IG		8, 5	162, 176	4.44E-01
VTA-DA	water licks	oral	perm. (2-sided) of activated neurons	vs. sham licks	0.981±0.128 vs. 0.07±0.005 pop-z	4, 5	39, 153	**1.90E-04**
VTA-DA	water licks	oral	perm. (2-sided) of inhibited neurons	vs. sham licks	–0.290±0.037 vs. –0.071±0.010 pop-z	4, 5	39, 153	**2.91E-04**
VTA-DA	Ensure licks	oral	perm. (2-sided) of activated neurons	vs. sham licks	0.591±0.042 vs. 0.07±0.005 pop-z	7, 5	232, 153	**3.90E-04**
VTA-DA	Ensure licks	oral	perm. (2-sided) of activated neurons	vs. sham licks	–0.101±0.004 vs. –0.071±0.010 pop-z	7, 5	232, 153	**1.70E-03**
VTA-DA	Ensure licks	oral	perm. (2-sided) of inhibited neurons	vs. water licks	0.591±0.042 vs. 0.981±0.128 pop-z	7, 4	232, 39	**6.90E-04**
VTA-DA	Ensure licks	oral	perm. (2-sided) of inhibited neurons	vs. water licks	–0.101±0.004 vs. –0.290±0.037 pop-z	7, 4	232, 39	**1.00E-05**
VTA-DA	water licks	oral	KS test	vs. sham licks		4, 5	39, 153	**4.64E-04**
VTA-DA	Ensure licks	oral	KS test	vs. sham licks		7, 5	232, 153	**2.63E-06**
VTA-DA	Ensure licks	oral	KS test	vs. water licks		7, 4	232, 39	2.43E-01
VTA-DA/CCK	water IG	GI	perm. (2-sided) of activated neurons	vs. sham IG	0.050±0.006 vs. 0.029±0.002 pop-z	8, 8	90, 90	**4.70E-03**
VTA-DA/CCK	water IG	GI	perm. (2-sided) of inhibited neurons	vs. sham IG	–0.132±0.029 vs. –0.088±0.006 pop-z	8, 8	90, 90	2.39E-01
VTA-DA/CCK	water IG	post–GI	perm. (2-sided) of activated neurons	vs. sham IG	0.173±0.023 vs. 0.068±0.022 pop-z	8, 8	90, 90	**2.98E-02**
VTA-DA/CCK	water IG	post–GI	perm. (2-sided) of inhibited neurons	vs. sham IG	–0.327±0.023 vs. –0.182±0.014 pop-z	8, 8	90, 90	**7.90E-03**
VTA-DA/CCK	Ensure IG	GI	perm. (2-sided) of activated neurons	vs. sham IG	1.274±0.162 vs. 0.029±0.002 pop-z	6, 8	77, 90	5.89E-02
VTA-DA/CCK	Ensure IG	GI	perm. (2-sided) of inhibited neurons	vs. sham IG	(no inhibited neurons)	6, 8	77, 90	
VTA-DA/CCK	Ensure IG	post–GI	perm. (2-sided) of activated neurons	vs. sham IG	0.510±0.050 vs. 0.068±0.022 pop-z	6, 8	77, 90	**2.50E-03**
VTA-DA/CCK	Ensure IG	post–GI	perm. (2-sided) of inhibited neurons	vs. sham IG	–0.089±0.019 vs. –0.182±0.014 pop-z	6, 8	77, 90	6.25E-02
VTA-DA/CCK	Ensure IG	GI	perm. (2-sided) of activated neurons	vs. water IG	1.274±0.162 vs. 0.050±0.006 pop-z	6, 8	77, 90	**2.59E-02**
VTA-DA/CCK	Ensure IG	GI	perm. (2-sided) of inhibited neurons	vs. water IG	(no inhibited neurons)	6, 8	77, 90	
VTA-DA/CCK	Ensure IG	post–GI	perm. (2-sided) of activated neurons	vs. water IG	0.510±0.050 vs. 0.173±0.023 pop-z	6, 8	77, 90	**1.00E-05**
VTA-DA/CCK	Ensure IG	post–GI	perm. (2-sided) of inhibited neurons	vs. water IG	–0.089±0.019 vs. –0.327±0.023 pop-z	6, 8	77, 90	**4.55E-02**
VTA-DA/CCK	Ensure IG	GI	rise time (3 sd)		35.5±6.9 s'	6	77	
VTA-DA/CCK	water IG	GI	KS test	vs. sham IG		6, 8	77, 90	8.53E-01
VTA-DA/CCK	water IG	post–GI	KS test	vs. sham IG		6, 8	77, 90	1.04E-01
VTA-DA/CCK	Ensure IG	GI	KS test	vs. sham IG		6, 8	77, 90	**1.98E-13**
VTA-DA/CCK	Ensure IG	post–GI	KS test	vs. sham IG		6, 8	77, 90	**1.75E-04**
VTA-DA/CCK	Ensure IG	GI	KS test	vs. water IG		6, 8	77, 90	**8.80E-13**
VTA-DA/CCK	Ensure IG	post–GI	KS test	vs. water IG		6, 8	77, 90	**3.78E-02**
VTA-DA/CCK	Ensure IG	GI	KS test	vs. all VTA-DA		6,8	77, 176	**4.15E-11**
VTA-DA/CCK	Ensure IG	post–GI	KS test	vs. all VTA-DA		6,8	77, 176	2.21E-01
VTA-DA/CCK	Ensure IG	GI	perm. (2-sided) of activity by mouse	vs. baseline	0.756±0.341 vs. 0.0±0.0 z	6	77	**1.41E-02**
VTA-DA/CCK	Ensure IG	post–GI	perm. (2-sided) of activity by mouse	vs. baseline	0.280±0.193 vs. 0.0±0.0 z	6	77	1.35E-01
VTA-DA/CCK	Ensure IG	GI	LME	vs. baseline	ICC= 0.212	6	77	**1.85E-02**
VTA-DA/CCK	Ensure IG	post–GI	LME	vs. baseline	ICC= 0.145	6	77	1.74E-01
VTA-DA/CCK	water licks	oral	perm. (2-sided) of activated neurons	vs. sham licks	0.832±0.060 vs. 0.067±0.010 pop-z	6, 8	61, 90	**6.69E-05**
VTA-DA/CCK	water licks	oral	perm. (2-sided) of inhibited neurons	vs. sham licks	–0.124±0.027 vs. –0.064±0.003 pop-z	6, 8	61, 90	**1.41E-02**
VTA-DA/CCK	Ensure licks	oral	perm. (2-sided) of activated neurons	vs. sham licks	1.674±0.143 vs. 0.067±0.010 pop-z	8, 8	73, 90	**5.70E-03**
VTA-DA/CCK	Ensure licks	oral	perm. (2-sided) of activated neurons	vs. sham licks	–0.052±0.005 vs. –0.064±0.003 pop-z	8, 8	73, 90	6.25E-02
VTA-DA/CCK	Ensure licks	oral	perm. (2-sided) of inhibited neurons	vs. water licks	1.674±0.143 vs. 0.832±0.060 pop-z	8, 8	73, 90	**3.00E-04**
VTA-DA/CCK	Ensure licks	oral	perm. (2-sided) of inhibited neurons	vs. water licks	–0.052±0.005 vs. –0.124±0.027 pop-z	8, 8	73, 90	1.88E-01
VTA-DA/CCK	water licks	oral	KS test	vs. sham licks		6, 8	61, 90	**5.92E-04**
VTA-DA/CCK	Ensure licks	oral	KS test	vs. sham licks		8, 8	73, 90	**2.05E-15**
VTA-DA/CCK	Ensure licks	oral	KS test	vs. water licks		8, 6	73, 61	**1.30E-03**
VTA-DA/CCK	Ensure licks	oral	KS test	vs. all VTA-DA		8, 7	73, 232	**4.53E-08**
VTA-DA/CCK	Ensure licks	oral	perm. (2-sided) of activity by mouse	vs. baseline	1.216±0.343 vs. 0.0±0.0 z	8	73	**3.40E-03**
VTA-DA/CCK	Ensure licks	oral	LME	vs. baseline	ICC=0.4499	8	73	**4.79E-05**
aBLA-D1R	sucrose licks	oral	rise time (sigmoid fit)		-0.183±0.165 s	9	77	
aBLA-D1R	sucrose licks	oral	peak time		3.356±0.339 s	9	77	
aBLA-D1R	sucrose licks	oral	perm. (2-sided, paired) of licks during 5s	vs. mock	16.446±2.155 vs. 4.791±0.523 licks	9		**2.06E-05**
aBLA-D1R	sucrose licks	oral	perm. (2-sided, paired) of z during 5s	vs. mock	0.528±0.157 vs. 0.056±0.053 z	9	77	**2.00E-05**
aBLA-D1R	sucrose licks	oral	perm. (2-sided, paired) of act-only z during 5s	vs. mock	0.984±0.247 vs. 0.081±0.087 z	9	77	**1.00E-05**
aBLA-D1R	sucrose licks	oral	perm. (2-sided, paired) of licks during 0.5s	vs. mock	2.609±0.166 vs. 2.45±0.264 licks	9		5.58E-01
aBLA-D1R	sucrose licks	oral	perm. (2-sided, paired) of z during 0.5s	vs. mock	0.309±0.133 vs. 0.101±0.037 z	9	77	**1.65E-02**
aBLA-D1R	sucrose licks	oral	perm. (2-sided, paired) of act-only z during 0.5s	vs. mock	0.695±0.264 vs. 0.231±0.067 z	9	77	**3.50E-03**
aBLA-D1R	sucrose licks	oral	linear regression model (z~licks; mean z in 0.5 s of each sucrose bout by mouse)		R^2=0.0299	9 (326 total bouts)		**1.73E-03**

Cells	Experiment	Phase	Test	Comparison	Statistics	n (mice)	n (cells)	p
aBLA-D1R	sucrose licks	oral	linear regression model (z~licks; mean z in 0.5 s of each mock bout by mouse)		R^2=0.000143	9 (27 total bouts)		9.53E-01
aBLA-D1R	sucrose licks	oral	KS test	vs. sham licks		9, 9	77, 120	**6.70E-15**
aBLA-D1R	sucrose licks	oral	KS test	vs. mock licks		9, 9	77, 77	**5.00E-03**
aBLA-D1R	sucrose licks	oral	perm. (2-sided, paired) of act-only z during 5s	vs. sucralose (cross-reg.)	0.738±0.16 vs. 0.652±0.197 z	6	51	6.12E-01
aBLA-D1R	sucrose licks	oral	linear regression model (sucrose z ~ sucralose z)	vs. sucralose (cross-reg.)	R^2=0.449	6	51	**7.66E-08**
aBLA-D1R	sucrose licks	oral	perm. (2-sided, paired) of act-only z during 5s	vs. water (cross-reg.)	0.973±0.33 vs. 0.397±0.095 z	6	51	**1.33E-02**
aBLA-D1R	sucrose licks	oral	linear regression model (z~licks; mean z in 5 s of each sucrose bout by mouse)		R^2=0.0176	9 (326 total bouts)		**1.65E-02**
aBLA-D1R	sucrose licks	oral	linear regression model (z~licks; mean z in 5 s of each mock bout by mouse)		R^2=0.0615	9 (27 total bouts)		2.12E-01
aBLA-D1R	sucralose licks	oral	linear regression model (z~licks; mean z in 5 s of each mock bout by mouse)		R^2=0.169	6 (153 total bouts)		**1.34E-07**
aBLA-D1R	water licks	oral	linear regression model (z~licks; mean z in 5 s of each mock bout by mouse)		R^2=0.076	7 (89 total bouts)		**8.93E-03**
aBLA-D1R	sucralose licks	oral	perm. (2-sided, paired)	vs. water licks	0.056±0.002 vs. 0.142±0.004 euclidian distance to sucrose trajectory	6	48	**1.00E-05**
aBLA-D1R	sucralose licks	oral	perm. (2-sided, paired)	vs. mock licks	0.056±0.002 vs. 0.101±0.004 euclidian distance to sucrose trajectory	6	48	**1.00E-05**
aBLA-D1R	sucrose licks	late ITI	perm. (2-sided) of activated neurons	vs. baseline	0.387±0.163 z	9	77	**1.89E-02**
aBLA-D1R	sucralose licks	late ITI	perm. (2-sided) of activated neurons	vs. baseline	0.102±0.096 z	6	81	2.90E-01
aBLA-D1R	water licks	late ITI	perm. (2-sided) of activated neurons	vs. baseline	–0.057±0.094 z	7	114	5.50E-01
aBLA-D1R	sucrose licks	late ITI	perm. (2-sided) of inhibited neurons	vs. baseline	0.127±0.133 z	9	77	3.44E-01
aBLA-D1R	sucralose licks	late ITI	perm. (2-sided) of inhibited neurons	vs. baseline	0.332±0.166 z	6	81	**3.95E-02**
aBLA-D1R	water licks	late ITI	perm. (2-sided) of inhibited neurons	vs. baseline	–0.032±0.103 z	7	114	7.55E-01
aBLA-D1R	sucrose licks	oral	perm. (2-sided) during early bouts	vs. baseline	0.864±0.260 z	9	77	**1.00E-05**
aBLA-D1R	sucralose licks	oral	perm. (2-sided) during early bouts	vs. baseline	0.660±0.204 z	6	81	**4.00E-05**
aBLA-D1R	water licks	oral	perm. (2-sided) during early bouts	vs. baseline	0.332±0.087 z	7	114	**3.00E-05**
aBLA-D1R	sucrose licks	oral	perm. (2-sided) during late bouts	vs. baseline	0.476±0.198 z	9	77	**1.00E-05**
aBLA-D1R	sucralose licks	oral	perm. (2-sided) during late bouts	vs. baseline	0.160±0.082 z	6	81	5.24E-02
aBLA-D1R	water licks	oral	perm. (2-sided) during late bouts	vs. baseline	0.018±0.035 z	7	114	6.15E-01
aBLA-D1R	sucrose licks	oral	perm. (2-sided, paired)	vs. sucralose licks (cross-reg.)	0.201±0.007 vs. 0.057±0.003 euclidian distance from first 5 to last 5 bout trajectory	6	51	**1.00E-05**
aBLA-D1R	sucrose IG	GI	KS test	vs. sham IG		10, 8	104, 120	**2.00E-03**
aBLA-D1R	sucrose IG	post–GI	KS test	vs. sham IG		10, 8	104, 120	**2.20E-03**
aBLA-D1R	sucrose IG	GI	perm. (2-sided) of activated neurons	vs. sham IG	0.177±0.020 vs. 0.039±0.003 pop-z	10, 8	104, 120	**3.00E-04**
aBLA-D1R	sucrose IG	GI	perm. (2-sided) of inhibited neurons	vs. sham IG	–0.044±0.003 vs. –0.034±0.002 pop-z	10, 8	104, 120	**2.53E-02**
aBLA-D1R	sucrose IG	post-GI	perm. (2-sided) of activated neurons	vs. sham IG	0.557±0.047 vs. 0.106±0.008 pop-z	10, 8	104, 120	**1.10E-04**
aBLA-D1R	sucrose IG	post-GI	perm. (2-sided) of inhibited neurons	vs. sham IG	–0.135±0.007 vs. –0.079±0.011 pop-z	10, 8	104, 120	**3.90E-04**
aBLA-D1R	sucrose IG	post-GI	perm. (2-sided) of mean z by mouse	vs. baseline	0.515±0.113 z	10	104	**5.41E-06**
aBLA-D1R	intralipid IG	GI	perm. (2-sided) of activated neurons	vs. sham IG	0.234±0.013 vs. 0.039±0.003 pop-z	9, 8	113, 120	**1.00E-05**
aBLA-D1R	intralipid IG	GI	perm. (2-sided) of inhibited neurons	vs. sham IG	–0.116±0.006 vs. –0.034±0.002 pop-z	9, 8	113, 120	**4.00E-05**
aBLA-D1R	intralipid IG	post-GI	perm. (2-sided) of activated neurons	vs. sham IG	0.365±0.049 vs. 0.106±0.008 pop-z	9, 8	113, 120	**3.70E-03**
aBLA-D1R	intralipid IG	post-GI	perm. (2-sided) of inhibited neurons	vs. sham IG	–0.150±0.011 vs. –0.079±0.011 pop-z	9, 8	113, 120	**1.00E-03**
aBLA-D1R	intralipid IG	post-GI	perm. (2-sided) of mean z by mouse	vs. baseline	0.330±0.196 z	9	113	**4.44E-02**
aBLA-D1R	Ensure IG	GI	perm. (2-sided) of activated neurons	vs. sham IG	0.162±0.020 vs. 0.039±0.003 pop-z	5, 8	76, 120	**4.90E-04**
aBLA-D1R	Ensure IG	GI	perm. (2-sided) of inhibited neurons	vs. sham IG	–0.034±0.003 vs. –0.034±0.002 pop-z	5, 8	76, 120	8.79E-01
aBLA-D1R	Ensure IG	post-GI	perm. (2-sided) of inhibited neurons	vs. sham IG	0.461±0.073 vs. 0.106±0.008 pop-z	5, 8	76, 120	**3.20E-03**
aBLA-D1R	Ensure IG	post-GI	perm. (2-sided) of activated neurons	vs. sham IG	–0.144±0.025 vs. –0.079±0.011 pop-z	5, 8	76, 120	**2.53E-02**
aBLA-D1R	Ensure IG	post-GI	perm. (2-sided) of mean z by mouse	vs. baseline	0.313±0.131 z	5	76	**4.35E-02**

Extended Data Table 3. Single cell imaging statistics. Summary information for all 1 and 2 photon miniscope recordings. Values are reported to 2 decimal places. P-values are reported for all statistical tests, and are shown in bold if below standard significance level (α=0.05). X' corresponds to the normalized value of X. For rise times, s' means the time is relative to either the onset of the licking bout or to the approximate entry of liquid into the stomach. Population-weighted activity (pop-z) is calculated for a group of neurons (e.g. activated or inhibited neurons) by multiplying activity by the fraction of neurons belonging to that group. Linear-mixed models (LME) treat mouse differences as both a fixed random effect and covariate (see Methods). The relative contribution of mouse differences to total variance is reported by intra-class correlations (ICC). Note that for PCA, the number of PCs is equal to the number of cells. Permutation (perm.) tests use an exact test (or 100,000 iterations if n>9) and are unpaired, unless otherwise mentioned (note: this means the lowest calculable p for those tests is 1E-5).

Methods

Experimental protocols using mice were approved by the University of California, San Francisco Institutional Animal Care and Use Committee, following the NIH Guide for the Care and Use of Laboratory Animals. The experimental protocols using humans were approved by the local ethics committee of the Medical Faculty of the University of Cologne, Germany for both the fMRI (No. 17-278) and the PET experiments (No. 16-320).

For reading ease, these methods are separated into sections for surgery, recordings, behavior, and analysis. Each subsection detailed a specific method and notes the species used (mouse or human).

Mouse strains

Experiments used adult mice (>6 weeks old) of both sexes, housed in temperature- and humidity-controlled facilities with 12-h light–dark cycle, and *ad libitum* access to water and standard chow (PicoLab 5053). We obtained Drd1a-cre (MMRRC #030989) mice from the Mutant Mouse Resource & Research Center. We obtained DAT-cre (Jackson #006660), CCK-cre (Jackson #012706), Vglut2-cre (Jackson #016963), Vgat-cre (Jackson #016962), DAT-flp (Jackson #033673), TiGRE-GCaMP7s (Jackson #034112), Rosa-GtACR1 (Jackson #033089), RosaFL-ReaChR (Jackson #024846) mice from Jackson Labs. We obtained LepR-cre mice from Martin Myers. Double mutants were generated with crosses.

SURGERY: General methods (mice only)

Mice were anesthetized with 2% isoflurane and placed on a heating pad. The mice were given a subcutaneous injection of 1.5 mg/kg sustained release buprenorphine and an intraperitoneal injection of 5 mg/kg meloxicam before surgery. Following these injections, ophthalmic ointment was applied to the eyes, and surgical areas were shaved and wiped down with betadine and ethanol. Finally, an injection of 0.25% bupivacaine was given subcutaneously at each surgical site for local anesthesia.

SURGERY: Intragastric catheters (mice only)

Sterile access veterinary catheters (C30PU-RGA1439, Instech Labs) were attached to sterile vascular access buttons (VABM1B/22, 22, Instech Labs). Mice were anesthetized as described above, and the catheter was surgically implanted into the avascular stomach, and the port on

the access button was secured to the mouse's upper back. Mice were allowed one week to recover following IG surgery before the start of experiments.

SURGERY: Intracranial implants (mice only)

Mice were anesthetized as described above, and a fiberoptic cannula was lowered into the brain (usually preceded by injection with an AAV expressing a fluorophore reporter). For miniscope recordings, we performed a second surgery four weeks later in which a baseplate (Inscopix 100-000279) was placed above the lens and affixed with adhesive cement (MetaBond) and then covered after surgery with a baseplate cover (Inscopix 100-000241). Mice were used for recordings 3–4 weeks after initial cannula implantation, allowing for at least a week recovery from any intracranial or intragastric surgery.

Mice were prepared for optogenetic experiments by first anesthetizing the mice with isoflurane, and two fiberoptic cannulae were lowered into either brain hemispheres (usually preceded by injection with an AAV expressing an opsin). Mice were used for behavior 3–4 weeks after initial cannula implantation, allowing for at least a week recovery from any intracranial or intragastric surgery.

<u>Dopamine imaging.</u> Wild-type mice were prepared for imaging by injecting AAV9-hSyn-GRAB-DA3m (200nL; 4–8e12 vg/mL; WZ Biosciences) into a given area and installing a fiberoptic cannula (Doric MFC_400/430-0.48_6mm_MF2.5_FLT) at 0.1 mm above the virus target site. For the initial recordings (Fig. 1 and associated Extended Fig. 2–3), the areas injected were left DLS (+1.5 mm AP, -1.5 mm ML, -3.0 mm DV), NAc core (+1.4 mm AP, -1.0 ML, -4.5 DV), left BLA (-1.7 mm AP, -2.9 mm ML, -4.8 DV), and left lateral BLA (-1.7 mm AP, -3.2 mm ML, -4.8 mm DV). For recordings comparing BLA subregions (Fig. 1 and associated Extended Fig. 4–5), the areas injected were left anterior BLA (-1.0 mm AP, -3.0 mm ML, -4.8 mm DV) and left posterior BLA (-2.4 mm AP, -3.3 mm ML, -4.7 mm DV). For recordings comparing left and right BLA (Fig. 1 and associated Extended Fig. 6), the areas injected were left and right BLA (-1.7 mm AP, ±2.9 mm ML, -4.8 DV).

<u>VTA-DA neuron imaging:</u> For recordings of all VTA-DA neurons (Fig. 3 and associated Extended Fig. 7),DAT-cre were prepared for imaging by injecting AAV1-FLEX-CAG-jGCaMP7s (300 nL; 6.3e12 vg/mL; Addgene 104495) into left VTA (-3.1 mm AP, -0.5 mm ML, -4.5 mm DV) and installing a GRIN lens (8.4 x 0.5 mm, Inscopix 1050-004629) at 0.15 mm above the virus

target site. For recordings of the VTA-DA-CCK subpopulation (Fig. 3 and associated Extended Fig. 7), CCK-cre x DAT-flp x RosaFL-GCaMP7s mice were prepared for imaging by installing a GRIN lens (8.4 x 0.5 mm, Inscopix 1050-004629) at 0.15 mm above left VTA (-3.1 mm AP, 0.5 mm ML, -4.5 mm DV).

BLA-D1R neuron imaging: For recording BLA neurons (Fig. 5 and associated Extended Fig. 10), Drd1a-cre mice were prepared for imaging by injecting AAV1-CAG-FLEX-GCaMP8s (200 nL; 5.9e-12 vg/mL; HHMI Janelia) into left anterior BLA (-1.0 mm AP, -3.0 mm ML, -4.8 mm DV) and installing a GRIN lens (8.4 x 0.5 mm, Inscopix 1050-004629) at 0.15 mm above the virus target site.

VTA-DA projection stimulation: For stimulating VTA-DA projections (Fig. 4 and associated Extended Fig. 8–9), DAT-cre mice were prepared for experiments by injecting AAV1-EF1a-DIO-hChR2(H134R)-mCherry (300 nL; 6.0e-12 vg/mL; Addgene 20297) into left and right VTA (-3.1 mm AP, ±0.5 mm ML, -4.5 mm DV) and installing two 200 μm fiberoptic cannulae (FT200EMT, CFLC230-10 Thorlabs) at 0.1 mm above downstream bilateral target sites, which included bilateral NAc (+1.4 mm AP, ±1.0 ML, -4.5 DV), bilateral anterior BLA (-1.0 mm AP, ±3.0 mm ML, -4.8 mm DV), and bilateral posterior BLA (-2.4 mm AP, ±3.3 mm ML, -4.7 mm DV). Control mice underwent the same surgery, except an injection of AAV1-hSyn-DIO-mCherry (300 nL; 5.7e-12 vg/mL; Addgene 50459) was injected instead.

VTA-DA neuron inhibition: For inhibiting VTA-DA neurons (Fig. 1 and associated Extended Fig. 1), DAT-cre x Rosa-GtACR mice (or littermate controls) were prepared for experiments by installing bilateral fiberoptic cannulae (Doric DFC_200/245-0.37_5mm_GS1.0_FLT) at 0.1 mm above VTA (-3.1 mm AP, ±0.5 mm ML, -4.5 mm DV).

aBLA-D1R neuron inhibition: For inhibiting aBLA-D1R neurons (Fig. 5 and associated Extended Fig. 11), Drd1a-cre x Rosa-GtACR mice (or littermate controls) were prepared for experiments by installing two 200 μm fiberoptic cannulae (FT200EMT, CFLC230-10 Thorlabs) at 0.1 mm above bilateral anterior BLA (-1.0 mm AP, ±3.0 mm ML, -4.8 mm DV).

RECORDINGS: General methods (mice only)

For all recordings (except for BLA neuron dynamics), mice were placed in sound-isolated behavioural chambers (Coulbourn Habitest Modular System). The chambers were cleaned

between experiments to remove any remaining olfactory cues from previous experiments. All mice were habituated for at least 1 hr to the behavioural chamber (with recording equipment and IG catheter simultaneously attached) before being used for any experiments on subsequent days. Mice were additionally re-habituated to the behavioural chamber for 10–20 min at the beginning of each testing session (during which the LED used for imaging was turned on, to reduce any initial bleaching artifacts at the beginning of the recording). For recording BLA neuron dynamics, the mice were headfixed using a custom titanium headplate (eMachineShop) in a miniature treadmill. These mice were habituated to the headfixed setup for at least three 1 hr sessions before being used for any experiments, and were re-habituated for 10–20 min at the beginning of each testing session. An approximately equal number of female and male mice were used for every recording in this paper.

Lick responses were recorded by giving mice access to different solutions when either water-deprived (for experiments involving water, 0.8% sucralose, or 32% sucrose consumption) or food-deprived (for experiments involving 35% Ensure consumption). Mice were then given access to a lickometer containing the appropriate solution after a ten-minute baseline period. All mice were habituated initially to the lickometer and recording setup by providing access to a bottle containing sucralose for one hour with the microendoscope camera attached. For recording BLA neuron dynamics during licking, mice were water-restricted and trained to lick the 32% sucrose solution during a 5 second long 2kHz cue. After three sessions of training, the mice were put through three subsequent recording sessions, where access to a spout and lickometer was given after a ten-minute baseline period. On each day, the spout provided one of the three solutions, and the order of the solutions presented was counterbalanced for each mouse.

IG responses were recorded by infusing solutions at a rate of 100 μL/min for 10 minutes using a syringe pump (Harvard Apparatus 70-2001) connected to plastic tubing and adapters (AAD04119, Tygon; LS20, PNP3M, Instech) terminating to the IG catheters described above. This tubing apparatus was assembled and attached to each mouse before chamber habituation, and the infusion began after a ten-minute baseline period. For experiments where various gut sensors were blocked, the drug was dissolved into the solution being infused (resulting in concentrations of 600μg/mL mizagliflozin, 50 μg/mL GW1100, 50 μg/mL AH7614, and 10 μg/mL sulfo-N-succinimidyl oleate). For experiments where CCK was blocked, 1 mg/kg devazepide (given in saline vehicle at 10 mL/kg) was injected 30 minutes before the start of the infusion. All

sugar solutions (sucrose, glucose, fructose, galactose, MDG, mannitol) were infused at 32% concentration, except for the sweetener sucralose, which was infused at 0.8% concentration. All other caloric solutions were infused at a concentration isocaloric to 32% sucrose (35% Ensure; 32% collagen peptide; 14% intralipid; diet A was 17.3% sucrose, 4.5% intralipid, and 4.5% collagen peptide; diet B was 6.5% sucrose, 8.5% intralipid, and 6.4% collagen peptide). For some control experiments, 14% mineral oil and double distilled water were used.

Hormone responses were recorded by injecting solutions in 10 mL/kg saline vehicle intraperitoneally (IP) on the right side of the mouse after a ten-minute baseline period (using the following concentrations: 2 mg/kg 5-hydroxy-tryptamine HCl, 10 μg/kg cholecystokinin octapeptide, 100 μg/kg peptide YY, 2mg/kg ghrelin, 2 mg/kg glucagon, 10 μg/kg amylin).

Visceral malaise responses were recorded by injecting 100 mg/kg lithium chloride in 10 mL/kg saline vehicle intraperitoneally (IP) on the right side of the mouse after a ten-minute baseline period.

RECORDINGS: Photometry (mice only)

Photometry traces were acquired using continuous excitation from 40 μW blue LED (470 nm) and UV LED (420 nm) with an integrated processor (RZ10X LUX-I/O, TDT). Digital signals were acquired at 1.0173 kHz and collected by Synapse (TDT). After the experiment, this data was exported via Browser (TDT), and in MATLAB temporally downsampled to 4 Hz.

RECORDINGS: Miniscope videos (mice only)

Videos were acquired at 8 Hz (0.2 mW/mm^2 455 nm LED power, 8.0 gain, 2x spatial downsampling) in freely moving mice using a miniscope camera (nVista 3.0, Data Acquisition Software 2.0, Inscopix). After acquisition, videos were first pre-processed, spatially (binning factor of 2) and temporally (binning factor of 2) downsampled, put through a spatial bandpass filter (to remove noise and out-of-focus cells), and motion-corrected using Inscopix Data-Processing Software (1.9). Videos were removed if excessive motion (larger than the diameter of the average neuron in any direction) occurred that could not be addressed by additional motion-correction. Activity traces for individual neurons were then extracted from these videos using the constrained non-negative matrix factorization (CNMF-E) pipeline[1] implemented in MATLAB (http://www.github.com/zhoupc/cnmfe). After initial CNMF-E segmentation, extracted neurons were manually refined to avoid uncorrected motion artefacts, region of interest

duplication and over-segmentation of the same spatial components. Neurons were removed if large bleaching artefacts (which fit a defined exponential decay function) occurred during the 10-minute baseline period.

RECORDINGS: 2-photon videos (mice only)

Videos were acquired at 20 Hz with 512x512 resolution using a 900 nm laser (Chameleon Discovery, Coherent) in head-fixed mice using a resonant-galvo scanner attached to a 2-photon microscope (Ultima Investigator, Prairie View 5.8, Bruker). After acquisition, videos were first pre-processed, spatially (binning factor of 2) and temporally (binning factor of 2) downsampled, put through a spatial bandpass filter (to remove noise and out-of-focus cells), and motion-corrected using Inscopix Data-Processing Software (1.9). The videos were then put through addition motion-correction followed by ROI detection using EZcalcium[2] modules built off NoRMCorre[3] and CaImAn[4] toolboxes (https://github.com/porteralab/EZcalcium). Extracted neurons were manually refined to remove artefacts using the CaImAn ROI refinement module, and neurons were cross registered across days using the CaImAn ROI matching module.

RECORDINGS: fMRI imaging (humans only)

We included 30 participants, balanced by sex for a controlled cross-over study design. On two separate days, each participant received either a 300 ml 25% glucose solution or 300 ml water. The order was counterbalanced across participants. Testing began with a standardized introduction to the procedure and a state rating. Next we collected blood samples from a peripheral vein to analyze basal plasma glycated haemoglobin (HbA1c), leptin, insulin, and glucose. Participants were placed into the MR scanner for 50 minutes, during which the participants conducted the “Drink Task” detailed below. Afterwards, we repeated the state rating and blood draw (45 and 60 minutes after the oral intake respectively) to monitor changes in state, glucose, and insulin levels relative to baseline. In a subsequent debriefing, we assessed participants’ body composition (seca mBCA 515, SECA GmbH, Hamburg, Germany) and self-reports relating to the testing as well as depression symptoms and socioeconomic status. The total procedure was the same for both testing days and lasted 2.5 hours in total on each day. All participants signed informed consent and received 15 Euros per hour as compensation for their participation in the study, plus a monetary bonus on the second fMRI session (approximately 5€).

fMRI imaging data were acquired using a 3T MRI scanner with a 64-channel head coil (MAGNETOM Prisma Fit, Siemens AG, Medical Solutions, Erlangen, Germany). Functional data were acquired using multiband echoplanar imaging covering the whole brain with the following parameters: repetition time (TR) = 700 ms, echo time (TE) = 37 ms, flip angle = flip angle = 52°, voxel size = 2×2×2 mm, 72 axial slices, field of view (FOV) = 208 × 208 × 144 mm, multiband acceleration factor of 8. The first fMRI session lasted approximately 25 minutes (dependent on the duration of the drinking phase) and included approx. 2,143 volumes and the second fMRI session lasted 19.7 min and included 1,699 volumes. High-resolution T1- and T2-weighted images were acquired in a preliminary MRI session, T1 using the magnetization prepared-rapid gradient echo (MPRAGE) sequence, TR = 2,300 ms, TE = 2.32 ms, voxel size = 0.9 × 0.9 × 0.9 mm, 213 sagittal slices, FOV = 256 × 256 × 192 mm; T2 using the sampling perfection with application-optimized contrasts using a different flip angle evolutions (SPACE) sequence, TR = 3,200 ms, TE = 460 ms, voxel size=0.8×0.8×0.8 mm, 224 sagittal slices, FOV = 256×256×179 mm.

"Drink Task" experiments were conducted after participants entered the scanner. We positioned a 300 ml test bottle (containing 25% glucose or water) and an additional bottle (containing water for rinsing) at the back of the MR tube within sight of the participant. The two bottles were attached to separate plastic tubing, placed on the participants' chest and within reach (the tubing attached to the test bottle was marked using tape to distinguish it for the participant). The fMRI measurement began with a 2-minute baseline, during which a fixation cross was shown on a monitor in sight. Next participants were instructed via the display to reach for the tube connected to the 300 ml test bottle (containing 25% glucose or water), to drink up, and to press a key (Response Pad, Current Designs). They subsequently rated the sweetness and taste on a visual analogue scale (VAS; ranging from 0, "not at all sweet/palatable," to 100, "very much sweet/palatable"). After the rating, they were instructed via the display to reach for the second tube, to drink from the rising water bottle until they had a neutral taste in their mouth, and to press the key. Lastly, the fixation cross was presented for the remaining fMRI session (20 minutes). The total duration of the "Drink Task" was approximately 25 minutes, varying across participants due to the self-paced drinking period. The procedure was conducted on a computer using MATALB (R2019b) and Psychophysics Toolbox (PTB-3 v3).

RECORDINGS: PET imaging (humans only)

This protocol has already been described in a previous publication[5], and that existing dataset was re-analyzed for this paper. Briefly, the dataset included 13 male participants, who were given one of two solutions (milkshake or a tasteless noncaloric solution) while imaged using a HRRT Siemens PET scanner. During the 60-minute-long scan, participants were instructed not to sleep and to lie still. To visualize dopamine release, the participants were injected with 220–370 MBq [11C]raclopride using a programmable syringe pump (Perfusor compact, Braun, Melsungen), where 70% of the solution was infused within the first minute and the remaining 30% was slowly infused throughout the next 59 minutes. Each subject participated on two testing days (where they received milkshake or a tasteless noncaloric solution), before which they had fasted for 10–11 hours.

BEHAVIOR: General methods (mice only)

For all behavioral experiments, mice were placed in sound-isolated behavioural chambers (Coulbourn Habitest Modular System). The chambers were cleaned between experiments to remove any remaining olfactory cues from previous experiments. All mice were habituated for at least 1 hr to the behavioural chamber (with recording equipment and IG catheter simultaneously attached) before being used for any experiments on subsequent days. Mice were additionally re-habituated to the behavioural chamber for 10–20 min at the beginning of each testing session. An approximately equal number of female and male mice were used for every behavioral group in this paper. For all behavioral recordings, experimenters were blinded as to which subjects were members of a test group (e.g. ChR2) or a control group (e.g. mCherry).

For optogenetic activation or inhibition, we used a DPSS 473-nm laser (Shanghai Laser and Optics Century BL473-100FC), attached to fiber optic cannulae on mice prepared for VTA-DA or BLA-D1R neuron inhibition or VTA-DA terminal activation as described above. The laser and cannulae were connected using patchcords (MFP_200/220/900-0.22_2m_FCM-ZF1.25 or SBP_200/220/900-0.22_2m_FCM-GS1.0, Doric). The laser power was measured at the beginning of every experimental day and was set to 1–2 mW for inhibition and 10–15 mW for activation studies.

BEHAVIOR: Flavor-nutrient conditioning (mice only)

Mice were put through a 9-day flavor-nutrient conditioning protocol (2 pre-training test days, 6 training days, and 1 post-training test day), during which the mice were continuously food restricted to 85–90% initial body weight. During the first two days of the protocol, the mice were

given a one-hour-long two bottle assay in which they had simultaneous access to two 0.2% saccharin solutions flavored with 0.1% Lemon-Lime or Grape Kool-Aid (Kraft Foods) to establish initial preference. The placement of the bottles (front or back of the chamber) was randomized for each mouse on the first day and then flipped for the second day. Training occurred over the next six days, after which preference was reassessed with a third one-hour-long two bottle assay (for which the placement of the bottles was again randomized). Mice were acclimatized to the behavioural chamber for 10–20 min before flavored solutions became accessible on every conditioning day. Mice were taken off food restriction immediately after the last two bottle assay. Licks were registered using a lickometer attached to the Coulbourn Habitest system

During training, mice were attached to IG catheters and given isolated access to one of two flavored solutions, which triggered IG infusion when consumed. Mice were separated out into four groups. For the first three days of training, the first group was given one-hour-long access to the Grape flavored solution, which triggered 1 μL IG infusion of 8% glucose when consumed. For the next three consecutive days, the solution was replaced with the Lemon-Lime flavored solution, which triggered 1 μL IG infusion of water when consumed. The second group went through the same training, but the order of the flavors was flipped. The third and fourth group went through the same protocols as groups one and two respectively, but instead grape was associated with water infusion and lime was associated with 8% glucose infusion. Briefly the groups were as follows:

Group 1: Grape→glucose infusion (days 1–3); Lime→water infusion (days 4–6)
Group 2: Lime→water infusion (days 1–3); Grape→glucose infusion (days 4–6);
Group 3: Grape→water infusion (days 1–3); Lime→glucose infusion (days 4–6)
Group 4: Lime→glucose infusion (days 1–3); Grape→water infusion (days 4–6)

Mouse placement within each group was randomized, with the exception that mice could not start with >90% initial preference for the flavored solution paired with glucose infusion. Mice were removed from the flavor-nutrient conditioning protocol if their body weight dropped below 85% or if their IG catheters became disconnected for the majority of any training day.

<u>Silencing during flavor-nutrient conditioning</u> was accomplished using a 1–2 mW laser applied via cannulae to mice prepared for VTA-DA or BLA-D1R silencing as described above. The laser was delivered continuously throughout each experimental training session. Mice were removed from the study if their body weight dropped below 85% or if their attached patchcords or cannulae disconnected during any training day.

Activation during flavor conditioning was accomplished using a 10–15 mW laser applied via cannulae to mice prepared for VTA-DA terminal activation as described above. For these mice, no glucose or water infusion was given during training, and instead of glucose infusion, the laser turned on for 10 Hz pulses (1 ms pulse width, 2 s ON, 3 s OFF, 12 cycles) after each lick following a 20 second delay. Mice were removed from the study if their body weight dropped below 85% or if their attached patchcords or cannulae disconnected during any training day.

Delayed during flavor-nutrient conditioning was accomplished by adapting the training sessions. In these adapted training sessions, the mice were allowed to consume the flavored solution for ten minutes, after which the bottle was removed from the chamber, and a 1.0 mL IG infusion of 8% glucose or water was delivered.

BEHAVIOR: Conditioned taste aversion (mice only)

Mice were put through a 3-day taste aversion protocol (2 training days and 1 test day). The mice were water deprived for 24 hours before each day, and the mice were allowed one week to recover in between each day. During the first two days of the protocol, the mice were given access to a 5% sucrose solution flavored with 0.2% Orange or Cherry Kool-Aid (Kraft Foods) for one hour. Before the first day, each mouse had never tasted either sucrose or the Kool-Aid flavoring. Ten minutes after the first lick bout each day, each mouse was received an intraperitoneal injection of 100 mg/kg LiCl. After the injection, the mouse was returned to the cage with continued solution access for the remainder of the session. On the third day, the mice were given access to two bottles containing either water or the flavored sucrose solution to access preference. The placement of the bottles (front or back of the chamber) was randomized for each mouse. Licks on each day were registered using a lickometer attached to the Coulbourn Habitest system.

Silencing during conditioned taste aversion accomplished using a 1–2 mW laser applied via cannulae to mice prepared for VTA-DA or BLA-D1R silencing as described above. The laser was delivered continuously throughout the two training days. Mice were removed from the study if their attached patchcords disconnected during any training day.

Activation during conditioned taste aversion was accomplished using a 10–15 mW laser applied via cannulae to mice prepared for VTA-DA terminal activation as described above. For these mice, no LiCl injection was given during training, and instead the laser turned on for continuous

10 Hz laser pulses (1 ms pulse width, 2 s ON, 3 s OFF) after the first lick following a 20-second delay. The stimulation lasted for the remainder of the session. Mice were removed from the study if their cannulae disconnected during any training day.

BEHAVIOR: Lever pressing assays (mice only)

In these assays, mice were allowed to self-stimulate VTA-DA terminals. This was accomplished using a 10–15 mW laser applied via cannulae to mice prepared for VTA-DA terminal activation as described above. Mice were put through a 3-day lever pressing protocol, where mice were given access to two levers for one hour. Pressing one of the two levers resulted in terminal stimulation (20 Hz, 1 ms pulse width, 5 s total). The initial location of this active lever was randomized for each mouse on the first day (front or back of the chamber), but the location did not change on the second or third day. Mice were removed from the study if their cannulae disconnected during any day.

BEHAVIOR: Feeding assays (mice only)

In a variety of related assays, mice were given access to flavored Ensure solutions during optogenetic inhibition or activation. On four separate days, the mice were given access to one of the flavored Ensure solutions for thirty minutes following a brief period (1 hour) of water and food deprivation. On two of these days, the laser providing inhibition or activation would be turned off, and on the other two days, the laser would be turned on. The total consumption for each mouse would be averaged across the two replicate “laser on” days and the two replicate “laser off” days. The time of day that each mouse was put through the experiment was kept constant within a 30-minute tolerance to control for circadian effects.

<u>Silencing during feeding</u> accomplished using a 1–2 mW laser applied via cannulae to mice prepared for VTA-DA or BLA-D1R silencing as described above. The laser was delivered continuously during access to a vanilla flavored Ensure solution. If a mouse’s cannulae disconnected during any “laser on” day, the licking data for that day was removed, and the experiment re-run.

<u>Activation during feeding</u> was accomplished using a 10–15 mW laser applied via cannulae to mice prepared for VTA-DA terminal activation as described above. These mice were put through three separate assays using different flavored Ensure solutions (vanilla, chocolate, strawberry). In the first assay, continuous laser pulses (10 Hz, 1 ms pulse width, 2 s ON, 3 s

OFF) were delivered during access to a vanilla flavored Ensure solution. In the second assay, the mice were given access to a chocolate flavored Ensure solution, with the same stimulation protocol except the laser would turn off for 2 seconds after every lick. In the third assay, the mice were given access to a strawberry flavored Ensure solution, where the laser would only turn on for 2 seconds after every lick (for 10 Hz stimulation at 1 ms pulse width). If a mouse's cannulae disconnected during any "laser on" day, the licking data for that day was removed, and the experiment re-run.

380 **ANALYSIS: Recordings (mice only)**

We analyzed all recording data using custom MATLAB (v. R2023a) scripts. Throughout the paper, values are generally reported as mean ± SE (error bars or shaded area). In figures with simple linear regressions, shaded areas represent the 95% confidence interval for the line of best fit. Except for linear regressions and K-S tests, nonparametric tests were uniformly used. We calculated P values for paired and unpaired comparisons using two-sided permutation tests (100,000 iterations or exact when possible). Occasionally, one-sided permutation tests were performed when the experiment called for it. For example, we used a one-sided test to determine whether terminal activation causes CTA (since the test cannot easily show that activation makes a flavor more preferrable since sucrose is already palatable). While each
390 recording method in mice (photometry, 2p, miniscope) was analyzed differently as detailed within this section, the same time windows were used to calculate activity during the licking ("oral phase"), during IG infusion ("IG phase"), and after IG infusion ("post-IG phase").

<u>The oral phase</u> was defined as 0–5 seconds after the first lick in a lick bout. Lick bouts were defined as a series of licks separated by at most 2 seconds and lasting at least 2 seconds. For almost all analysis (see 2-photon analysis below), only the first lick bout was considered for this analysis. This time window was chosen since post-ingestive sensation by the GI tract should be minimal. Considering that mice consume 9.6 μL/s at maximum speed[6] and mice swallow at a rate of 1 Hz[7], the amount swallowed in 5 s would be at most 38.4 μL (roughly 10% of a mouse's
400 stomach volume at baseline[8]). Our choice of this time window was later justified by our finding that DA release in the BLA only occurs after 80±18 μL of Ensure has entered the stomach (i.e. after 48±11 seconds of a 100 μL/min infusion entering the stomach; Extended Fig. 2e–g).

<u>The GI phase</u> was defined as 20–600 seconds after the start of IG infusion. The beginning of this time window was chosen due to the approximate time (20s) it takes for Ensure to travel

through the internal tubing to reach the mouse's stomach after the onset of an infusion. The end is simply when the 10-minute IG infusion ends.

The post-IG phase was defined as 1200–3000 seconds after the start of IG infusion. This is the 30-minute time window starting ten minutes after the IG infusion ends. Since our previous study found that liquid by oral gavage can be found five minutes after delivery[9], we decided to allow for additional time to allow for further drainage.

The hormone phase was defined as 0–300 seconds after IP injection. This time window was used to determine responses to all injections other than aversive stimuli such as LPS, which were analyzed using a different time window.

The malaise phase was defined as 300–1800 seconds after IP injection. This time window was used to determine responses to LPS, due to its delayed effects.

Photometry recordings provided signal traces using isosbestic (420 nm) and activity-dependent (470 nm) excitation wavelengths. To account for movement artefacts, we normalized the activity-dependent signal using the function $\frac{\Delta F}{F_0} = \frac{F - F_0}{F_0}$, where F is the activity-dependent signal and F_0 is the fluorescence predicted by the isosbestic signal (by applying the total isosbestic signal to a linear regression model of both signals during the 10 min baseline period). Additionally, we subtracted every photometry trace during IG infusions or IP injections by the trace acquired when that same mouse underwent a sham infusion or a saline injection. These traces are shown un-subtracted in the mean and example traces in each figure, but this subtracted trace was used for statistical tests and to generate datapoints for every other graph

Miniscope and 2-photon recordings provided activity traces following neuron segmentation as described above. All responses were z-scored using the standard deviation of activity during the 10 minute baseline period. Licking data was acquired via TTL signal to get activity data during lick bouts. For miniscope recordings, only the first lick bout was considered for analysis. For 2-photon recordings, since lick bouts were short (<5 seconds) and separated by relatively large windows of time (>20 seconds), we combined all lick bouts for analysis, except when the text directly says otherwise.

Activated/inhibited populations were determined using activity cutoffs drawn from empirical data distributions. Neurons were considered activated if they showed z-scored activation over 95% of the same population of neurons during a similar time window where no manipulation was given. Inhibited neurons were those that showed decreases in z-scored activity below 95% of the same population of neurons during a similar time window where no manipulation was given. As an example, 5% of $VTA_{DA/CCK}$ neurons were found to increase by more than 0.5378 z during the "IG phase" of sham infusion, so $VTA_{DA/CCK}$ neurons were said to have been activated during other infusions if their activity increased by more than 0.5378 z. Since neuronal recordings have an inherent drift, we used a different cutoff for determining whether neurons were activated during the "post-IG phase." As an example, we found that 5% of $VTA_{DA/CCK}$ neurons increased by more than 0.6917 z during the "post-IG phase" of sham infusion, so $VTA_{DA/CCK}$ neurons were said to have been activated after other infusions if their activity increased by more than 0.6917 z. For determining neurons activated during licking, the TTL data acquired while licking Ensure (for miniscope recordings) or sucrose (for 2p recordings) was applied to recordings of the same population of neurons where no manipulation was given. This allowed us to generate activity during sham lick bouts to generate cutoffs for activated and inhibited neurons using the methodology detailed above. In total, this empirical method for determining activity cutoffs was used to account for the fact that some neuron populations are more active than others and to account for differences in neuronal drift over different timescales.

Population-weighted activity was calculated for populations of activated neurons, by multiplying the mean z-scored activity for each neuron by the proportion of neurons activated in the total sample. The opposite procedure was done for inhibited neurons, with activated and inhibited neurons determined using the method above. This method allows us to determine the degree of activation or inhibition of the neuron population as a whole.

Area under the receiver operator curve (auROC) was used to quantify responses of aBLA-D1R neurons during bouts of sucrose ingestion. Receiver operator curves were calculated for each timepoint by comparing the distribution of z-score across sucrose trials, to the distribution of z-score across sham trials. In this analysis, auROC>0.5 represents greater activation than seen in sham.

Rise time dynamics were calculated for dopamine release using individual traces during IG infusion, using the time window starting 1 minute before the infusion started and ending 5

minutes into the infusion. These traces were fitted with a sigmoid curve, and the time point at which the fitted curve reached 5% of the final value was used to calculate $T_{5\%}$. The first time point that the trace exceeded baseline fluorescence by 3σ (where σ was the standard deviation of fluorescence during the baseline period) was used to calculate $T_{3\sigma}$. These values are shown unadjusted in Extended Fig. 2. In the text, however, catheter transit time was subtracted in order to obtain an adjusted rise times for $T_{5\%}$ and $T_{3\sigma}$ which were then averaged (note: the reported mean rise time also required averaging standard errors according to the rule $\overline{SE} = \frac{\sqrt{\overline{var}}}{\sqrt{n}}$, where SE was standard error, var was variance, n was number of observations, and $\bar{x}$ is the mean of x). Individual cell recordings could not use both rise time measurements ($T_{5\%}$ and $T_{3\sigma}$), as responses during IG infusion did not follow a sigmoid curve (and thus only $T_{3\sigma}$ could be used) and while responses during licking did follow a sigmoid, they did not typically rise above 3σ (and thus only $T_{5\%}$ could be used). For this reason, in the text neuron activity rise times are given by one of these two measurements, and are compared to dopamine release rise time using the same measurement method (e.g. IG rise time for activity and release is compared using $T_{3\sigma}$ alone). Fall time dynamics were calculated similarly to rise time dynamics, except a different time window was used, starting 5 minutes before the end of infusion and ending 40 minutes after the infusion ended.

Peak time dynamics were calculated for dopamine release during licking by looking at the time window starting at the beginning of the first lick of the first lick bout and ending 30 seconds after. The time reported is the time that dopamine reached its peak over this time window. Peak timing is also noted for aBLA activity, but this uses a shorter time window starting at the beginning of each lick bout and ending 5 seconds after (due to the much shorter access windows).

Statistical corrections for subject effects were utilized when noted. For some neuron activity recordings, a linear mixed-effects model was performed to account for effects emerging from individual mouse differences. This model treated mouse differences as a random effect and a possible covariate, using the matlab function fitlme("activity ~ 1 + manipulation + (1|mouse) + (manipulation|mouse)"). Additionally, intra-class correlations (ICC) are also noted to show how the relative effect of differences between mice and experimental conditions, using the formula $\frac{var(mice)}{var(total)}$ to get the fraction of variance between mice of the total variance. In cases where this

appeared relevant, we graphed activity responses averaged by mouse (e.g. Extended Fig. 10v) to visually demonstrate ICC.

Principal-component analysis was accomplished using the built-in MATLAB 'pca', which centers the data with single value decomposition. Prior to this, the data was down sampled (to 1 Hz for IG responses or 4 Hz for lick responses) and then normalized by the absolute maximum change over the activity trace. The variance explained by each PC was shown with a scree plot, which was used to determine the number of plotted PCs in cases where a clear "elbow" was present (Fig. 3g). Neuron trajectories were always plotted using the first two principal components to create a 2-dimensional PC space. For determining trajectory similarity, we calculated Euclidian distances between paired timepoints in this 2-dimensional space. For analysis of VTA-DA/CCK neurons, the input matrix for PCA was each neuron's activity trace during Ensure IG infusion. For analysis of aBLA-D1R neurons, two separate PCAs were run, the first to determine response similarity across solutions and the second to determine response similarity across time. In the first case, videos were cross registered across days to get mean individual neuron responses during bouts of sucrose, sucralose, and water. The response during mock trials was averaged across all three days to get each neuron's mean mock trial response. These four matrices were concatenated (sucrose, sucralose, water, mock) for use in PCA. In the second case, videos were cross-registered only across sucrose and sucralose sessions, and activity during bouts 2–5 and the last 5 bouts were averaged to get four separate matrices which were concatenated (early sucrose bouts, late sucrose bouts, early sucralose bout, late sucralose bouts) for use in PCA.

K-means clustering was accomplished using the built-in MATLAB 'kmeans' function, after determining the number of clusters using the silhouette method. Prior to this, the data was down sampled (to 1 Hz for IG responses or 4 Hz for lick responses) and then normalized by the absolute maximum change over the activity trace. This pipeline gave indices for the n clusters, which were plotted using data that had not been normalized by absolute maximum change.

ANALYSIS: fMRI recordings (humans only)

Before statistical analysis, all fMRI datasets were preprocessed, and the first 10 volumes were discarded to allow for magnetic saturation. The first preprocessing step was to correct functional images for motion and distortion using FSL tools 'mcflirt'[10] and 'topup'[11]. Next, the T2 image was co-registered to functional images, and T1 was then co-registered to the T2 image and

normalised to the Montreal Neurological Institute (MNI) reference space using the unified segmentation approach in SPM12. Finally, functional images were normalised using the ensuing deformation parameters and smoothed using a 6 full-width-half-maximum Gaussian kernel. Moreover, the following confounds were computed to be used as nuisance regressors for 1st-level fMRI analyses: 24 motion parameters (6 motion parameters relating to the current and the preceding volume, respectively, plus each of these matrices squared[12]), mean signal extracted from the ventricular cerebrospinal fluid (computed using 'fslmeants'), and a matrix with motion-outlier volumes (identified using fsl_motion_outliers, based on framewise displacement between subsequent volumes, at a threshold of > 1 mm[13]).

Statistical analysis of discrete data was performed using MATLAB (v2019b) and preprocessing and analyses of fMRI data were performed using SPM12 (version 6225, Wellcome Trust Centre for Neuroimaging), implemented in MATLAB and the FMRIB Software Library (FSL, version 5.0.10, Oxford UK). Analyses of fMRI data were conducted using the mass-univariate approach by fitting general linear models (GLMs) in SPM12.

To assess the time course of the BOLD response within the 20 min after the oral intake, relative to the 2-min baseline before the oral intake, we specified 2-min time bins: one for the baseline at the beginning of the Drink Task and ten for the period after the oral intake. In 1st-level GLMs estimated for each testing day, we modelled these time bins as separate regressors using a boxcar reference vector with their onsets and durations, convolved with the canonical hemodynamic response function and its time and dispersion derivatives. Furthermore, the drinking phase (including drinking, taste rating, and rinse) was modelled on an additional regressor (with varying durations dependent on participants' behavior), and the confounds described above were specified as nuisance regressors. Low-frequency signal drifts were filtered using a cutoff of 128 s. Finally, we estimated 10 contrast images comparing each of the post-ingestion time bins against the baseline time bin (contrast weights: [-1 1]). At the 2nd level, we specified a flexible factorial design with the factors subject and condition (dependency present in the latter), with all variances set to equal, and with the following covariates: sex, age, testing day, insulin sensitivity (mean Homeostatic Model Assessment of Insulin Resistance, HOMA-IR), and subjective hunger (before oral intake). For each subject, the condition included 20 contrast images corresponding to post-ingestion time bins relative to baseline, 10 after water intake and 10 after glucose intake. We identified brain regions that were modulated in response

to glucose relative to water by analyzing the contrasts water > glucose (contrast weights: [ones(1,10)ones(1,10)*-1]) and glucose>water(contrast weights:[ones(1,10)*-1 ones(1,10)]).

ANALYSIS: Behavior (mice only)

All behavioral analysis used Coulbourn output data of licking or lever pressing. Lick data is presented as cumulative totals or as flavor preferences. Flavor preferences are calculated as a percent preference towards the flavor associated with neuronal stimulation, glucose infusion, or LiCl injection, where preference is calculated as $\frac{A}{A+B}$, where A is the total licks of one flavor and B is the total licks of the other flavor. Lever pressing data is presented in the paper as the total number of active lever presses subtracted by the total number of inactive lever presses. Where appropriate (Fig. 4 and associated Extended Fig. 8–9), statistical tests utilized a Benjamini-Hochberg correction for multiple comparisons (i.e. the p-value was adjusted using the equation $p' = \frac{m}{i} \times p$, where m is the number of brain regions tested, and i is the individual p-value's rank).

ANALYSIS: Histology (mice only)

Mice were trans-cardially perfused with phosphate-buffered saline (PBS) followed by 10% formalin. Whole brains were dissected, and kept in 10% formalin overnight at 4°C. The brains were transferred to 15% sucrose the next day, and then transferred to 30% sucrose the following day (still at 4°C). Once brains had fully absorbed the 30% sucrose solution, they were embedded in Tissue-Tek OCT Compound (Sakura) and sectioned using a cryostat. For immunostaining, these brain sections (50 μm) were washed 3 x 5 min with PBS-T (0.1% Triton X-100 in PBS) and incubated for 2 hours at room temperature with NGS blocking solution (2% Normal Goat Serum + 3% Bovine Serum Albumin in PBS-T). Then, the sections were incubated for 12–48 hours at 4°C with primary antibodies in NGS blocking solution. Afterwards, the sections were washed 3 x 5 min with PBS-T and incubated at room temperature with secondary antibodies in NGS blocking solution. Finally, the sections were washed again 3 x 5 min with PBS, mounted with DAPI Fluoromount-G (Southern Biotech), and then imaged with an Eclipse Ti2 inverted microscope (Nikon). Images underwent minimal processing using ImageJ (v.1.53t). Coordinates were determined from these images by eye. For GFP staining, the primary antibody was anti-GFP chicken (Abcam, ab13970) and the secondary antibody was goat anti-chicken Alexa Fluor 488 (Abcam, ab150169). For RFP staining, the primary antibody was anti-RFP rabbit (Abcam, ab124754) and the secondary antibody was goat anti-rabbit Alexa Fluor 568 (Abcam, ab175471).

ANALYSIS: Graphing

For presentation purposes, many of the traces in figures were down sampled and smoothed using a moving average filter with a kernel size of 2. The traces depicting many minutes of recording (as seen with IG responses) were down sampled to 0.1–0.2 Hz. The mean traces depicting only a few seconds (as seen with lick responses) were down sampled to 1 Hz (except for single neuron activity traces during lick bouts, which is shown at 4 Hz). Graphs showing PC space of licking responses were kept at 4 Hz. In some cases, the same data was used for multiple graphs to make different comparisons (such as DA responses during Ensure IG infusion in left BLA, which is plotted in bar graphs in Fig. 2b, Fig. 2f, and Extended Fig. 2b, to compare responses to striatum, to right BLA, and during water infusion respectively).

Acknowledgements

Author Contributions

Competing Interests

The authors declare no competing interests.

Bibliography (Methods)

1. Zhou, P. *et al.* Efficient and accurate extraction of in vivo calcium signals from microendoscopic video data. *eLife* **7**, e28728 (2018).
2. Cantu, D. A. *et al.* EZcalcium: Open-Source Toolbox for Analysis of Calcium Imaging Data. *Front. Neural Circuits* **14**, (2020).
3. Pnevmatikakis, E. A. & Giovannucci, A. NoRMCorre: An online algorithm for piecewise rigid motion correction of calcium imaging data. *J. Neurosci. Methods* **291**, 83–94 (2017).
4. Giovannucci, A. *et al.* CaImAn an open source tool for scalable calcium imaging data analysis. *eLife* **8**, e38173 (2019).
5. Thanarajah, S. E. *et al.* Food Intake Recruits Orosensory and Post-ingestive Dopaminergic Circuits to Affect Eating Desire in Humans. *Cell Metab.* **29**, 695-706.e4 (2019).
6. Boughter Jr, J. D., Baird, J.-P., Bryant, J., St. John, S. J. & Heck, D. C57BL/6J and DBA/2J mice vary in lick rate and ingestive microstructure. *Genes Brain Behav.* **6**, 619–627 (2007).
7. Lever, T. E. *et al.* Adapting Human Videofluoroscopic Swallow Study Methods to Detect and Characterize Dysphagia in Murine Disease Models. *J. Vis. Exp. JoVE* 52319 (2015) doi:10.3791/52319.
8. McConnell, E. L., Basit, A. W. & Murdan, S. Measurements of rat and mouse gastrointestinal pH, fluid and lymphoid tissue, and implications for in-vivo experiments. *J. Pharm. Pharmacol.* **60**, 63–70 (2008).
9. Bai, L. *et al.* Genetic Identification of Vagal Sensory Neurons That Control Feeding. *Cell* **179**, 1129-1143.e23 (2019).
10. Jenkinson, M., Bannister, P., Brady, M. & Smith, S. Improved Optimization for the Robust and Accurate Linear Registration and Motion Correction of Brain Images. *NeuroImage* **17**, 825–841 (2002).

11. Andersson, J. L. R., Skare, S. & Ashburner, J. How to correct susceptibility distortions in spin-echo echo-planar images: application to diffusion tensor imaging. *NeuroImage* **20**, 870–888 (2003).

12. Friston, K. J., Williams, S., Howard, R., Frackowiak, R. S. J. & Turner, R. Movement-Related effects in fMRI time-series. *Magn. Reson. Med.* **35**, 346–355 (1996).

13. Power, J. D., Barnes, K. A., Snyder, A. Z., Schlaggar, B. L. & Petersen, S. E. Spurious but systematic correlations in functional connectivity MRI networks arise from subject motion. *Neuroimage* **59**, 2142 (2012).